MODELING SHALLOW GROUNDWATER TABLE CONTRIBUTION TO SOIL WATER RETENTION IN THE UNSATURATED ZONE OF A CALCAREOUS SOIL OF SOUTH FLORIDA

By

LUIS PABLO BARQUIN VALLE

A THESIS PRESENTED TO THE GRADUATE SCHOOL
OF THE UNIVERSITY OF FLORIDA IN PARTIAL FULFILLMENT
OF THE REQUIREMENTS FOR THE DEGREE OF
MASTER OF SCIENCE

UNIVERSITY OF FLORIDA

2009

To Regina and my family

ACKNOWLEDGMENTS

I would like to thank the University of Florida, the Agricultural and Biological Engineering Department, the College of Agricultural and Life Sciences and the Tropical Research and Education Center for granting the opportunity of pursuing my graduate studies and research with such a prestigious and recognized institution.

Special thanks to Dr. Kati Migliaccio, for her leadership, trust and patience. But specially for conferring me the opportunity of learning and developing my interests in water resources research with her team as a graduate research assistant. Special thanks to Dr. Rafael Muñoz Carpena for giving me the first chance to be at UF and develop my interests in hydrology during the EARTH undergrad internship as well as all his time patience and intellectual support in great part of this thesis. Special thanks to Dr. Yuncong Li for giving me the opportunity to return to UF-TREC and work with his team before joining graduate school. Special thanks to Dr. Bruce Schaffer and Dr. Jonathan Crane for being not only great committee members and professors but also for being such great persons and friends.

The author would also like to acknowledge Michael Gutierrez for all the field support and instrumental training. Special thanks to Sikavas Na-Lampang for sharing his programming skills and special thanks to Tina Dispenza, Nicholas Kiggundu, Isaya Kisseka and Bridgette Castro for all their team support.

Last but not least I would like to recognize Regina Incer for all her love, patience and support and my family, specially my parents, for giving me all the opportunities and education necessary to pursuit many of my dreams and professional goals.

TABLE OF CONTENTS

LIST OF TABLES

LIST OF FIGURES

Abstract of Thesis Presented to the Graduate School
of the University of Florida in Partial Fulfillment of the
Requirements for the Degree of Master in Science

MODELING SHALLOW GROUNDWATER TABLE CONTRIBUTION TO SOIL WATER RETENTION IN THE UNSATURATED ZONE OF A CALCAREOUS SOIL OF SOUTH FLORIDA

By

Luis Pablo Barquin Valle

August 2009

Chair: Kati White Migliaccio
Cochair: Rafael Muñoz-Carpena
Major: Agricultural and Biological Engineering

Quantifying the relationship between groundwater table level and root zone soil water content in shallow groundwater conditions is important in South Florida due to the potential changes in groundwater level related to the Comprehensive Everglades Restoration Plan (CERP) and the resulting impacts these changes may have on deep rooted agriculture. Thus, soil water dynamics of the capillary fringe of a Krome very gravelly loam soil profile from a lychee grove (Litchi chinensis) were evaluated using data collected from September 2008 to March 2009. Thirty-two EnviroSCAN capacitance sensors distributed at four depths (10, 20, 40 and 60 cm) and pressure transducers located in four adjacent monitoring wells were installed with the goal of characterizing the shallow groundwater contribution to the soil water content in a soil profile composed of two layers: a scarified layer and an underlying layer of limestone bedrock. The analysis was conducted in three main objectives (1) develop a multi sensor capacitance onsite calibration equation for limestone bedrock by comparing readings of scaled frequency to suction readings of tensiometers, (2) determine the existence, location and statistical significance of diurnal peaks in soil water content and groundwater levels and (3) test the validity of the drain to equilibrium hydrostatic assumptions for predicting the soil water content using groundwater

level as a reference. The Krome soil scarified layer's water holding capacity was primarily attributed to the loam fraction as the limestone fraction had very low water retention properties. Limestone water loss was equivalent to 20% volumetric water content compared to 40% in the Krome scarified soil at 1,000 cm of suction. Four regression models were proposed for calibration purposes in spite of measured spatial and depth variability of the soil. Diurnal peaks of soil water content and groundwater level were statistically identified with circular statistics using Rayleigh test. Mean vectors of soil water content at deeper depths were found to be more related with groundwater fluctuations and soil water content at shallower depths was associated with peaks of solar radiation and soil temperature. A hydrostatic model based on the drained to equilibrium principle and van Genucthen's equation (1980) was able to capture the general and most representative trends of soil water content changes in response to shallow groundwater fluctuations, accuracy of predictions had an overall Nash Sutcliffe (1970) coefficient of efficiency of 0.72. Results are intended to provide agricultural producers with science-based information on the benefits and challenges of the shallow groundwater table in this area.

CHAPTER 1
GENERAL INTRODUCTION

Background

Shallow Groundwater Capillarity

Contribution to irrigation from shallow water tables has been a subject of extensive research around the world. A brief review of such studies is provided in Babajimopoulos et al. (2007). Shallow groundwater tables have been shown to provide a portion of the crop water needs for cotton replacing 60% of the evapotranspiration (ET) (Wallender et al., 1979) and 37% of ET (Ayars and Schoneman, 1986). Others have suggested that irrigation could be reduced by 80% under shallow groundwater conditions (Prathapar and Qureshi, 1999). Also, assessment tools and models of water movement from a shallow water table to the root zone have been developed such as Upflow (Raes and Deproost, 2003) and DRAINMOD (Skaggs, 1978a).

Diurnal fluctuations of groundwater have been documented by several authors around the world. Most of the groundwater hydrology literature suggests diurnal fluctuations are principally induced by three factors: evaporation, barometric pressure and tidal actions. Diurnal fluctuations of groundwater caused by daily evaporative cycles are documented by White (1932), Tromble (1977), Bauer et al. (2004), Merrit (1996) and Chin et al. (2008). Temperature effects on groundwater fluctuations were originally studied by Bouyoucos (1915) and developed by Smith (1939), Taylor (1962) and Meyer (1960). Effects of pressure changes on groundwater levels have also been suggested. Peck (1960) attributed the upward movement of groundwater to the effect of atmospheric pressure on entrapped air in the pore space. Turk (1975) in attempt to explain this phenomenon attributed the fluctuations to temperature induced atmospheric changes acting upon the capillary zone. This process was also supported by Weeks (1979) who described how changes in barometric pressure generally affect diurnal patterns of groundwater levels. The effect

of pressure on water levels was explained by Rasmussen and Crawford (1997) who described how unconfined aquifers generally experience a unit decrease in groundwater level with each unit increase in barometric pressure and vice versa.

Previous anecdotal evidence has been reported in Miami-Dade County, Redland agricultural area of South Florida suggesting that groundwater may be contributing to plant water requirements. Al-Yahyai et al. (2005) reported a lack of physiological response between irrigated and non irrigated carambola (Averrhoa carambola) in a study conducted in the Redland's agricultural area and assumed this result was due to shallow groundwater capillary rise. Additional work characterizing the soil water retention in this orchard described the difficulty in obtaining suction values greater than 125 cm in the field treatments without irrigation (Al-Yahyai et al., 2006). Similarly, Migliaccio et al. (2008a) reported evidence of capillary influences on soil water status. They investigated soil suction in Marl soils of South Florida, and identified diurnal patterns during the dry season.

Drained to Equilibrium Concept

In order to model the shallow groundwater contribution to the soil water status in the unsaturated zone, it is necessary to understand the process of capillary rise and find alternatives to interpret its fluctuations. A simple approach to interpret the soil water dynamics is through the drained to equilibrium concept explained in detail by Wellings and Bell (1982).

The unsaturated zone of an unconfined aquifer is generally categorized into three zones: the soil zone, the intermediate zone and the capillary fringe (Todd, 1959). The soil zone contains roots and is characterized by rapid water content changes due to rainfall and evapotranspiration. The intermediate zone is below the soil zone and varies in thickness according to the water table depth and is the region where water movement is downwards due to percolation. The capillary fringe is the zone extending from the water table into the intermediate zone for a distance,

limited by the pore size distribution of the soil. This zone is partially saturated and holds water at negative pressures. The three zones form a dynamic continuum from the water table to the soil surface (Figure 1-1). Thus, capillary rise is a function of porosity and hydraulic conductivity. When water drains, a capillary moisture distribution curve is formed. After drainage, there is a relationship between water content and negative water pressure which relates to the pore size distribution.

The concept of potential energy of soil water with respect to an arbitrary reference datum was first suggested by Buckingham (1907). Above the water table, the soil is unsaturated and the matric potential is negative. In a soil with high permeability and a shallow water table, an equilibrium profile is equivalent to the traditional concept of field capacity. When the profile is at equilibrium with the water table, the matric potential equals the height above the water table and its relationship with soil water content is equivalent to the water content characteristic of the soil because the water potential profile will always move towards equilibrium with the water table. As a result, the water retention curve can be determined either in laboratory or field conditions.

The soil water content and suction relationship (and also the soil water content and water table relationship) is unique for a given vadose zone. Depending on the path the soil water is moving (drainage or wetting), the soil water content at a given water level can be represented by more than one pressure (Nielsen, 2006). This phenomenon is called hysteresis and is caused by the variation of the pore sizes in the soil.

Characterization of the soil water retention functions requires parametric models. A commonly used retention model is the Van Genuchten (1980) closed form analytical expression. The closed form equation consists of four independent parameters which have to be estimated

from observed soil water retention data. Many curve fitting and parameter optimization codes such as RETC software (Van Genuchten et al., 1991) are widely used today. These types of relationships are empirical in nature with a physical basis. The van Genuchten (1980) equation is expressed as

$$\theta = \theta_r + \frac{(\theta_s - \theta_r)}{\left[1 + (\alpha h)^n\right]^m} \tag{1-1}$$

where θ is the volumetric water content; h is the pressure head; θ_s and θ_r represent the saturated and residual water contents, respectively; and α, n and m are empirical shape parameters. The parameters generally adopt values in the following ranges: $0 < \alpha < 1$, $n > 1$, $0 < m < 1$, $h \geq 0$.

Study Site Characteristics: Southeast Florida Hydrology

The Biscayne Aquifer in southeast Florida is an unconfined coastal aquifer with a shallow layer of highly permeable limestone that covers an area of 10,360 km^2 underlying Broward County, Miami-Dade County, Monroe County and Palm Beach County (Klein and Hull, 1978) (Figure 1-2 and 1-3). Groundwater recharge from annual rainfall of 1,448 mm/yr (Ali and Abtew, 1999) is 46% (USGS, 2009) (Figure 1-4); approximately 70% of the total direct groundwater recharge (Klein and Hull, 1978) occurs through storm events greater than 15 mm during the rainy season (June to October) (Delin et al., 2000). The aquifer's specific yield is 0.26 m of water table rise for every 1 mm of rain (Chin et al., 2005). Thus, the Biscayne Aquifer characteristics of unconfinement, high permeability and shallow depth result in water table fluctuations that are fairly responsive to storm events and canal system management (Pitt, 1976; Ritter and Muñoz-Carpena, 2006).

Weather patterns also influence aquifer water losses as the principal process of withdrawal from the Biscayne Aquifer is evaporation which has a close correlation with solar radiation and consequently a corresponding seasonal variation (Merrit, 1996). This finding was supported by

Abtew (1996) which indicated that solar radiation explained 70% of the variations in South Florida's reference evapotranspiration. Likewise, Chin et al. (2008) reported that shallow saturated-zone evaporation rate equaled the potential evaporation rate to a depth of 1.4 m decreasing to zero at a depth of 2.5 m.

One of the most dominant features of flood control and water management in southeast Florida is the hydraulic connection of the Biscayne Aquifer with the South Florida Water Management District (SFWMD) canal system. This relationship brings benefits and challenges. The benefits of the system are that it provides an effective and fast response to flood prevention and a protective freshwater head against saltwater intrusion. The challenges of such a drainage system are related to the reduced retention time or water storage in the watershed during the wet season that results in potential salt water intrusion during drought periods (Klein and Hull, 1978). A great part of the SFWMD's canal management decisions are integrated into the Comprehensive Everglades Restoration Plan (CERP) which represents an ambitious effort to rehabilitate the Everglades National Park (ENP) quantity and distribution of water (Perry, 2004). The effort of maintaining sustainable groundwater levels capable of restoring ENP natural flow, protecting agricultural and urban areas from flooding and preventing saltwater intrusion along the coast results in a complex and sometime conflicting challenge for canal management. As management goals are adjusted to meet the CERP objectives, there exists a greater potential for elevated groundwater levels and resulting water movement by capillary forces into the underlying unsaturated soil. The potential impact of increased soil water content is of particular concern to deep rooted crops, such as tropical fruits in respect of flooding tolerance and water use efficiency (Schaffer, 1998).

Soils

Krome soils are loamy skeletal, carbonatic, hyperthermic Lithic Udorethents (Noble et al., 1996) made of rock plowed oolitic limestone. A Krome soil's typical profile is composed of a scarified layer (15 cm) of very gravelly loam texture and an underlying layer of limestone bedrock (Li, 2001) (Figure 1-5). Muñoz-Carpena et al. (2002) and Al Yahyai et al. (2006) describe the Krome scarified layer physical structure in two solid fractions, 51% coarse particles (>2 mm) and 49% loam particles, with a complex bimodal soil water retention patterns where the gravel fraction contributes to very rapid soil water depletion and the loamy fraction provides for soil water retention.

Available information on the properties of the limestone bedrock layer is limited since most soil analytical methods are designed for traditional loose soil and not for solid, bedrock material. The information that is available focuses on the hydro-geological characterization of the Biscayne Aquifer (Klein and Hull, 1978; Fish and Stewart, 1991; Chin, 2005; Cunningham et al., 2004; 2006) and its geotechnical properties (Saxena, 1982). Klein and Hull (1978) describe the aquifer as a system of limestone, sandstone and sand, highly permeable and extremely porous. The geotechnical specifications for material engineering classify the underlying layer as Miami limestone; the bulk density ranges from 1.31 to 1.64. g/cm^3 and porosity is between 20 to 50% or greater (Saxena, 1982). Cunningham (2004) characterized the Biscayne Aquifer as a triple porosity: (1) interparticle vug porosity providing much of the storage, (2) touching vug porosity creating groundwater flow passageways and (3) conduit porosity cavernous vugs.

Tropical Fruit Industry

According to the 2007 Census of Agriculture, Miami-Dade County has about 27,134 ha of agricultural land distributed among 2,498 agricultural producers where subtropical and tropical fruit production is estimated to cover about 4,600 ha with a crop valued at $35.8 million/yr (2002

crop value; 2007 crop value unavailable). Eighty-eight percent of these fruit crops are located in the Redlands of Miami-Dade County (Minkowski and Schaffer, 2001), an area of 18,080 ha (Figure 1-3 and 1-6). Agricultural land use encompasses 14,265 ha of this area representing 36.5% of all agriculture in Miami-Dade County. Minkowski and Schaffer (2001) reported that 91% of Miami-Dade County's fruit groves are located in Krome soils (Figure 1-6).

Lychee (Litchi chinensis)

Lychee (Litchi chinensis) was introduced in Florida in the 1880s and gained importance as a commercial crop in the 1940s. The two main varieties in South Florida are Brewster and Mauritius. It is a polyaxial species with synchronous growth pattern characterized by alternating root and shoot growth and vegetative reproductive growth separated in time (Crane, 2008). The two environmental factors that mainly influence the potential to flower are ambient temperature and available soil water content. However, the most dominant factor to induce consistent flowering is cool non-freezing temperatures. Studies in South Florida have concluded that around 390 hrs of non-freezing temperatures below 15.5 °C correspond to the best crop yield potential (Crane et al., 2004).

Vegetative flush usually occurs between June and October. Root flush is characterized by two cycles, the first cycle occurs between February and May and the second cycle is simultaneous to the vegetative flush (June to October). Flower bud development begins in November and peaks in January and fruit set occurs between December and March peaking in February. The crop's season is from March to June in the case that anthesis is successfully initiated after the quiescence induced by non-freezing temperatures. Critical periods to restrict irrigation in South Florida are from October to February to limit vegetative flush. Generally,

drought stress synchronizes the vegetative shoots dormancy and influences on flowering increase as long as the plant has been exposed to cold temperatures.

As many of the tropical crops in South Florida Krome soils, lychees are planted in trenches. They are typically planted at a density of 286 trees/ha. Crane et al. (1994) indicates that growers have found it beneficial to create these soil filled trenches to about 0.6 m deep in the bedrock beneath the rock plowed surface layer to resist greater winds during the hurricane season and to increase the root development (Figure 1-7). Fruit trees grown in trenched environments in South Florida develop a root system that is characterized by deep roots in a localized area within the trench and a "pancake" superficial root layer that interconnects (over time) with the rest of the trees planted in the orchard (Crane, 2008). The stress physiology caused by the root growth restriction provides stimulus to produce more carbon and biomass and therefore a better yield (Schaffer, 2008).

Research Objectives

Employing these concepts to interpret and predict the shallow groundwater contribution due to capillary movement on soil water content in the unsaturated zone will provide some understand and realistic benefits and challenges posed by potential changes in groundwater levels considering the hydro-geological conditions in the area. This research was focused into three objectives:

- To develop an onsite capacitance sensor calibration equation for limestone bedrock by comparing readings of scaled frequency to soil water suction readings of tensiometers.
- To determine the existence, location and statistical significance of diurnal peaks in soil water content and groundwater level.
- To test the validity of the drain to equilibrium hydrostatic assumptions for predicting the soil water content using groundwater level as a reference.

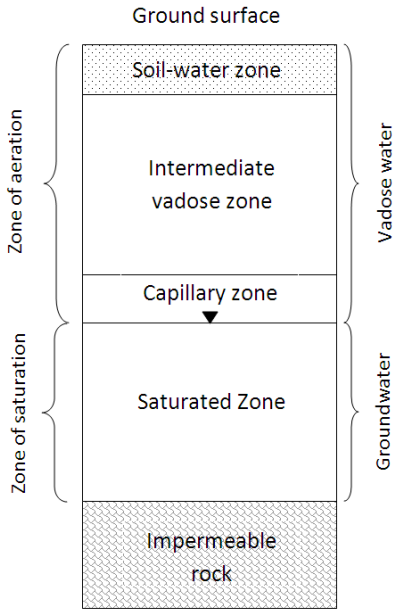

Figure 1-1. Divisions of subsurface water (Todd, 1959).

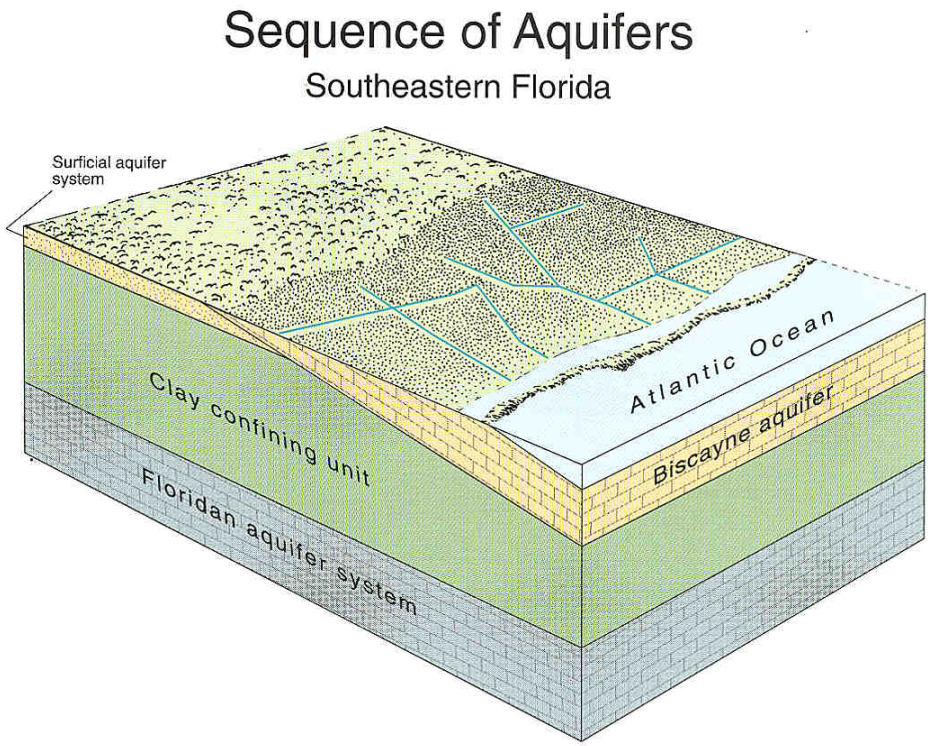

Figure 1-2. Southeastern Florida aquifer allocation from the Water Resources Atlas of Florida (Fernald et al., 1998).

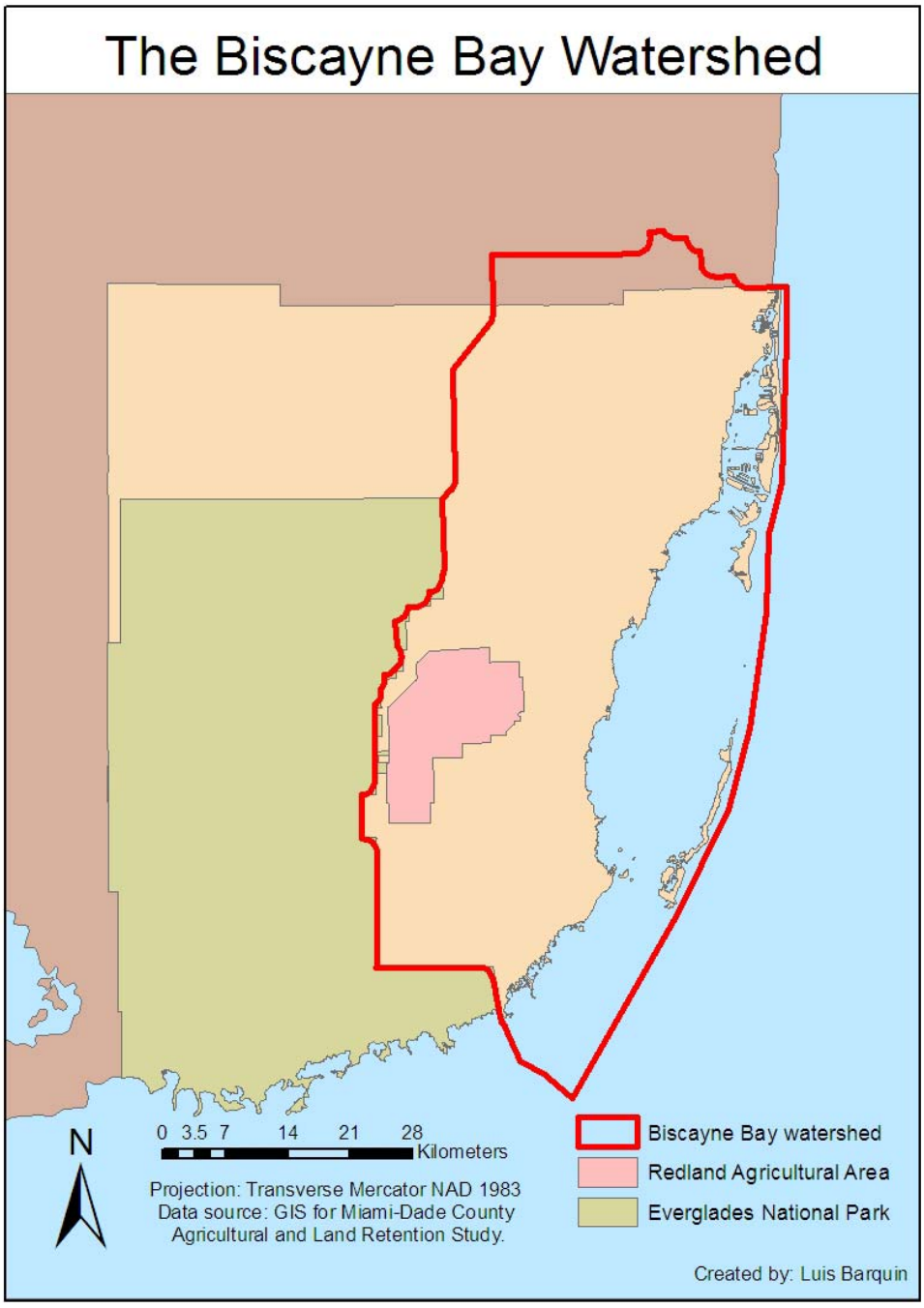

Figure 1-3. General view of the Biscayne Bay Watershed, South Florida.

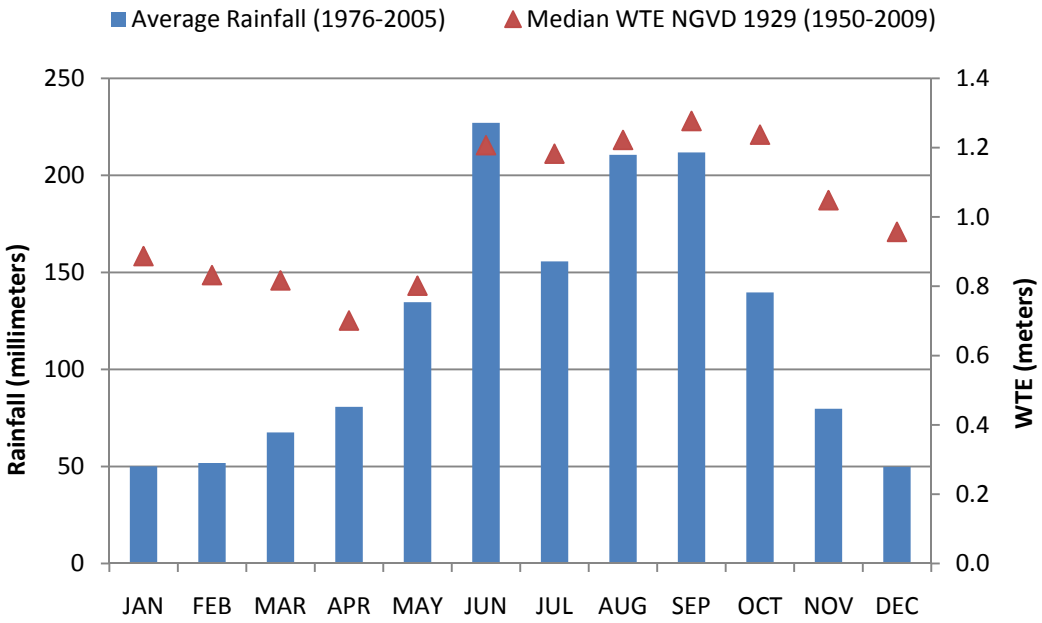

Figure 1-4. South Florida Water Management District (1976-2005) monthly average rainfall of Miami-Dade County and US Geological Survey (1950-2009) monthly median water table elevation WTE NGVD1929 of Well 196A at UF-TREC Homestead, Florida. (SFWMD, 2009; USGS, 2009).

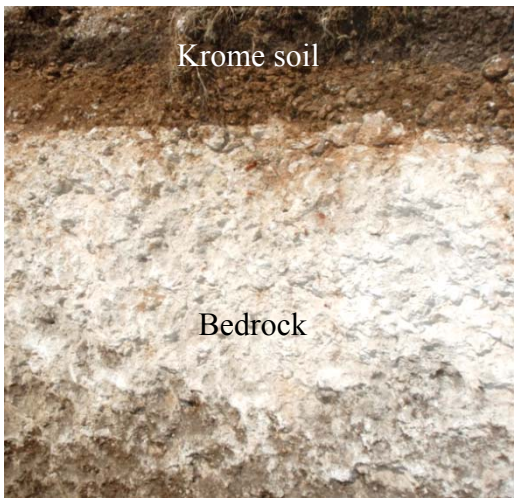

Figure 1-5. Krome soil typical profile consisting of a scarified layer of Krome soil (15 cm) and underlying permeable layer of limestone bedrock.

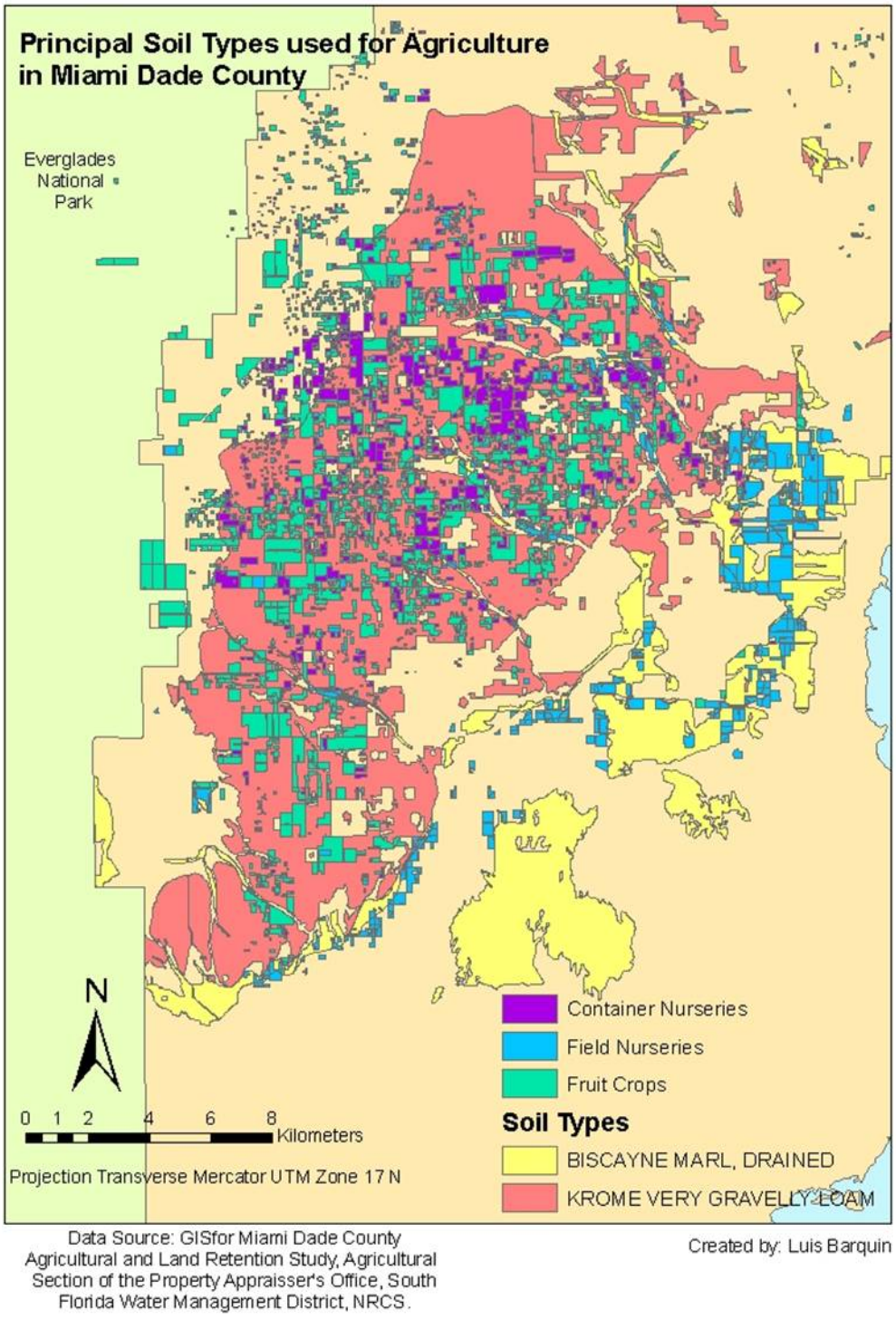

Figure 1-6. Classification of the principal soil types and principal agricultural land use in the study area of South Miami-Dade County, FL.

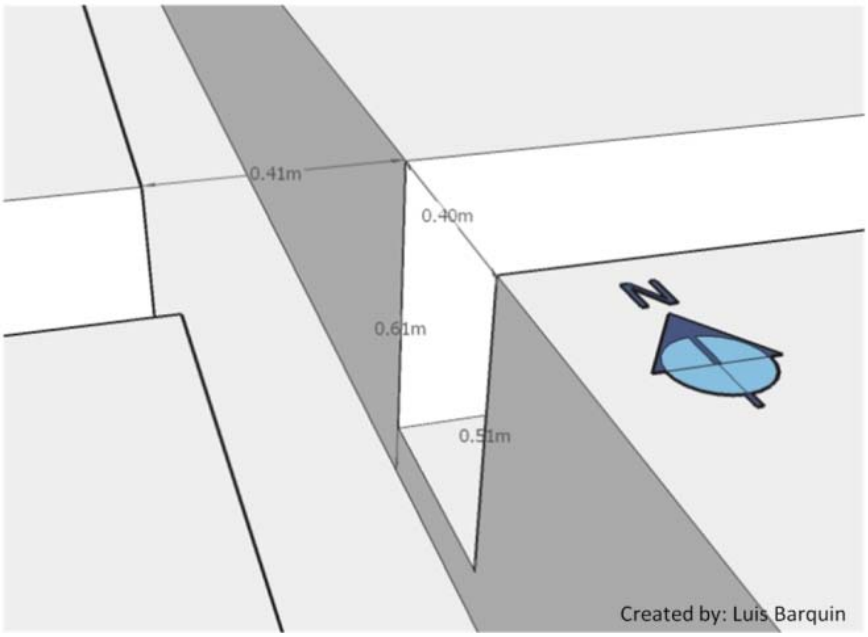

Figure 1-7. Dimension of trenches for tropical crops in Krome soils of Miami-Dade County.

CHAPTER 2
NON DESTRUCTIVE ONSITE CALIBRATION OF MULTISENSOR CAPACITANCE PROBES IN A LIMESTONE BEDROCK PROFILE

Introduction

Soil water content monitoring based on electromagnetism generally use the soil medium as a circuit component. This type of method is based on the dielectric constant of the soil and relates the apparent dielectric constant of the soil-air-water mixture and the volumetric water content at different electromagnetic field frequencies. This concept is employed in capacitance sensors, where the dielectric constant of the soil is used to measure the soil volumetric water content considering the soil matrix around the sensor as part of the capacitor system (Gardner et al., 1998).

EnviroSCAN multi sensor capacitance probes (Sentek Ltd. Pty., Stepney, Australia) are commonly used in soil water content monitoring; the system is detailed in Paltineanu and Starr (1997). Each capacitance sensor consists of two brass cylindrical rings that function as electrodes (Fares and Alva, 2000). EnviroSCAN operates using a high frequency range (150 Mhz) which minimizes sensitivity to changes in salinity or temperature. Sensors are capable of measuring volumetric water content values ranging from a saturated soil to almost oven dry soil with a resolution of 0.1% (Buss, 1993). However, the multi sensor capacitance system requires soil specific calibration to produce accurate estimates of soil water content due to large variability in soils.

The calibration consists of a relationship between volumetric water content and scaled frequency of a sensor usually determined by regression analysis using a sample dataset. Depending on the nature of the soil, the manufacturer recommends two calibration procedures to obtain the absolute values of volumetric soil water content: field calibration and laboratory calibration. Laboratory calibration procedures require the extraction of samples in containers to

track the scaled frequency readings at specific volumetric water contents; Paltineanu and Starr (1997) and Mead et al. (1995) describe in detail this method. Field calibration procedures are site specific calibrations described in detail by Morgan et al. (1999) and Polyakov et al. (2005) and can be destructive and laborious. Accurate field calibrations usually require minimizing the uncertainty of soil bulk density and volumetric water content sampling using sub sampling techniques. The relationship between soil water content and scaled frequency can be developed by collecting a soil sample for a range of scaled frequency values. These samples would be analyzed for bulk density and water content and then results would lead to development of a site specific calibration curve.

South Florida (specifically, Miami-Dade County) is characterized by very unique, complex calcareous soils that are derived from limestone. A dominant soil type in Miami-Dade County's agricultural area is Krome soil. Krome soils are loamy skeletal, carbonatic, hyperthermic Lithic Udorethents (Noble et al., 1996) made of rock plowed oolitic limestone. A Krome soil's typical profile is composed by a scarified layer (15 cm) of very gravelly loam texture and an underlying layer of limestone bedrock (Li, 2001). The available information on the properties of the limestone bedrock layer is focused on the hydro geological characterization of the Biscayne aquifer (Klein and Hull, 1978; Fish and Stewart, 1991; Chin, 2005; Cunningham et al., 2004, 2006) and the material's geotechnical properties (Saxena, 1982) since most of the soil analysis standard methods of physical properties are difficult to be applied and the material is not considered for agronomical functions. Al-Yahyai et al. (2006) developed a capacitance sensor calibration equation for the scarified layer of Krome soil using the laboratory method. However the relationship of volumetric water content and scaled frequency of limestone bedrock has not been calibrated for this equipment. Thus, an additional calibration equation for limestone

bedrock is needed to relate EnviroSCAN measurements to volumetric water content at depths greater than 15 cm in a Krome soil profile.

Determination of calibration equations that predict soil water content based on EnviroSCAN measurements require non-traditional methods when the media (i.e., bedrock) is not a loose soil or when it is difficult to maintain structural characteristics when the media is transported to a laboratory for analysis. For these types of circumstances, the development of procedures to calibrate sensors without removing significant amounts of media is needed. Jabro et al. (2005) developed on site calibration procedures of EnviroSCAN capacitance sensors by comparing readings of scaled frequencies with soil water content of neutron probes that had been calibrated using the gravimetric method. The approach of capacitance sensor calibration using a different soil water monitoring technology can be applied in limestone conditions.

The main goal of this study was to develop a calibration equation for limestone bedrock by comparing readings of scaled frequency to another soil water monitoring technology. The analysis was conducted in four steps: (1) equipment installation and data collection, (2) development of soil water characteristic curves of Krome soil scarified and limestone bedrock layer in laboratory conditions, (3) conversion of suction values from tensiometers to volumetric water content using the laboratory soil water characteristic curves of limestone bedrock and (4) onsite calibration of capacitance sensors in limestone by comparing tensiometers values to those of capacitance sensors.

Materials and Methods

Equipment and Data Collection

The experiment was conducted at the University of Florida (UF) Tropical Research and Education Center (TREC), Homestead, Florida. Data were collected from two sites of limestone bedrock. Data from site 1 was collected from 16 September to 4 December 2008 and from site 2

from 22 January to 23 March 2009. Each site was equipped with two EnviroSCAN multi sensor capacitance probes (Sentek Ltd. Pty., Stepney, Australia) and five automated recording remote sensing tensiometer units (RSU model, Irrometer Co. ®, Riverside, CA, USA). Sensors were localized at 20 and 40 cm depths on each EnviroSCAN capacitance probe. RSU tensiometers were installed so that porous tips were located at similar depths: 20 cm (2 RSU units) and 40 cm depth (3 RSU units) (Figure 2-1). Equipment was programmed to collect data every 15 minutes; data collected was categorized by depth and site and then summarized to daily means to avoid lag response between scaled frequencies and suction. It was assumed that suction values at 20 cm of depth and scaled frequency values at 20 cm depth were comparable. Likewise, suction values at 40 cm depth and scaled frequency values at 40 cm were paired. Site 1 and site 2 could not be statistically compared because data collection occurred during different time periods. However, relationships among calibration equations permitted the comparison of similarities in sites and depths.

Development of Soil Water Characteristic Curves of Krome Soil Scarified and Limestone Bedrock Layer in Laboratory Conditions

Soil water characteristic curves for the complete Krome soil profile were analyzed with Tempe cells using a laboratory soil water retention procedure (Klute, 1986). A total of five core samples were collected to characterize the complete soil profile. Cores were organized into two categories: the Krome scarified layer and the limestone bedrock layer. Two core samples from Krome scarified layer were analyzed to compare with the current soil water characteristic curve reported in literature for this soil type (Al-Yahyai, 2006). Three core samples from the limestone bedrock were analyzed as part of the onsite capacitance calibration equation procedure.

The two samples of Krome scarified layer were not used for calibration purposes but to characterize the complete soil profile. One of the samples was collected as an undisturbed core

and the other sample was separated into two subsamples. Using a 2 mm sieve (mesh #10), one core contained the loam fraction (< 2 mm) and the other contained the gravel fraction of the soil (>2 mm). The gravel and loam fractions were separated considering previous findings that suggest that coarse particles also contribute to the water holding capacity (Coile, 1953; Berger, 1976; Hanson and Blevins, 1979).

Cores of limestone bedrock were extracted near each experimental site at 40 and 60 cm of depth using an auger, a hammer and a chisel. The cores were shaped according to the Tempe cell's dimensions (10 cm diameter and 10 cm length) using an emery wheel. The dimensions of the cores used in this Tempe cells experiment are greater than the standard cores normally used in this type of analysis. These cores are designed for soils with gravel fractions greater than 2 mm, hence core sizes were greater than typical Tempe cell equipment.

Sample preparation included saturation with 0.005 M $CaSO_4$ and Thymol solution for 30 days, securing samples in Tempe cell apparatus and draining cells at atmospheric pressure for 2 days, weighing samples at field capacity and gradually applying increasing pressure while measuring water volumes draining from each Tempe cell. Ten pressure steps were used (i.e., 15, 25, 35, 55, 105, 255, 505, 755, 930, and 980 cm H_2O). Pressure steps did not include the first low pressure phase (<15 cm H_2O) were soil water is governed by macro pores and drainage which reflects the first step of soil water depletion due to our interest in hydrostatic or drained to equilibrium conditions. Tempe cell laboratory soil water retention procedure is explained in detail by Klute (1986). Volumes of water depleted were used to characterize water release curves and fitting parameters were calculated using van Genuchten's (1980) for the soil water suction range previously described:

$$\theta = \theta_r + \frac{(\theta_s - \theta_r)}{\left[1 + (\alpha h)^n\right]^m} \tag{2-1}$$

where θ is the volumetric water content; h is the applied pressure head; θ_s and θ_r represent the saturated and residual soil water contents, respectively; and α, n and m are empirical shape parameters. The fitting parameters for all curves were estimated with the RETC program by van Genuchten et al. (1991). For a more holistic relationship, the data collected for all limestone cores was used to generate a general limestone release curve representative of the site.

Conversion of Suction Values from Tensiometers to Volumetric Water Content Using the Laboratory Soil Water Characteristic Curves of Limestone Bedrock

Data from both instruments was summarized to daily means to avoid differences of time response between tensiometers (Towner, 1980) and capacitance sensors (Buss, 1993). Soil water characteristic curves for limestone bedrock were used to relate soil matric potential (suction) values recorded by the RSU tensiometers to volumetric water content. Using van Genuchten's Equation 2-1 with the respective parameters for limestone, daily mean records of volumetric water content from RSU tensiometers were paired with simultaneous daily mean records of scaled frequency from the capacitance sensors.

Onsite Calibration of Capacitance Sensors in Undisturbed Limestone by Comparing Tensiometers Values to Those of Capacitance Sensors

EnviroSCAN scaled frequency values were normalized considering the frequencies of air and water. The following equation described by Paltineanu and Starr (1997) was used to convert field frequencies into scaled frequency (*SF*):

$$SF = \frac{\left(F_A - F_S\right)}{\left(F_A - F_W\right)} \tag{2-2}$$

where F_A is the frequency reading in air, F_W is the reading in water and F_S are the subsequent readings of the soil water content.

The relationship of scaled frequency and volumetric water content was evaluated as:

$$SF = A\theta^B + C \tag{2-3}$$

where θ is the volumetric water content (independent variable) and A, B, and C are the regression fitted parameters (Paltineanu and Starr, 1997). Data collected from capacitance sensors and RSU tensiometers was used to determine the fitted parameters (A, B, C) at each site (site 1 and site 2) and depth (20 and 40 cm) combination. Resulting parameter sets for each site-depth combination were used to predict soil water content based on scaled frequency.

$$\theta = \left(\frac{SF - C}{A} \right)^{1/B} \tag{2-4}$$

Limestone calibration equations were compared to the calibration equation for Krome soils (Al-Yahyai et al., 2006) using correlation analysis.

Results and Discussion

Development of Soil Water Characteristic Curves of Krome Soil Scarified and Limestone Bedrock Layer in Laboratory Conditions

Scarified Krome soil

Soil physical properties and results from the Tempe pressure cell study of gravel and loam subsamples are summarized in Table 2-1. Four soil water characteristic curves shown in Figure 2-2 represent the Krome scarified layer. As depicted in Figure 2-2, the sieved loam portion of the Krome scarified layer had the greatest water retention characteristics. This was expected due to the small particle size of the loam fraction. The gravel fraction of the soil sample in this study constituted 36% of the total volume compared to 51% which was reported by Al-Yahyai et al. (2006). The effective porosity and bulk density also differed between Al-Yahyai et al. (2006) and that collected in this study. Soil water characteristic curves in Figure 2-2 depict volumetric water content depletion in the first 100 cm of pressure head for the sieved loam, while the gravel remained at relatively constant volumetric water content from 15 to 1,000 cm of pressure. Thus, the drainage of soil water contained in the macro pores of gravel was not captured in the pressure

steps studied. Since the application of study results will be for evaluation of hydrostatic conditions, macro pore gravity drainage characterization of the limestone is not required.

Results for the core soil water characteristic curve of Krome scarified layer suggest its retention properties are between the partitioned loam and the gravel fractions. The Al-Yahyai et al. (2006) soil water characteristic curve and the Krome scarified soil water characteristic curve from our study were similar. However, some differences were observed which could be attributed to the greater loam content of our samples (64%) compared to Al- Yahyai et al. (2006) (51%). Thus, water retention characteristics of our soil allowed for greater volumetric water contents at greater suctions and field capacity is primarily dependent upon the proportion of the soil that is in the loam fraction.

Limestone bedrock

Physical properties and soil water characteristic curves for the limestone bedrock cores are presented in Figure 2-3. Results indicated that effective porosity of the limestone bedrock was approximately 0.25. The three cores had an average bulk density of 1.4 g/cm^3, similar to the range reported by Saxena (1982) of 1.31 and 1.64 g/cm^3. The van Genuchten inflection point parameter for limestone was lower than that for the Krome scarified sample (θ_{inf} = 0.20 limestone; θ_{inf} = 0.30 Krome). It is important to consider the excessive volume of water drained between the saturation of thymol and the phase of equilibrium saturated content (zero suction). Macro porosity is not considered in the effective porosity (Table 2-2) and it is not included in determining water holding capabilities.

As a result, we can conclude that the limestone bedrock has in general very low saturated water content and a characteristic of low volumetric water content changes to large changes in matric potential (suction) increments. This feature was previously described by Muñoz-Carpena et al. (2002) for the scarified Krome soil and now is confirmed in the underlying limestone

bedrock as well. The results also indicate that the soil water characteristic of the gravel fraction in Krome scarified layer was similar to the soil water characteristic of the limestone bedrock layer.

All the limestone data were pooled to create a general limestone curve ($r^2 = 0.38$) for onsite EnviroSCAN calibration purposes. The low coefficient of determination suggests that there was heterogeneity in the structure of the limestone profile not only in depth but also in terms of horizontal variability, adding a level of complexity and uncertainty to measuring, predicting and modeling soil water conditions in this region.

Characterizing the Krome soil profile

Physical properties and Tempe pressure cell results are summarized in Table 2-3. The limestone (all) ($r^2 = 0.38$) and the Krome scarified layer cores ($r^2 = 0.99$) were found to have different soil water retention properties and therefore water management properties. If we consider the field capacity of a soil as 100 cm of suction, the Krome scarified layer's field capacity is approximately 0.27 and at the same suction the volumetric water content of the limestone is 0.22. In addition, at 1,000 cm of pressure the Krome soil water content decreases to 60% while a similar pressure change in limestone results in 20% reduction in water content. The Krome soil scarified layer retains up to 9% and limestone only retains 1.7% of volumetric water content between the field capacity (100 cm of suction) and the effective saturated water content. Models for all individual curves (Tables 2-1, 2-2 and 2-3) had in general good fits with measured data ($r^2 > 0.9$) with the exception of the limestone (all) model ($r^2 = 0.38$). The limestone (all) model is considered an overall fit that includes the diverse porosities found in the study.

Conversion of Suction Values from Tensiometers to Volumetric Water Content Using the Laboratory Soil Water Characteristic Curves of Limestone

The soil water characteristic from limestone (all) curve ($r^2 > 0.38$; Table 2-2) was used to convert the measured suction of the RSU tensiometers to volumetric water content. Suction (h) measured by the RSU tensiometers and the fitted parameters α (0.00779), n (1.05816), m (0.05496), θ_s (0.2371) and θ_r (0.0) in the Van Genuchten's Equation (2-1) were used to estimate the volumetric water content regression with scaled frequency.

Estimating Onsite Calibration of Capacitance Sensors in Undisturbed Limestone by Comparing Tensiometers Values to Those of Capacitance Sensors

Calibration equations for each site and depth were developed by comparing the capacitance sensor's readings (SF) with the converted soil water contents from the RSU tensiometers. Calibration equations are presented in Figures 2-4 to 2-7 and equation coefficients are summarized in Table 2-4. All calibrations were linear regressions (B = 1). Measured scaled frequency from the capacitance sensors and measured suction from the RSU tensiometers resulted in good fits ($r^2 > 0.70$; Table 2-4). However, when all data was combined a general relationship could not be defined (Figure 2-8).

The non-destructive site specific calibration of the scaled frequency values provided a good site and depth specific relationship between the EnviroSCAN observations and the simultaneous RSU suctions (converted to volumetric water content with the limestone (all) soil water characteristic curve). These results support the idea of using field measurements of other instruments to calibrate sensor readings instead of using more destructive techniques such as field or laboratory calibrations, similar to the methods proposed by Jabro et al. (2005) for calibrating neutron probes. However, the site specific calibration required in limestone conditions makes it unpractical and similar to the field calibration recommended by the manufacturer. Comparison of calibration results between the new limestone regressions and the

calibration regression used by Al-Yahyai et al. (2006) was evaluated by converting the scaled frequencies from capacitance sensors to volumetric water content using the new coefficients (Table 2-4) and the typical coefficients from Al-Yahyai et al. (2006) (A = 0.011, B = 1, C = 0.5206) at equilibrium conditions (no rainfall or irrigation).

Results for the calibration regression from site 1 at 40 cm depth from September to December 2008 are plotted in Figure 2-4 ($r^2 = 0.96$). Relationship of the new calibration equation with the Al-Yahyai et al. (2006) calibration equation at equilibrium conditions was strong ($r^2 = 0.960$). The regression equation for site 2 at 40 cm depth considering data from January to March 2009 ($r^2 = 0.70$) (Figure 2-5) relation with Al-Yahyai et al. (2006) calibration equation resulted in a lower coefficient of determination of ($r^2 = 0.51$). The deviation between the methods is further observed in storm or irrigation observations, where the Al-Yahyai et al. (2006) equation showed a greater response to volumetric water content increase. Limestone low response to storm events is due to low water holding capacity expressed in parameters shown in Table 2-3 and Figure 2-3.

Regression analysis of scaled frequency and volumetric water content at site 2 ($r^2 = 0.96$) indicated a better fit than site 1 ($r^2 = 0.74$) at the 60 cm depth (Figures 2-6 and 2-7). The lower coefficient of determination for Site 1 was due to a parallel scatter attributed to site heterogeneity and instrument uncertainty. Comparisons of the new calibration equations at 60 cm depth with the Al-Yahyai et al. (2006) calibration equation (Figures 2-7) are presented in Table 2-5 and indicate there is a relatively similar degree of correlation for site 1 ($r^2 = 0.82$) and site 2 ($r^2 = 0.83$) with Al-Yahyai et al. (2006).

If all graphs are combined, similarities and differences of the resulting regression models and respective data for each case are evident (Figure 2-8). Results suggest that horizontal

variability influences volumetric water content more than depth. The four site specific limestone regression models are characterized by different slopes. The site specific calibration regressions and the Al-Yahyai et al. (2006) model are presented in Figure 2-9. It is clear that all of our regression models have a greater slope compared to the Al-Yahyai et al. (2006) model.

Results indicated that large changes in scaled frequencies correlate with small changes in volumetric water content. This relationship was derived from the conversion of field suction using the laboratory experiments which observed small changes in volumetric water content with large changes in soil water suction. Finally, despite the valuable and important relationships found with this technique, in general a small range of volumetric water content (range of $\theta < 0.01$) was measured (Figures 2-4 to 2-7). A primary difference between the limestone soil water characteristic curve and the curve presented by Al-Yahyai et al. (2006) is their response to water inputs. For purposes of equilibrium conditions, the volumetric water content values seem to be similar.

Conclusion

The soil water characteristic of a Krome soil profile was evaluated using pressure Tempe cells. The results of the experiment suggest that most of the water holding capacity of the soil is due to the loam fraction. The difference in volumetric water content of the Krome scarified layer at effective saturation and volumetric water content at 1,000 cm of suction was 40%. The gravel fraction of Krome scarified soil had a similar soil water characteristic to that of limestone bedrock. The difference in volumetric water content at limestone effective saturation and volumetric water content at 1,000 cm of suction was 20%.

EnviroSCAN field calibration using suction from tensiometers as a reference to determine volumetric water content is a site specific technique for conditions where standard calibration procedures are not possible and soil structure is uniform. The regression equations were different

for all sites and depths but confirmed the dominance of spatial variability over depth variability. Thus, four site specific regression models for limestone bedrock are proposed. Similarities between the calibration equation from Al-Yahyai et al. (2006) Krome and the proposed limestone calibration equation were strong during soil water equilibrium conditions while differences were observed during periods of rainfall or irrigation.

Table 2-1. Soil physical properties and fitted parameters of van Genucthen's model (1980) used to describe laboratory soil water characteristics of a scarified Krome soil partitioned into its gravel and loam fraction.

Parameter	Sieved gravel	Sieved loam
α	0.01473	0.02979
n	1.05522	1.71126
m	0.05233	0.41564
θ_s	0.23264	0.56603
θ_r	0.00000	0.18313
r^2	0.970	0.990
Effective Porosity	0.248	0.528
Bulk Density (g/cm^3)	2.062	0.907

Table 2-2. Soil physical properties and fitted parameters of van Genucthen's model (1980) used to describe laboratory soil water characteristics of the underlying limestone bedrock layer of a typical Krome soil profile using three rock samples, sieved gravel and data from all samples.

Parameter	Limestone(all)	Limestone 1	Limestone 2	Limestone 3	Sieved gravel
α	0.00779	0.01060	0.00027	0.00744	0.015
n	1.05816	1.09145	1.23822	1.05346	1.055
m	0.05496	0.08379	0.19239	0.05075	0.052
θ_s	0.23712	0.24331	0.28184	0.19149	0.233
θ_r	0.00000	0.00000	0.00000	0.00000	0.000
r^2	0.380	0.950	0.970	0.980	0.970
Effective Porosity	0.244	0.253	0.284	0.192	0.248
Bulk Density (g/cm^3)	1.524	1.469	1.449	1.117	2.062

Table 2-3. Soil physical properties and fitted parameters of van Genucthen's model (1980) used to describe laboratory soil water characteristic of the limestone and the scarified layer of a Krome soil profile. Al-Yahyai et al. (2006) Krome scarified layer characterization is shown for comparison.

Parameter	Limestone (all)	Krome	Al-Yahyai (2004)
α	0.00779	0.02419	0.09000
n	1.05816	1.76556	1.46000
m	0.05496	0.43361	0.31507
θ_s	0.23712	0.36580	0.47000
θ_r	0.00000	0.19487	0.10000
r^2	0.380	0.990	0.930
Effective Porosity	0.244	0.350	0.470
Bulk Density (g/cm^3)	1.524	1.271	1.400

Table 2-4. EnviroSCAN onsite calibration equation coefficients for limestone bedrock from sites 1 and 2 at 40 and 60 cm depths. Regression parameters are result from the relationship between scaled frequency from capacitance sensors and suction from tensiometers converted to volumetric water.

Site	Period	Depth	A	B	C	r^2
1	Sep to Dec	40	3.4857	1	0.0039	0.96
1	Sep to Dec	60	5.5125	1	-0.4049	0.74
2	Jan to Mar	40	6.0519	1	-0.6362	0.70
2	Jan to Mar	60	2.2536	1	0.2343	0.96

Table 2-5. Correlation of capacitance sensor scaled frequencies calibrated using Al-Yahyai et al. (2006) Krome coefficients and onsite calibration coefficients proposed for each site and depth. Dataset includes only volumetric water content in state of equilibrium.

Site	Period	Depth	r^2
1	Sep to Dec	40	0.96
1	Sep to Dec	60	0.82
2	Jan to Mar	40	0.51
2	Jan to Mar	60	0.83

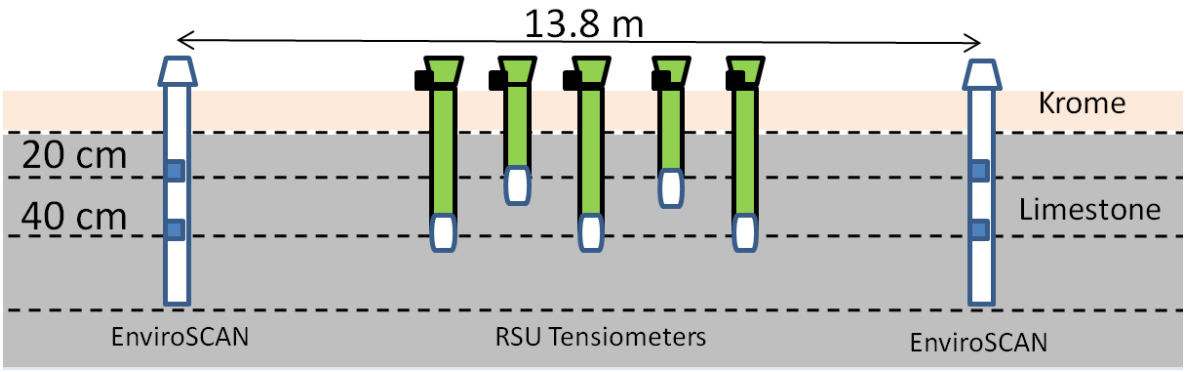

Figure 2-1. Schematic diagram of EnviroSCAN and RSU tensiometers installed at each site. Two EnviroSCAN probes with sensors at 20 and 40 cm and five RSU tensiometers installed at 20 cm (2 units) and 40 cm (3 units).

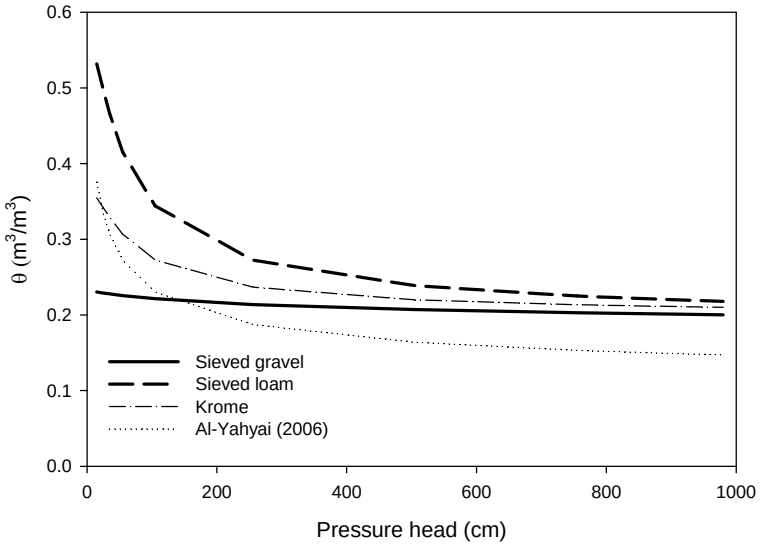

Figure 2-2. Laboratory soil water characteristic curves of Krome scarified layer. Samples with the partitioned gravel and loam fraction are compared to a sample without sieve and Al-Yahyai et al. (2006) characterization. The suction and soil water content were determined with pressure Tempe cells and fitted with van Genuchten (1980) model.

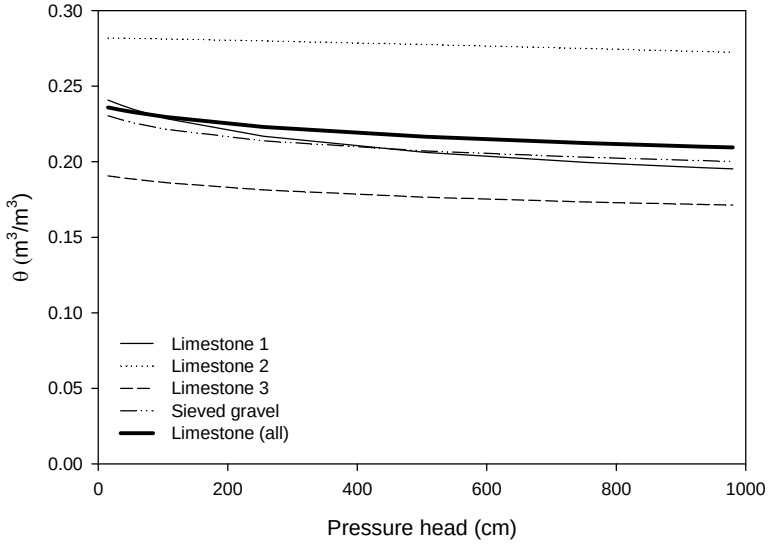

Figure 2-3. Laboratory soil water characteristic curves of limestone bedrock layer. A general curve Limestone (all) was fitted from three limestone samples and compared to the sieved gravel from Krome. The suction and soil water content were determined with pressure Tempe cells and fitted with van Genuchten (1980) model.

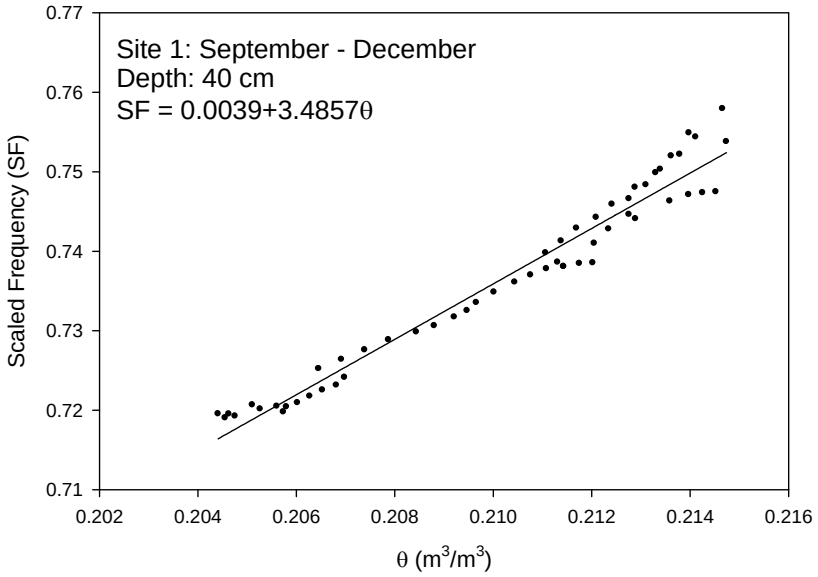

Figure 2-4. EnviroSCAN capacitance sensor onsite calibration of limestone bedrock from site 1 at 40 cm depth. Scaled frequency (SF) was determined by EnviroSCAN and volumetric water content (θ) was derived from suction observations of RSU tensiometers.

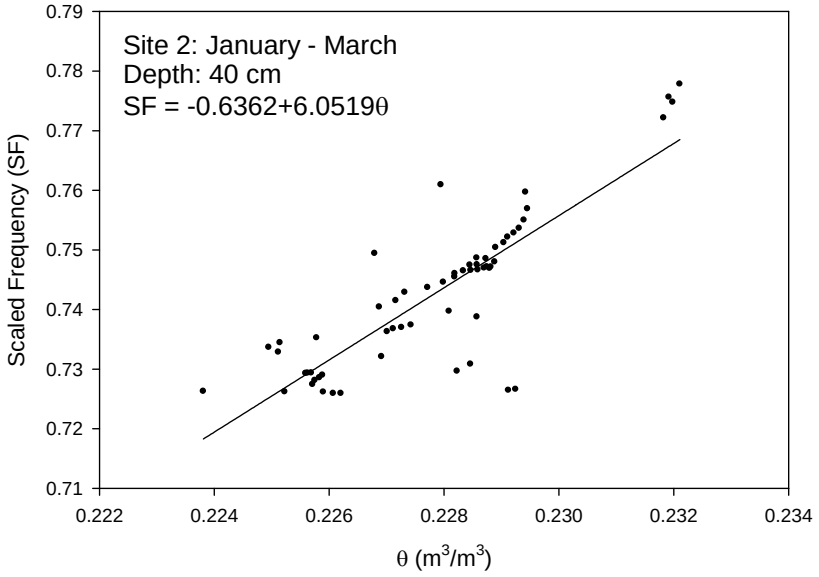

Figure 2-5. EnviroSCAN capacitance sensor onsite calibration of limestone bedrock from site 2 at 40 cm depth. Scaled frequency (SF) was determined by EnviroSCAN and volumetric water content (θ) was derived from suction observations of RSU tensiometers.

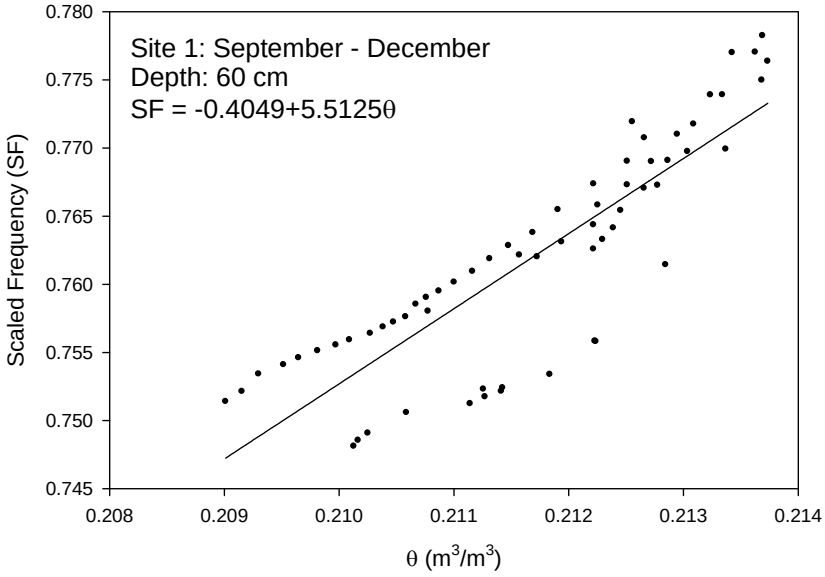

Figure 2-6. EnviroSCAN capacitance sensor onsite calibration of limestone bedrock from site 1 at 60 cm depth. Scaled frequency (SF) was determined by EnviroSCAN and volumetric water content (θ) was derived from suction observations of RSU tensiometers.

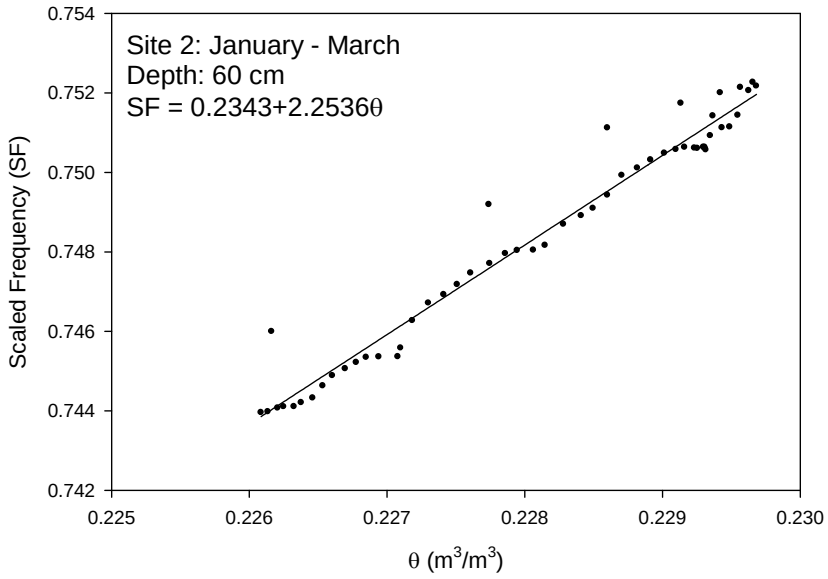

Figure 2-7. EnviroSCAN capacitance sensor onsite calibration of limestone bedrock from site 2 at 60 cm depth. Scaled frequency (SF) was determined by EnviroSCAN and volumetric water content (θ) derived from suction observations of RSU tensiometers.

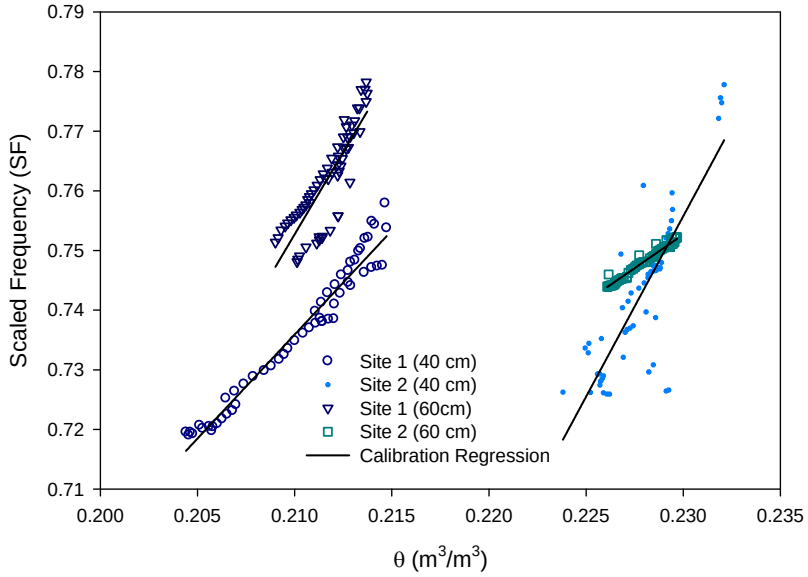

Figure 2-8. Comparison site specific EnviroSCAN capacitance sensor onsite calibrations of limestone bedrock from sites 1 and 2 at 40 and 60 cm depths. Scaled frequency (SF) was determined by EnviroSCAN and volumetric water content (θ) was derived from suction observations of RSU tensiometers.

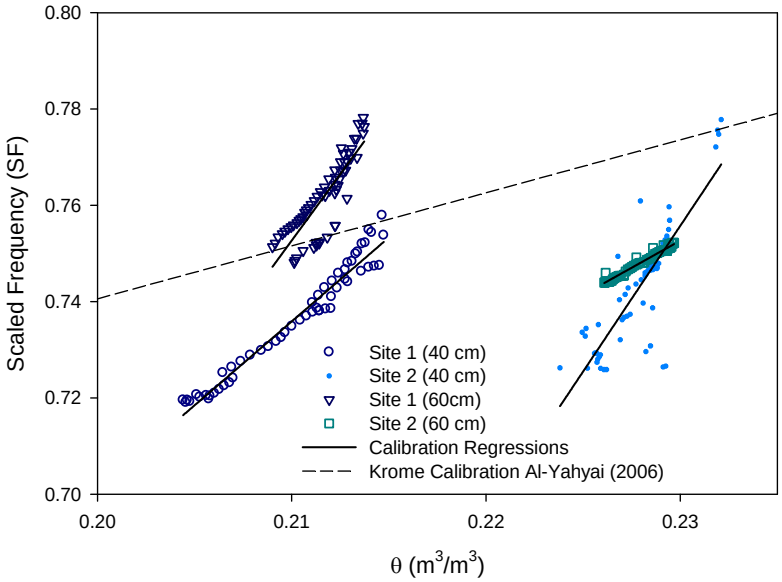

Figure 2-9. Comparison of site specific EnviroSCAN capacitance sensor onsite calibrations of limestone bedrock from sites 1 and 2 at 40 and 60 cm depths with Al-Yahyai et al. (2006) calibration of Krome soil. Limestone scaled frequency (SF) was determined by EnviroSCAN and limestone volumetric water content (θ) derived from suction observations of RSU tensiometers.

CHAPTER 3
USING CIRCULAR STATISTICS TO IDENTIFY CAPILLARY RISE DIURNAL FLUCTUATIONS IN CALCAREOUS SOILS

Introduction

Southeast Florida Biscayne aquifer is an unconfined coastal aquifer with a shallow layer of highly permeable limestone that covers an area of 10,360 km^2 including portions of Broward County, Miami-Dade County, Monroe County and Palm Beach County (Fish and Stewart, 1991). Biscayne aquifer characteristics of unconfinement, high permeability and shallow depth result in water table fluctuations that are fairly responsive to storm events and canal system management (Pitt, 1976; Ritter and Muñoz-Carpena, 2006).

Due to its shallow nature, the groundwater is subject to upward movement due to capillary forces into the unsaturated zone of the soil profile. The potential contribution of groundwater to unsaturated soil water content increases as distance to groundwater level decreases (Wellings and Bell, 1982; Raes and Deproost, 2003). As water management goals are adjusted to meet the Comprehensive Everglades Restoration Plan (CERP) objectives, there exists a greater chance of elevated groundwater levels and resulting water movement by capillary forces into overlying unsaturated soil. Given this scenario, characterizing groundwater fluctuations provide information that could be used to evaluate capillary rise in the unsaturated zone.

Anecdotal evidence combined with previous research findings has documented the effect of capillary rise in the agricultural area of South Miami-Dade County. Al-Yahyai et al. (2005) reported a lack of physiological response between irrigated and non irrigated carambola (Averrhoa carambola) grown in Miami-Dade County Krome soil and assumed this result was due to shallow groundwater capillary rise. Additional work characterizing the soil water retention in this orchard described the difficulty in obtaining suction values greater than 125 cm in the field treatments without irrigation (Al-Yahyai et al., 2006). Similarly, Migliaccio et al.

(2008) reported evidence of capillary influences on soil water status. They investigated soil suction in Marl soils of South Florida and identified diurnal patterns during the dry season.

Diurnal fluctuations of groundwater have been documented by several authors around the world. Most of the groundwater hydrology literature suggests diurnal fluctuations are principally induced by three factors: evaporation, barometric pressure and tidal actions.

Evaporation of the water table is a negative recharge and thus an important process to consider during extended periods of no rainfall. Diurnal fluctuations of groundwater caused by daily evaporative cycles were documented by White (1932), Tromble (1977) and Bauer et al. (2004). Merrit (1996) recognized the principal process of water flux from the Biscayne aquifer as evaporation which has a close correlation with solar radiation and consequently a corresponding seasonal variation. This finding was supported by Abtew (1996) confirming solar radiation explains 70% of the variations in South Florida's reference evapotranspiration.

Groundwater fluctuations may also be a due to temperature gradients where soil water moves from warmer to cooler profiles in response to vapor pressure differences. This was originally suggested by Bouyoucos (1915) and developed by Smith (1939) and Taylor (1962). Meyer (1960) also found diurnal fluctuations of shallow groundwater accompanied by capillary rise of soil water induced by temperature changes. South Florida's distribution of mean temperature is strongly related to solar radiation distribution and, in consequence, temperature fluctuations are associated to the evaporative processes (Abtew, 1996).

Pressure change impacts on groundwater levels have also been suggested by several authors. For example Peck (1960) attributed the upward movement of groundwater to the effect of atmospheric pressure on entrapped air in the pore space. Turk (1975), in attempt to explain this phenomenon, attributed the fluctuations to temperature induced atmospheric changes acting

upon the capillary zone. This process was supported by Weeks (1979) who described how changes in barometric pressure generally affect diurnal patterns of groundwater levels. The influence pressure has on water levels was also explained by Rasmussen and Crawford (1997) which described how unconfined aquifers generally experience a unit decrease in water level with unit increase in barometric pressure and vice versa.

Groundwater level can also be influenced by tidal changes in coastal areas (Todd, 1959). Todd (1959) also explained how monitoring wells installed near tidally influenced water bodies could experience periodic fluctuations in water levels. This type of signal is not only observed in sites close to the coast but also in locations like Southeast Florida, where groundwater levels are responsive to canal level changes (Ritter and Munoz-Carpena, 2006).

As a result, several factors are involved in water table daily recharge and decline. The fluxes of water from the groundwater into the unsaturated zone of the local soil profiles are currently uncharacterized and the impact of weather parameters on this process is not understood specifically in Southeast Florida Krome soils.

Characterization of groundwater level fluctuations can be used to assist with interpreting fluctuations in soil water content, particularly in regions with unconfined shallow aquifers (Bouyoucos, 1915; Migliaccio et al., 2008) during hydrostatic conditions (i.e., absence of rainfall or irrigation). The relationship between groundwater level and soil water content during hydrostatic conditions is governed predominantly by capillary forces. However, other factors (previously discussed) may also play a role in this relationship.

Determination of peak occurrence can be used to explain soil water content changes due to daily groundwater fluctuations or to identify other factors that are influencing soil water content. Thus, a useful approach is needed to evaluate diurnal cycles, such as circular statistics. Circular

statistics are methods used to interpret the frequency of occurrence for each daily peak identified in a time series. This method relates the time of the day to a location on the circumference of a circle and data points distributed on a circle are analyzed as directional data. The mean direction or mean vector of a circle (μ) is a measure based on trigonometry using a center of gravity, *C* (Figure 3-1). In this example, three equal masses are represented as vertices of a triangle (representing peak frequencies in a dataset) and the direction of this center of gravity to the origin *O* is the mean direction of the dataset or unit vector. Circular statistical analyses are described in detail by Batschelet (1981). To the author's knowledge, this method has not been previously published in literature to evaluate capillary rise. However, circular statistics have been used to evaluate seasonality and timing variability of flooding (Magilligan and Graber, 1996; Black and Werritty, 1997), meteorology (Hassan et al., 2009) and principally biology and animal behavior (Mennill and Ratcliffe, 2004; Oliveira et al., 1998; Paton et al., 2003; Peach, 2003).

The goal of this study was to determine the existence, location and statistical significance of diurnal peaks in soil water content of Krome soil and groundwater levels. Circular statistics were used to answer these questions and to find a relationship among the directions found in soil water content and groundwater level with weather variables. The specific objectives were to: (1) extract and compile diurnal peaks of soil water contents, groundwater levels and weather variables, (2) perform circular statistical analysis and (3) interpretation of mean vectors.

Materials and Methods

Experimental Site

Diurnal fluctuations of soil water contents, groundwater levels and weather variables were collected in Homestead South Miami-Dade County, Florida, at the University of Florida (UF) Tropical Research and Education Center (TREC) (80.5^0W, 25.5^0N). The site is located 16 km west of Biscayne Bay and 250 m south of the South Florida Water Management District

(SFWMD) Mowry Canal C-103. The mean elevation is 3.12 m National Geodetic Vertical Datum (NGVD) 1929 and is identified by a subtropical, marine climate. The study was conducted in a lychee (Litchi chinensis) orchard. The dominant soil type in the area is Krome soil; classified as loamy skeletal, carbonatic, hyperthermic Lithic Udorethents (Noble et al., 1996) made of rock plowed oolitic limestone. The complete soil profile is composed of a scarified layer (15cm) of very gravelly loam texture and an underlying layer of limestone bedrock. The lychee orchard (as most of the tropical fruit crops in the area) is planted in rock plowed trenches 0.40 m wide and 0.60 m deep filled with scarified Krome soil. The experimental site (as seen in Figure 3-2) consists of six rows: two rows with lychee trees planted in trenches (hence after referred as "lychee trench"), one row without lychee trees but with trenched soil (hence after referred as "trench"), two rows without lychee trees but with surficial roots and no trenched soil (hence after referred as "lychee no trench") and one row without lychee trees roots and without trenches (hence after referred as "no trench"). Each lychee row consists of 12 trees spaced at 4.6 m within row and 7.6 m between rows with a planting density of 286 trees/ha. Data collected from this site represent diurnal fluctuations of a typical tropical fruit orchard in this region.

Equipment and Data Collection

To track soil water content, three data loggers recorded measurements from 24 EnviroSCAN multi sensor capacitance probes (Sentek Ltd. Pty., Stepney, Australia) distributed in the six rows previously described. Each row had four probes installed within 13.8 m and each probe had four sensors positioned at 10, 20, 40 and 60 cm depths (Figure 3-2). The installed system of 96 sensors measured soil water content as a function of the apparent bulk dielectric constant of the soil, imposed frequency and electrode configuration, as described in detail by Paltineanu and Starr (1997). Sensors were programmed to record volumetric water content

values every 15 min at a resolution of 0.1% (Buss, 1993; Fares and Alva, 2000). A sensor normalization procedure was used to determine the scaled frequency (SF). A regression equation for the Krome soil, previously developed by Al-Yahyai et al. (2006), was used to calibrate scaled frequency (*SF*) to volumetric water content (θ). Considering that the 24 probes were installed in the experimental plot for a systematic sampling, six probes were randomly selected to represent 24 of the 96 sensors (Figure 3-2). Thus, six selected probes were used to capture the daily peaks of soil water content per depth. Probe sites were named so that locations in trenches were assigned as "A" and locations outside trenches were assigned as "B". Sensor identification included the probe id and installation depth (e.g., A11-20 corresponds to a sensor at probe A11 located at 20 cm depth).

Groundwater level was measured using Levelogger LT 3001 (Solinst Ltd., Ontario, Canada) pressure transducers. The Leveloggers were suspended and submerged at 3.6 m depth (accuracy = 0.1%, -10^0C to 40^0C) in four monitoring wells located along the perimeter of the study site (Figure 3-2). Groundwater levels were compensated using data collected by Barologger air barometric pressure. Groundwater levels were also adjusted and validated based on weekly manual water table depth readings from each monitoring well. Barometric pressure records from the Barologger were included in the data analysis as part of the weather variables. Additionally, weather records (i.e., solar radiation, relative humidity, temperature) from the Florida Automated Weather Network (FAWN) station located at UF TREC, within 100 m of the site, were used.

Data Extraction and Compilation of Diurnal Peaks

Data were collected every 15 min for soil water content at 10, 20, 40 and 60 cm depths, water table elevation, barometric pressure, relative humidity, solar radiation and soil temperature (Table 3-1). The dataset for each instrument contained 18,144 observations corresponding to189

days from 16 September 2008 to 23 March 2009. The dataset collected was filtered to include only data points that were representative of equilibrium conditions so that potential capillary influences could be evaluated. Thus, data points associated with storm events and freeze protection were removed. The filtering criteria reduced the representative data to 12,480 observations per variable corresponding to 130 days. Each day was summarized according to the time its maximum observed daily value (or peak) occurred. For each daily peak identified in the time series, the corresponding time of day was translated into a location on the circumference of a circle (e.g., 360° corresponds to 0:00 hr). The procedure was repeated for each variable (soil water content, groundwater level, barometric pressure, relative humidity, solar radiation and soil temperature). Data from the 24 soil water sensors were also combined to obtain a mean vector according to the installed depth (i.e., 10, 20, 40 and 60 cm depths). Water table elevation observations from the four wells were also merged to obtain a mean vector of water table elevation. All circular data analyses were performed using the ORIANA software (Kovach, 2009).

Circular Statistical Analysis

Frequencies of occurrence of maximum daily values during the day were interpreted with circular statistics. Temporal measurements were converted to angular measurements to calculate the mean vector length (r).

$$r = \frac{1}{n}\sqrt{\left(\sum_{i=1}^{n}\cos\phi_i\right)^2 + \left(\sum_{i=1}^{n}\sin\phi_i\right)^2} \quad (3\text{-}1)$$

where r is the mean vector length, n is the sample size and Φ are the angular measurements. When events were distributed uniformly during the entire period (i.e., all day) the results for r were close in value to 0. When a significant concentration of events was located at a specific time during the day, values of r were closer to 1. The mean vector length (r) is a useful measure

of data concentration but an additional test was needed to confirm if the mean vector length significantly exceeded the length of a uniform distribution.

The Rayleigh test of significance of the mean vectors was used to test the null hypothesis of uniform distribution (no mean direction) for each of the six variables. This method tested the existence of a significant mean angle or mean direction and consequently the location of a consistent peak during the day. For each rejected null hypothesis, a diurnal peak was statistically confirmed and identified. The Rayleigh test of uniform distribution is calculated through the *z* value of the population:

$$z=nr^2 \tag{3-2}$$

Thus, the greater the mean vector, the larger the value of *z* and the greater the concentration of the observations will be around the mean. If the critical level of *P* from the Rayleigh test of randomness table is less than the assigned alpha level, the null hypothesis is rejected. Significance occurs when $z \geq z(\alpha)$. The statistical significance of *r* was first studied by Lord Rayleigh in 1880 and its statistical applications were developed in detail by Beran (1969) and Greenwood and Durand (1955). One assumption of the circular parametric test (for purposes of comparison) is that the data is random with a von Mises distribution (unimodal). To test the validity of such an assumption with our dataset, the Watson's U test was used to test the null hypothesis of a theoretical unimodal distribution for each dataset.

Frequencies of daily peak data were summarized in circular histograms showing the number of cumulative maximum values observed at each hour of the day during the study period. The mean vector and vector length were determined according to the frequency distributions and concentration of observations. Thus, length of the mean vector at each histogram was illustrated with an arrow symbol and concentrations of frequencies were represented by bars projected from

the circle's center. For each variable, the following circular statistic parameters were calculated: mean vector, length of mean vector, median, circular variance, circular standard deviation, standard error mean, 95% confidence interval, Watson U test for theoretical distribution and Rayleigh test for uniform distribution.

Significance of a presumed bivariate dependence (e.g. between groundwater level and soil water content) was tested with correlation analysis. Usually this procedure is completed when the angles of both variables are uniformly distributed on the circle and the difference between the observed angles of the two variables (Equation 3-3) can be used to fit Equation 3-4 and determine the mean vector length *r*. A high value of *r* indicates a strong positive correlation and a low value indicates that the angles from the two variables are weakly correlated. The values of *r* range from 0 to 1 and can be used as a correlation coefficient.

$$\delta_i = \psi_i - \phi_i \tag{3-3}$$

$$r = \frac{1}{n}\sqrt{\left[\sum_{i=1}^{n}\cos\delta_i\right]^2 + \left[\sum_{i=1}^{n}\sin\delta_i\right]^2} \tag{3-4}$$

where δ is the difference of the angles Ψ and Φ from two different variables. The δ is then used in Equation 3-2 instead of Φ in order to get the vector length of the two variables. For datasets that violated the assumption of uniform distributions, the circular-circular correlation method (explained in detail by Batschelet [1981]) was used to calculate the strength of the relationship between two circular variables. Circular-circular correlation uses the Fisher and Lee (1983) method, analogous to the Pearson product moment correlation normally used in linear data analysis. This coefficient ranges from -1 to +1, according to a perfect negative or positive correlation and tests the null hypothesis that correlation between two variables is 0. Circular-circular correlation analysis tests the hypothesis that there is no correlation between two circular variables. The main objective of completing this statistical analysis was to determine the possible

statistical relationships between weather and groundwater level and soil water content variables. This statistic evaluation is intended to help identify the main factors influencing the capillary effect or diurnal peaks identified.

Results and Discussion

Data Extraction and Compilation of Diurnal Peaks

A time series plot of soil water content, groundwater level and barometric pressure is depicted in Figure 3-3. Some general features of the datasets can be observed in this figure. One pattern that was identified is the decline in groundwater table level, observed from October 2008 to March 2009. This decline has been previously documented and is characteristic of groundwater levels in southeast Florida during the dry season (Klein and Hull, 1978). Groundwater level data from wells 2 and 4 also captured the influence of barometric pressure changes. This relationship was more evident in data from wells 2 and 4 than that from wells 1 and 3. This can be contributed to instrumentation, as equipment used to measure groundwater levels from wells 2 and 4 were more sensitive to temperature and pressure changes due to the greater range of barometric compensation (5000 cm) compared to wells 1 and 3 (500 cm). Therefore compensated groundwater levels were smoother at smaller ranges of barometric compensation (Figure 3-3).

Plots considering a greatly reduced time scale were created (Figures 3-4, 3-5 and 3-6) to identify patterns that might be less evident at the greater time scale. The period plotted for the reduced time scale represents a randomly selected pair of days from the study period (21 November to 22 November 2008). Each figure includes six datasets: soil water content, water table elevation (WTE), solar radiation, relative humidity, soil temperature and barometric pressure. Soil water contents plotted in these figures were from probe A11 (trenched no lychee). Peaks of soil water content at 10 and 20 cm depths coincided with peaks of soil temperature and

solar radiation and minimum values of WTE and barometric pressure (Figure 3-4 and 3-5). Alternatively, the minimum values in soil water content at 60 cm depth coincided with peaks of solar radiation and soil temperature and minimum values of WTE and barometric pressure (Figure 3-6). The relationship between barometric pressure and groundwater level was anticipated as it has previously been observed (Peck, 1960). Similarly, it was expected that solar radiation and soil temperature would follow a similar pattern.

While Figure 3.3 includes the entire period of record, values corresponding to storm events or freeze protection were discarded using a filtering process. The remaining, filtered dataset was further evaluated to identify prevalent patterns. One pattern identified was that ranges of soil water fluctuations were less at greater depths. For example, ranges of soil water content for probe B8 (lychee no trench) at 10, 20, 40 and 60 cm depths were 0.002, 0.003, 0.0006, and 0.0004, respectively. Similarly, for probe A6 (lychee trench) shallower depth (10 and 20 cm) ranges of soil water content (0.012 and 0.02) were greater than soil water content (0.006 and 0.0025) at deeper points (40 and 60 cm depths).

Circular Statistical Analysis

Results from circular statistical analysis are summarized in Tables 3-2 to 3-6 and simplified using circular histograms in Figures 3-7 to 3-10. All mean vectors had statistical significance based on the Rayleigh test ($\alpha = 0.05$). The significant differences of mean directions found in all the variables using Rayleigh test is attributed in great part to the number of observations. For datasets that were characterized by multimodal distributions, vector lengths decreased and the von Mises distribution hypothesis was rejected in all cases ($P<0.05$).

Circular histograms of water table elevation (Figure 3-9, Table 3-5) suggest a different mean vector for maximum daily values found at wells 1 and 3 compared to wells 2 and 4. In this case the differences in water level ranges for each pair of sensors were influenced by the level of

sensitivity to temperature and atmospheric pressure fluctuations (as previously discussed). Results considering a pooled dataset of water table elevation (WTE) data indicated a significant mean vector and median value of 5:00 am (r = 0.61). The significant mean vectors for wells 1 and 3 were consistently observed at 4:11 am (r = 0.76) and 4:09 am (r = 0.79), respectively. Alternatively, the mean vectors for well 2 (7:03 am) and well 4 (7:31 am) had lower mean vector lengths (r = 0.36 and 0.34, respectively) due to greater variances and standard deviations in the dataset (see Figure 3-3). Thus, groundwater levels whose range of pressure compensation is too high tend to have greater standard deviations due to a poor compensation of barometric and temperature fluctuations.

The weather variables were more consistent in the frequency concentrations compared to WTE and soil water content results. Figure 3-10 and Table 3-6 mean vector lengths were greater than 0.81 except for relative humidity (r = 0.57) where the dataset was characterized by a bimodal distribution. The greatest frequency for relative humidity occurred at 7:00 am. This frequency location is likely associated with the cooler temperatures observed during morning hours and is a typical weather response. The second greatest frequency in relative humidity occurred at 11:00 am. One possible explanation for this is that ponded water (residual from storm events or irrigation where days did not meet removal criteria during dataset filtering process), evaporation, and increasing temperature combine to form optimum conditions for a mid-morning peak in relative humidity. However, this was not confirmed and further investigation is needed to identify true causes of the observed bimodal distribution. The mean vectors for barometric pressure, solar radiation and soil temperature were found at 11:14 am (r = 0.81), 12:42 pm (r = 0.97) and 3:58 pm (r = 0.98), respectively.

Circular histograms of soil water content (Figure 3-7 and Figure 3-8) illustrate the variability in peak values that were observed. This variability translated into reduced mean vector lengths (r values) for mean vectors describing soil water content peaks (Table 3-2, Table 3-3 and Table 3-4). For example, mean vectors of soil water contents at 10 and 20 cm depths (Figure 3-8 and Table 3-4) were located at 4:10 pm (r = 0.46) and 11:16 pm (r = 0.46), respectively. Mean vectors for soil water content datasets at 40 and 60 cm depths were at 3:23 am (r = 0.39) and 7:23 am (r = 0.31), respectively. The 40 and 60 cm soil water content depths were found to be similar to mean vectors found in groundwater levels of well 2 (7:03 am) and well 4 (7:31 am). This corresponds with general observations previously discussed for Figures 3-4 to 3-6.

Given the rejected null hypotheses of Rayleigh test in all variables (Tables 3-2 to 3-6) circular-circular correlation analysis was used to determine the strength of the relationship between soil water content and groundwater level, barometric pressure, soil temperature, relative humidity and solar radiation. For all variable combinations except soil water probe A11-10 and barometric pressure (r = -0.000105), the null hypothesis of zero correlation was rejected. Although the probability of zero relationship was rejected, most of the *r* coefficients were low (r < 0.5) and therefore the relationship between soil water content, groundwater level and the rest of the weather variables were not strong. Thus, correlation analysis confirmed relationships among all variables but the results did not provided a good level of interpretation due to the weak relationships.

Further Discussion

The circular methods applied captured significant patterns in all variables of diurnal fluctuations expressed as mean vectors. Visual examination of the variables' mean vector results provided some interesting concepts to consider.

Soil water content in the shallow layer of the soil profile (10 cm) seemed to be more influenced by weather than soil water content at the 40 and 60 cm depths. This concept is based on the fact that the soil water content mean vector for 10 cm depth was at 4:10 pm. This peak value corresponded to mean vectors for solar radiation (12:42 pm) and soil temperature (3:58 pm). (It is expected that solar radiation would peak prior to soil temperature peak as soil temperature is a function of heat transfer primarily driven by solar radiation.) Additionally, these peaks coincided with minimum values for groundwater level. These combined events could be explained by the following phenomenon: groundwater evaporation, transport of water vapor up through the soil profile, and subsequent condensation (at shallower soil depths) when temperatures start to decrease. Groundwater evaporation of the shallow aquifer is supported by results in Chin et al. (2008) that indicated the shallow saturated zone evaporation rate equals the potential evaporation rate to a depth of 1.4 m decreasing to zero at a depth of 2.5 m. While the 10 cm depth peak mean vector may be explained (in some part) by this phenomenon, the 20 cm depth peak vector values were not directly correlated with other measured variables. The 20 cm depth peak mean vector for soil water content, which occurred at 11:16 pm, could potentially be explained by other physical phenomenon. For example, soil water movement has been observed due to temperature gradients where soil water moves from warmer to cooler and wet to dry profiles (Bouyoucos, 1915). Thus, the later peak at 20 cm could possibly be due to water movement from 10 cm to 20 cm depths due to these gradients and therefore the 20 cm depth peak vector for soil water content would occur after the peak vector for the 10 cm depth, which was observed.

While soil water content mean vectors for shallower depths could potentially be linked to weather factors, results for deeper depths suggested a different relationship. Our results indicated

that soil water mean vectors at depths of 40 (3:23 am) and 60 cm (7:23 am) were similar to groundwater mean vectors (WTE-W1 = 4:11 am; WTE-W2 = 7:03 am). Although the multimodal response in most of the soil water content and groundwater level data analyzed suggests that more than one variable is important in describing soil water content and groundwater level fluctuations, probes located in lychee trenches at 40 and 60 cm depth (A1-40, A1-60, A6-40 and A6-60) captured mean vectors with unimodal distributions with consistent peaks of soil water content similar to groundwater peak mean vectors (Table 3-2 and Table 3-5). The results suggest a tree effect which isolates the groundwater effect from other variables. Also, mean vectors for trenches with lychee trees had greater vector lengths ($r > 0.5$) than mean vectors found at trenches without lychee trees ($r < 0.5$).

To understand diurnal cycles in soil water content, it is essential to characterize diurnal fluctuations in groundwater level. Groundwater levels in our study were influenced by different factors as evident by the multimodal distributions (Figure 3-9). Primary recharge for the aquifer is from precipitation during the rainy season (June to October), as approximately 70% of the total direct groundwater recharge (Klein and Hull, 1978) is from storms greater than 15 mm (Delin et al., 2000). The time series data collected during this study (dry season) captured a declining trend in groundwater levels. Mean vectors and frequencies observed in early morning hours could be associated with rates of depletion greater than diurnal peaks (i.e., Figure 3-7, probe B8-40, B3-40 and B9-40). Another possibility is that groundwater peaks vectors occurring during this time might be related to an inverse effect of the mean vectors found in barometric pressure (11:14 am). As barometric pressure reaches minimum values, a reduction of entrapped air in the unsaturated zone as described by Turk (1975) and Peck (1960) may result. Other peaks observed in groundwater circular histograms might be attributed to canal stage management. Studies by

Merrit (1996), Ritter and Muñoz-Carpena (2006) and Klein and Hull (1978) have noted the interconnection of canal stages and groundwater levels. As suggested, data collected could not provide a definite explanation for observed patterns. Further investigation is needed to accurate access driving factors influence groundwater level fluctuations.

Capillary Contribution Relative Significance

Although Rayleigh test determined the existence and location of the diurnal peaks in all the variables studied, the relative importance of this increase of soil water content during the day needs to be studied in detail to determine its contribution to plant water uptake purposes. According to the results shown in Table 3-8, the soil water content daily difference between the maximum daily values and the daily mean soil water content was less than 1% of volumetric water content in all cases. This daily peak <1% of soil water content could be attributed to the relatively low groundwater daily mean diurnal range (< 4 cm). Thus, despite statistical significance of the mean vectors found, suggested hypothesis of possible daily contribution to plant water uptake through diurnal capillarity requires further research. Considering an actual ET of 3.3 mm/day (Migliaccio et al., 2008b) groundwater diurnal fluctuations would be able to contribute an average of 0.58 ± 0.46 mm of daily soil water content equivalent to 18% of mean actual daily ET.

Conclusions

Location and statistical significance of diurnal fluctuations were confirmed with circular statistical analysis. The technique represents a practical approach to locate and confirm the existence of mean vectors of soil water content and groundwater level using the Rayleigh test of uniform distribution. The mean vectors had statistical significance in all the tests and circular histograms provided a method for better evaluating the large dataset.

Many of the mean vectors found were characterized by multimodal distributions attributed to multivariate effects. The mean vector of groundwater was closer to the mean vectors of soil water content at 40 and 60 cm depths which also corresponded with the mean vectors of relative humidity at dew point hours. Results suggest that soil water at 10 and 20 cm depths were more similar to solar radiation (evapotranspiration) and soil water temperature mean vectors. Most of the variables evaluated did not met unimodal Von Mises distribution for purposes of parametric comparisons among variables. Circular-circular correlation analysis confirmed in general a weak relationship between soil water content and the weather and groundwater peak mean vectors.

Table 3-1. Equipment used to identify diurnal peaks using circular statistics.

Equipment	Variable	Number of Instruments
EnviroSCAN	Soil water content	24
Levelogger LT 3001	Water table elevation	4
Barologger	Barometric pressure	1
FAWN[1] weather station	Relative humidity	1
FAWN weather station	Solar radiation	1
FAWN weather station	Temperature	1

[1] Florida Automated Weather Network (FAWN) weather station at Homestead, Miami-Dade County, Florida.

Table 3-2. Circular statistical analysis of the occurrence of maximum daily soil water content in trenched conditions at 10, 20, 40 and 60 cm depths.

Variable	A6-10	A6-20	A6-40	A6-60	A1-10	A1-20	A1-40	A1-60	A11-10	A11-20	A11-40	A11-60
Mean Vector (μ)	11:42 PM	6:55 AM	8:33 AM	9:09 AM	3:14 PM	11:03 PM	7:43 AM	9:24 AM	4:13 PM	9:06 PM	2:50 AM	6:48 AM
Length of Mean Vector (r)	0.347	0.419	0.894	0.896	0.669	0.878	0.577	0.766	0.654	0.637	0.448	0.282
Median	12:00 AM	9:00 AM	8:45 AM	9:15 AM	3:15 PM	12:00 AM	8:45 AM	9:45 AM	4:00 PM	8:15 PM	2:00 AM	8:00 AM
Concentration	0.74	0.923	5.022	5.091	1.83	4.386	1.419	2.503	1.753	1.668	1.001	0.588
Circular Variance	0.653	0.581	0.106	0.104	0.331	0.122	0.423	0.234	0.346	0.363	0.552	0.718
Circular Standard Deviation	83.361°	75.545°	27.088°	26.88°	51.354°	29.28°	60.069°	41.826°	52.781°	54.45°	72.615°	91.165°
Standard Error of Mean	9.917°	8.078°	2.371°	2.353°	4.541°	2.561°	5.552°	3.629°	4.692°	4.876°	7.505°	12.342°
95% Confidence Interval (-/+) μ	10:25 PM	5:52 AM	8:15 AM	8:50 AM	2:38 PM	10:43 PM	6:59 AM	8:55 AM	3:36 PM	8:28 PM	1:51 AM	5:11 AM
	1:00 AM	7:59 AM	8:52 AM	9:27 AM	3:49 PM	11:23 PM	8:26 AM	9:52 AM	4:49 PM	9:44 PM	3:49 AM	8:25 AM
Watson's U^2 Test (von Mises, U^2)	1.708	1.385	2.592	2.89	0.389	1.114	1.701	1.525	1.683	0.903	0.914	0.711
Watson's U^2 Test (p)	< 0.005	< 0.005	< 0.005	< 0.005	< 0.005	< 0.005	< 0.005	< 0.005	< 0.005	< 0.005	< 0.005	< 0.005
Rayleigh Test (Z)	15.654	22.853	103.961	104.317	58.218	100.121	43.31	76.297	55.642	52.69	26.084	10.338
Rayleigh Test (p)	1.59E-07	1.19E-10	< 1E-12	< 1E-12	< 1E-12	< 1E-12	< 1E-12	< 1E-12	< 1E-12	< 1E-12	4.70E-12	3.24E-05

Table 3-3. Circular statistical analysis of the occurrence of maximum daily soil water content in non trenched conditions at 10, 20, 40 and 60 cm depths.

Variable	B8-10	B8-20	B8-40	B8-60	B3-10	B3-20	B3-40	B3-60	B9-10	B9-20	B9-40	B9-60
Mean Vector (μ)	6:15 PM	4:16 AM	12:47 AM	1:56 AM	3:11 PM	10:44 PM	1:00 AM	1:54 PM	3:22 PM	9:45 PM	12:17 AM	2:10 AM
Length of Mean Vector (r)	0.312	0.403	0.492	0.305	0.795	0.831	0.633	0.2	0.593	0.683	0.902	0.646
Median	5:00 PM	2:52 AM	12:15 AM	11:45 PM	2:45 PM	11:45 PM	12:15 AM	1:45 PM	3:00 PM	11:45 PM	11:45 PM	1:30 AM
Concentration	0.656	0.879	1.127	0.64	2.799	3.292	1.653	0.408	1.482	1.903	5.41	1.714
Circular Variance	0.688	0.597	0.508	0.695	0.205	0.169	0.367	0.8	0.407	0.317	0.098	0.354
Circular Standard Deviation	87.483°	77.281°	68.241°	88.343°	38.847°	34.914°	54.766°	102.793°	58.554°	50.078°	25.975°	53.528°
Standard Error of Mean	11.111°	8.444°	6.748°	11.384°	3.37°	3.039°	4.912°	17.584°	5.36°	4.409°	2.274°	4.774°
95% Confidence Interval (-/+) μ	4:48 PM	3:10 AM	11:54 PM	12:27 AM	2:44 PM	10:20 PM	12:21 AM	11:36 AM	2:40 PM	9:10 PM	11:59 PM	1:32 AM
	7:42 PM	5:22 AM	1:40 AM	3:26 AM	3:37 PM	11:07 PM	1:39 AM	4:12 PM	4:04 PM	10:19 PM	12:35 AM	2:47 AM
Watson's U^2 Test (von Mises, U^2)	0.682	0.754	0.529	0.674	2.392	1.111	0.938	0.945	1.653	1.925	1.839	0.998
Watson's U^2 Test (p)	< 0.005	< 0.005	< 0.005	< 0.005	< 0.005	< 0.005	< 0.005	< 0.005	< 0.005	< 0.005	< 0.005	< 0.005
Rayleigh Test (Z)	12.632	21.079	31.468	12.063	82.092	89.676	52.138	5.201	45.747	60.559	105.849	54.311
Rayleigh Test (p)	3.27E-06	7.01E-10	< 1E-12	5.77E-06	< 1E-12	< 1E-12	< 1E-12	0.006	< 1E-12	< 1E-12	< 1E-12	< 1E-12

Table 3-4. Circular statistical analysis of the occurrence of maximum daily pooled soil water content at 10, 20, 40 and 60 cm depths.

Variable	Soil Water 10 cm	Soil Water 20 cm	Soil Water 40 cm	Soil Water 60 cm
Mean Vector (μ)	4:10 PM	11:16 PM	3:23 AM	7:23 AM
Length of Mean Vector (r)	0.464	0.466	0.399	0.315
Median	3:30 PM	12:00 AM	2:00 AM	8:45 AM
Concentration	1.045	1.05	0.871	0.665
Circular Variance	0.536	0.534	0.601	0.685
Circular Standard Deviation	71.04°	70.852°	77.623°	87.055°
Standard Error of Mean	2.948°	2.934°	3.478°	4.482°
95% Confidence Interval (-/+) μ	3:47 PM 4:33 PM	10:53 PM 11:39 PM	2:55 AM 3:50 AM	6:48 AM 7:59 AM
Watson's U^2 Test (von Mises, U^2)	3.171	2.17	2.053	1.574
Watson's U^2 Test (p)	< 0.005	< 0.005	< 0.005	< 0.005
Rayleigh Test (Z)	167.666	169.037	124.449	77.536
Rayleigh Test (p)	< 1E-12	< 1E-12	< 1E-12	< 1E-12

Table 3-5. Circular statistical analysis of the occurrence of maximum daily water table elevation at four wells and all data combined.

Variable	WTE-W1	WTE-W2	WTE-W3	WTE-4	WTE
Mean Vector (μ)	4:11 AM	7:03 AM	4:09 AM	7:31 AM	4:41 AM
Length of Mean Vector (r)	0.768	0.365	0.792	0.341	0.614
Median	4:45 AM	8:45 AM	4:45 AM	9:00 AM	5:00 AM
Concentration	2.521	0.783	2.77	0.727	1.569
Circular Variance	0.232	0.635	0.208	0.659	0.386
Circular Standard Deviation	41.626°	81.392°	39.108°	83.991°	56.551°
Standard Error of Mean	3.611°	9.405°	3.392°	13.023°	2.955°
95% Confidence Interval (-/+) μ	3:43 AM 4:39 AM	5:49 AM 8:16 AM	3:43 AM 4:36 AM	5:49 AM 9:13 AM	4:18 AM 5:04 AM
Watson's U^2 Test (von Mises, U^2)	0.279	1.527	0.272	0.38	0.991
Watson's U^2 Test (p)	< 0.005	< 0.005	< 0.005	< 0.005	< 0.005
Rayleigh Test (Z)	76.686	17.28	81.585	9.096	147.227
Rayleigh Test (p)	< 1E-12	3.13E-08	< 1E-12	1.12E-04	< 1E-12

Table 3-6. Circular statistical analysis of the occurrence of maximum daily observations of weather factors.

Variable	Barometric Pressure	Soil Temperature	Relative Humidity	Solar Radiation
Mean Vector (μ)	11:14 AM	3:58 PM	4:58 AM	12:42 PM
Length of Mean Vector (r)	0.814	0.983	0.57	0.97
Median	11:00 AM	4:00 PM	7:00 AM	12:45 PM
Concentration	3.05	30.523	1.392	17.045
Circular Variance	0.186	0.017	0.43	0.03
Circular Standard Deviation	36.707°	10.458°	60.752°	14.091°
Standard Error of Mean	3.188°	0.917°	5.641°	1.236°
95% Confidence Interval (-/+) μ	10:49 AM 11:39 AM	3:51 PM 4:05 PM	4:13 AM 5:42 AM	12:32 PM 12:52 PM
Watson's U^2 Test (von Mises, U^2)	2.586	0.317	1.645	0.155
Watson's U^2 Test (p)	< 0.005	< 0.005	< 0.005	< 0.025
Rayleigh Test (Z)	86.237	125.74	42.235	122.37
Rayleigh Test (p)	< 1E-12	< 1E-12	< 1E-12	< 1E-12

Table 3-7. Circular-circular Pearson product moment correlation tests between soil water sensor data and groundwater level as well as weather variables during the study period.

Variable	WTE-W1		WTE-W2		WTE-W3		Barometric Pressure		Soil Temperature		Relative Humidity		Solar Radiation	
	r	P	r	P	r	P	r	P	r	P	r	P	r	P
A6-10	-0.075	< 0.05	0.043	< 0.05	-0.02	< 0.05	0.019	< 0.05	-0.073	< 0.05	-0.117	< 0.05	-0.026	< 0.05
A6-20	0.065	< 0.05	0.064	< 0.05	0.072	< 0.05	-0.089	< 0.05	-0.225	< 0.05	0.077	< 0.05	0.002	< 0.05
A6-40	0.324	< 0.05	-0.046	< 0.05	0.253	< 0.05	-0.042	< 0.05	0.093	< 0.05	0.427	< 0.05	0.011	< 0.05
A6-60	0.34	< 0.05	2.98E-04	< 0.05	0.238	< 0.05	-0.046	< 0.05	-0.007	< 0.05	0.37	< 0.05	0.067	< 0.05
B8-10	-0.102	< 0.05	0.031	< 0.05	-0.114	< 0.05	0.072	< 0.05	-0.022	< 0.05	-0.095	< 0.05	-0.043	< 0.05
B8-20	0.045	< 0.05	-0.028	< 0.05	0.138	< 0.05	-0.048	< 0.05	0.134	< 0.05	0.073	< 0.05	0.037	< 0.05
B8-40	-0.06	< 0.05	0.004	< 0.05	-0.042	< 0.05	0.044	< 0.05	-0.118	< 0.05	-0.051	< 0.05	-0.112	< 0.05
B8-60	0.025	< 0.05	0.018	< 0.05	0.019	< 0.05	-0.019	< 0.05	6.24E-04	< 0.05	-0.03	< 0.05	0.07	< 0.05
A1-10	-0.079	< 0.05	-0.151	< 0.05	-0.015	< 0.05	-0.053	< 0.05	0.192	< 0.05	-0.015	< 0.05	-0.011	< 0.05
A1-20	-0.186	< 0.05	-0.125	< 0.05	-0.163	< 0.05	0.038	< 0.05	-0.214	< 0.05	-0.083	< 0.05	-0.121	< 0.05
A1-40	0.059	< 0.05	-0.034	< 0.05	0.078	< 0.05	0.025	< 0.05	-0.039	< 0.05	0.208	< 0.05	0.026	< 0.05
A1-60	0.095	< 0.05	-0.069	< 0.05	0.177	< 0.05	-0.021	< 0.05	0.126	< 0.05	0.165	< 0.05	0.087	< 0.05
B3-10	-0.006	< 0.05	-0.011	< 0.05	-0.123	< 0.05	0.002	< 0.05	0.069	< 0.05	-0.112	< 0.05	-0.078	< 0.05
B3-20	-0.134	< 0.05	-0.082	< 0.05	-0.131	< 0.05	0.122	< 0.05	-0.12	< 0.05	-0.087	< 0.05	-0.157	< 0.05
B3-40	0.01	< 0.05	0.006	< 0.05	0.003	< 0.05	-0.049	< 0.05	-0.009	< 0.05	-0.011	< 0.05	0.008	< 0.05
B3-60	0.016	< 0.05	-0.023	< 0.05	-0.002	< 0.05	0.023	< 0.05	-0.015	< 0.05	-0.037	< 0.05	-0.002	< 0.05
A11-10	-0.002	< 0.05	-0.085	< 0.05	-0.063	< 0.05	-1.05E-04	ns	0.257	< 0.05	0.019	< 0.05	-0.065	< 0.05
A11-20	0.001	< 0.05	-0.119	< 0.05	-0.059	< 0.05	0.166	< 0.05	0.031	< 0.05	-0.044	< 0.05	-0.148	< 0.05
A11-40	0.069	< 0.05	0.046	< 0.05	0.059	< 0.05	0.037	< 0.05	-0.062	< 0.05	0.054	< 0.05	0.007	< 0.05
A11-60	0.058	< 0.05	0.066	< 0.05	0.064	< 0.05	-0.059	< 0.05	-0.025	< 0.05	0.063	< 0.05	0.069	< 0.05
B9-10	-0.023	< 0.05	0.039	< 0.05	0.027	< 0.05	0.065	< 0.05	0.043	< 0.05	0.031	< 0.05	-0.003	< 0.05
B9-20	-0.127	< 0.05	-0.008	< 0.05	-0.216	< 0.05	0.062	< 0.05	0.007	< 0.05	-0.147	< 0.05	-0.095	< 0.05
B9-40	0.013	< 0.05	-0.017	< 0.05	-0.017	< 0.05	0.011	< 0.05	0.086	< 0.05	0.044	< 0.05	0.106	< 0.05
B9-60	0.075	< 0.05	-0.085	< 0.05	0.133	< 0.05	-0.094	< 0.05	-0.055	< 0.05	0.104	< 0.05	0.171	< 0.05

Table 3-8. Estimated daily contribution of groundwater diurnal fluctuations to soil water content at four different depths and soil conditions of a typical Krome soil profile. Soil water contribution is the difference of the daily mean and the maximum daily value at each soil condition.

Depth (cm)	Overall		Trench		No Trench	
	$\theta\%_{mean}$	$\theta\%_{stdev}$	$\theta\%_{mean}$	$\theta\%_{stdev}$	$\theta\%_{mean}$	$\theta\%_{stdev}$
10	0.490	0.331	0.592	0.454	0.388	0.191
20	0.239	0.111	0.217	0.100	0.261	0.138
40	0.150	0.101	0.152	0.140	0.148	0.075
60	0.087	0.032	0.082	0.031	0.092	0.040

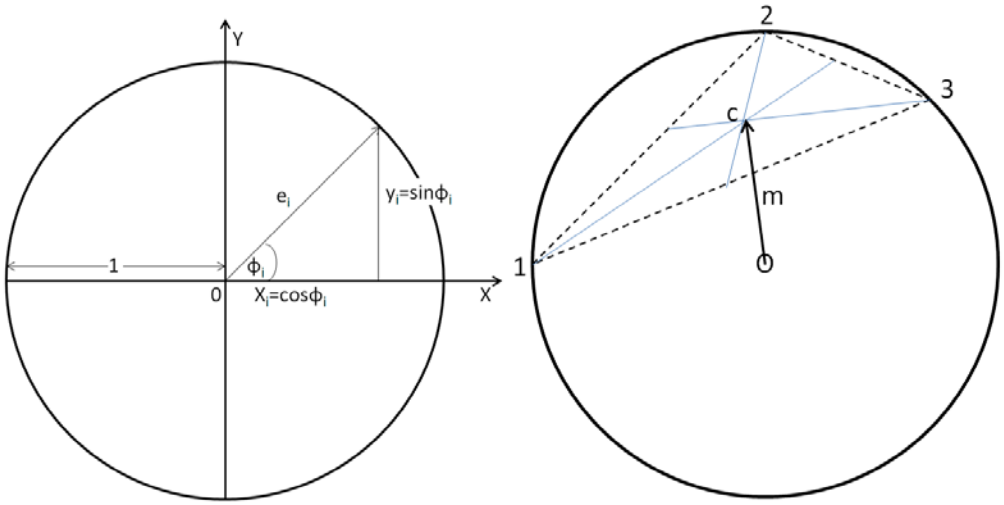

Figure 3-1. The circular statistic's rectangular components of a mean vector and its determination through the construction of the center of gravity from three observations.

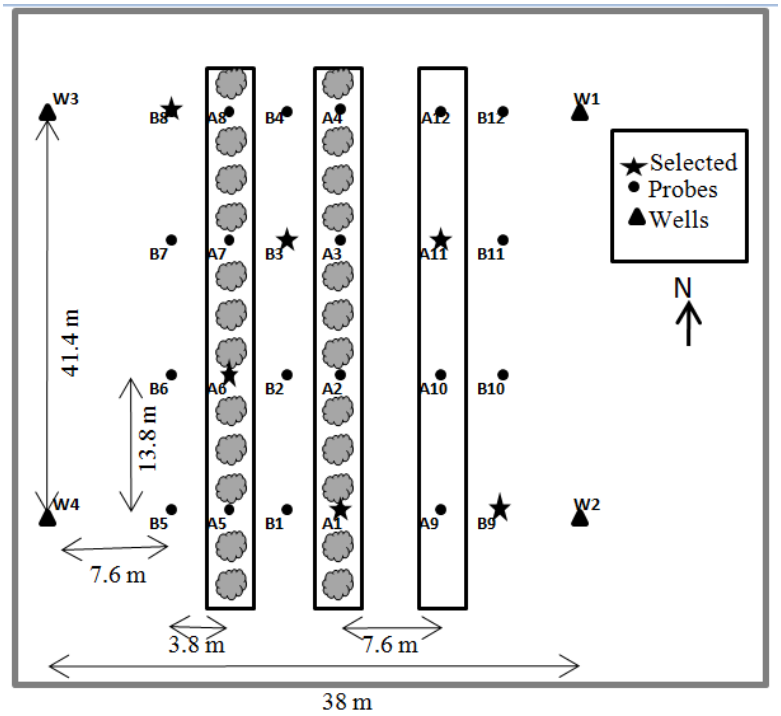

Figure 3-2. Schematic of selected probes and location of monitoring wells in experimental site at University of Florida Tropical Research and Education Center (TREC). "A" symbolized probes located in a trenched Krome soil condition and "B" symbolizes probes located in a non trenched limestone soil condition.

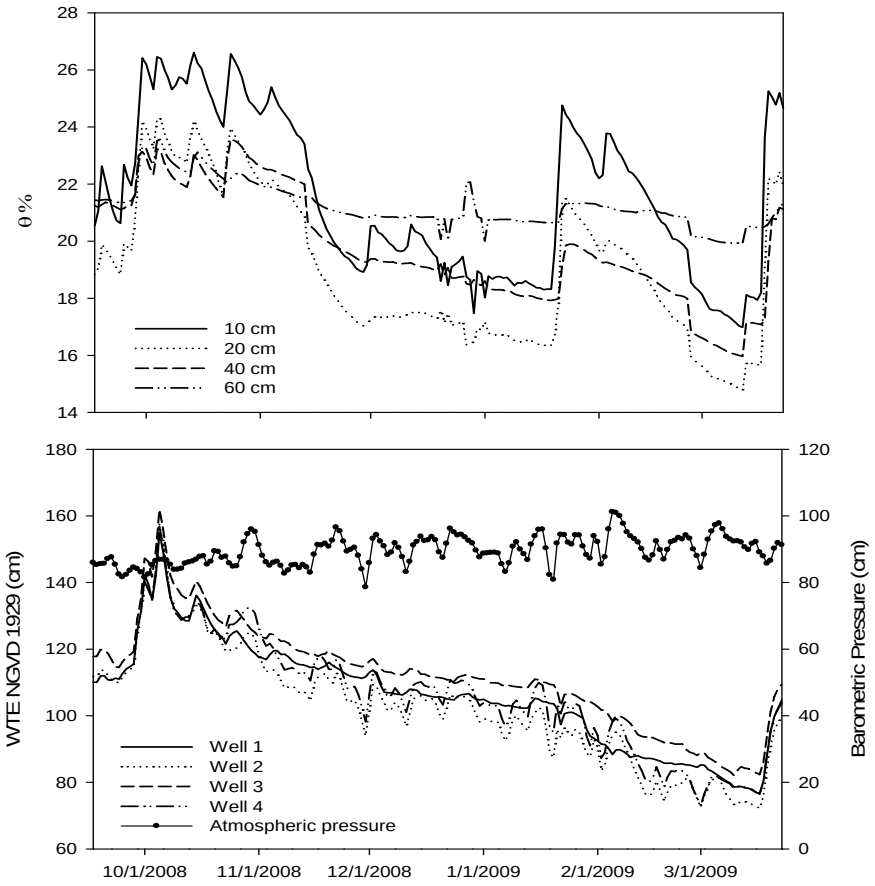

Figure 3-3. Daily means for the entire dataset of groundwater level, barometric pressure and overall soil water content at 10, 20, 40 and 60 cm depths. Study period from16 September 2008 to 23 March 2009.

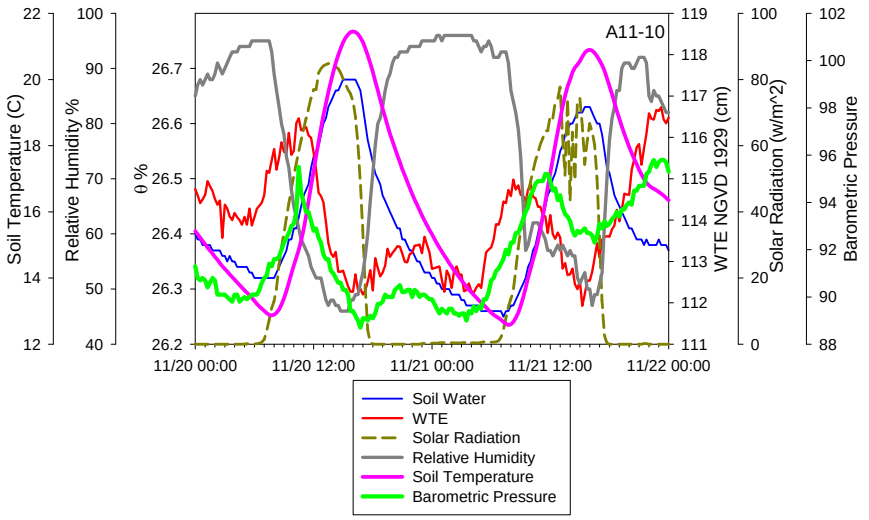

Figure 3-4. Diurnal fluctuations from November 20 to November 22, 2008; Influence of groundwater level (WTE), solar radiation, relative humidity and soil temperature in the soil water content of probe A11-10 (depth: 10 cm).

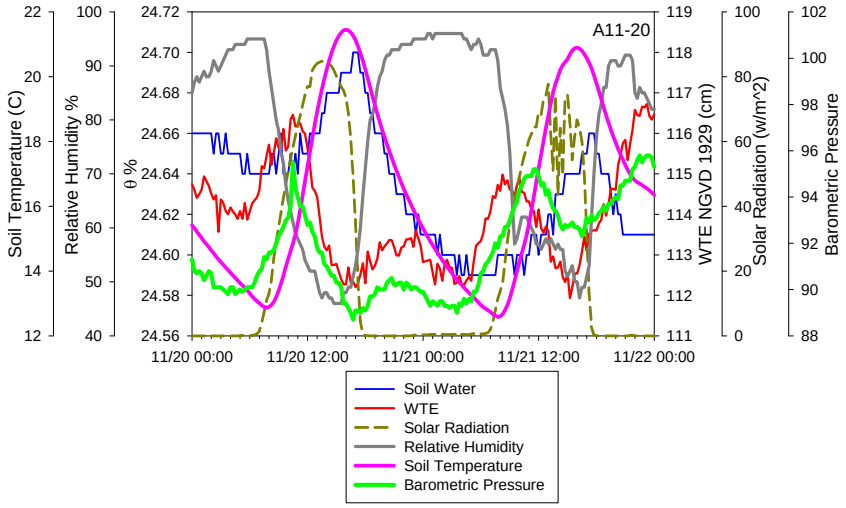

Figure 3-5. Diurnal fluctuations from November 20 to November 22, 2008; Influence of groundwater level (WTE), solar radiation, relative humidity and soil temperature in the soil water content of probe A11-20 (depth: 20 cm).

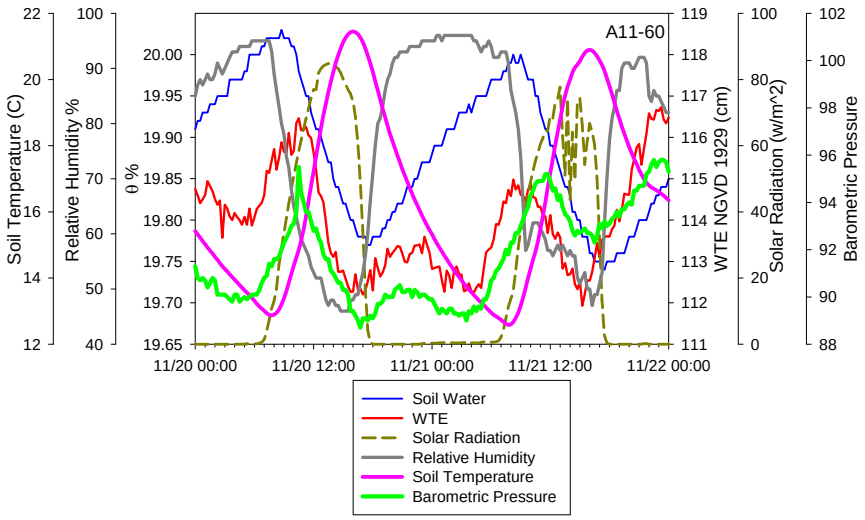

Figure 3-6. Diurnal fluctuations from November 20 to November 22, 2008; Influence of groundwater level (WTE), solar radiation, relative humidity and soil temperature in the soil water content of probe A11-60 (depth: 60 cm).

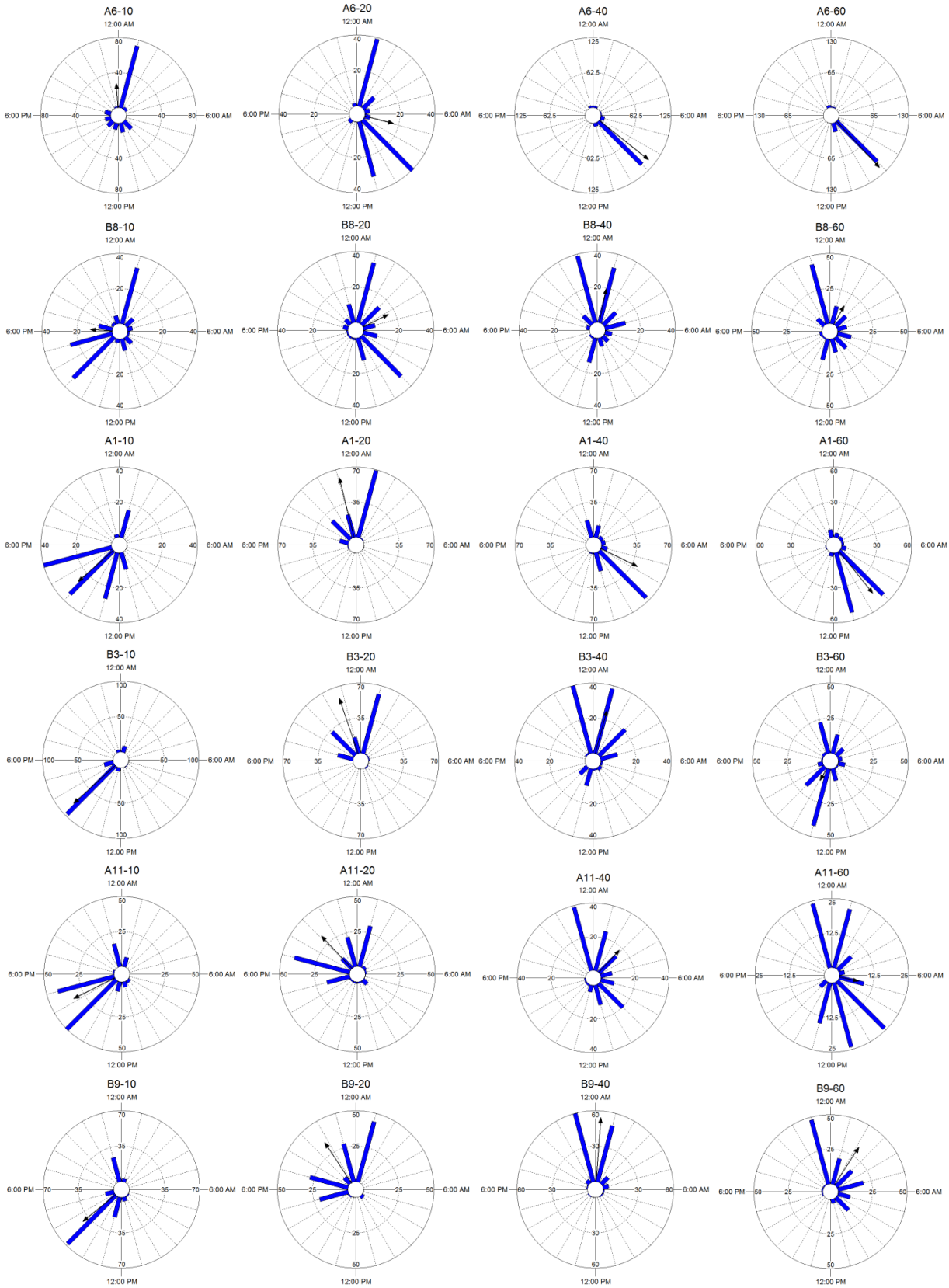

Figure 3-7. Circular histograms and mean vectors of filtered soil water maximum daily values.

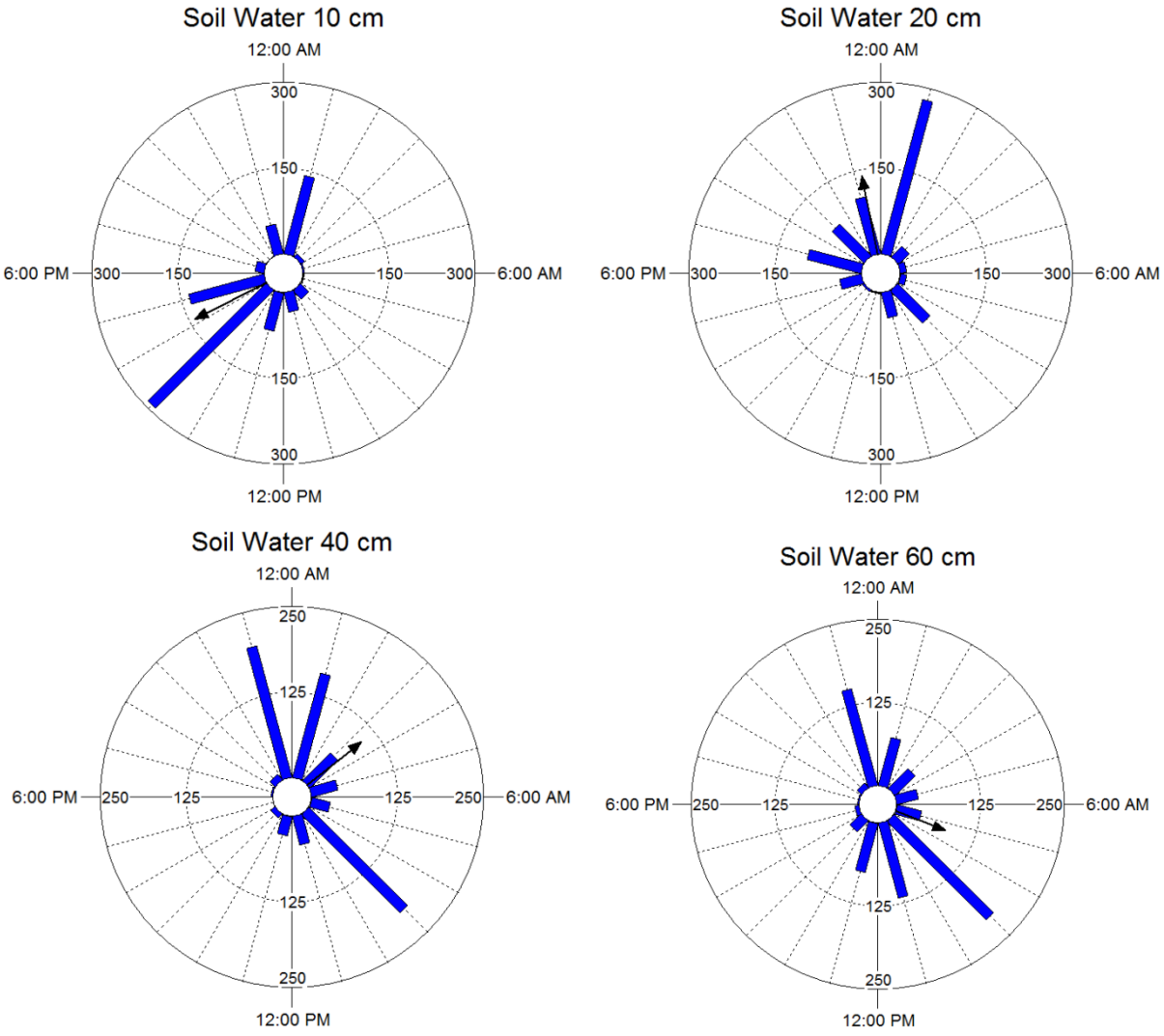

Figure 3-8. Circular histograms and mean vectors of pooled, filtered soil water maximum daily values at 10, 20, 40 and 60 cm depths.

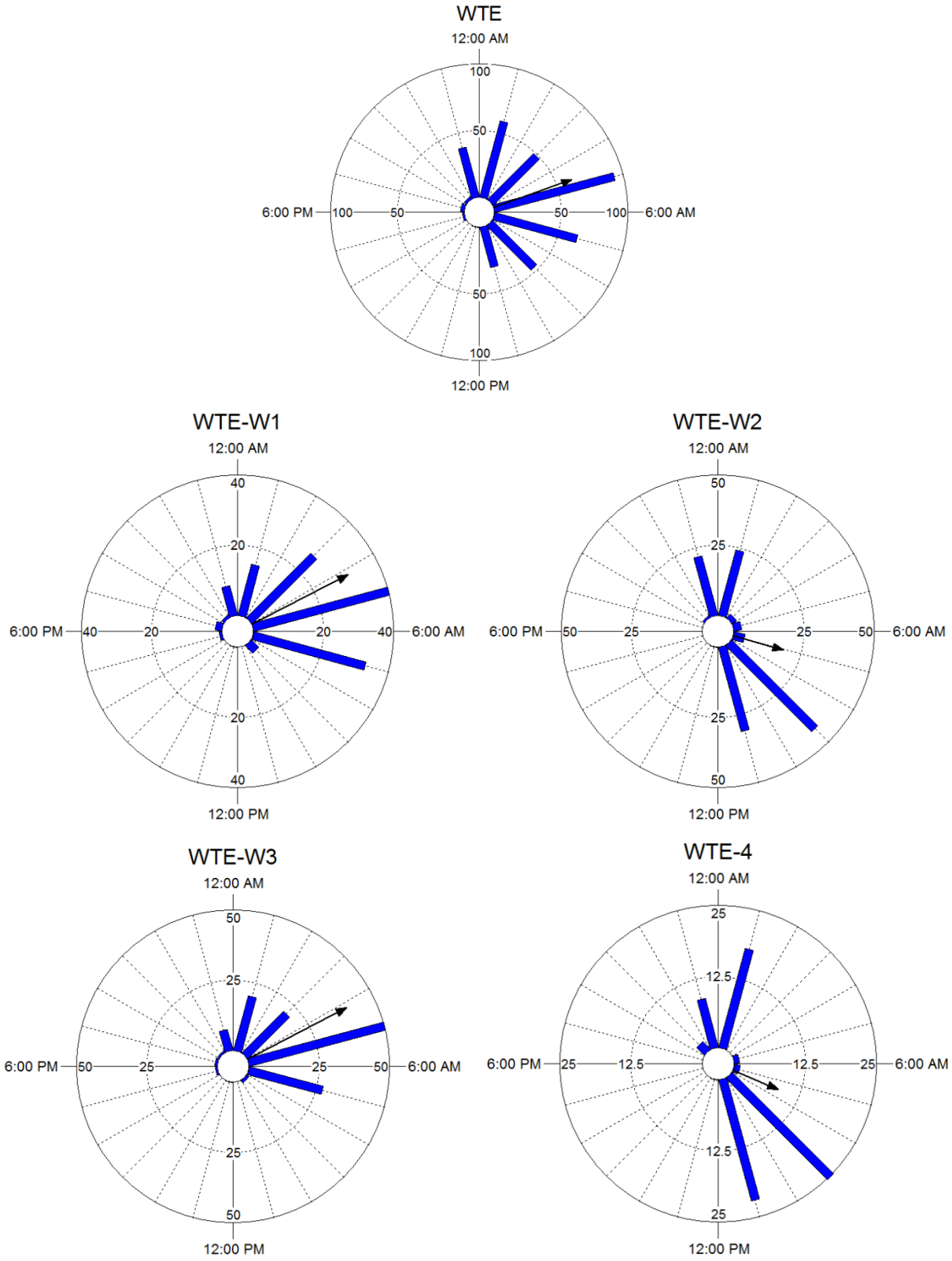

Figure 3-9. Circular histograms and mean vectors of filtered groundwater level maximum daily values from all wells (WTE), well 1 (WTE-W1), well 2 (WTE-W2), well 3 (WTE-W3) and well 4 (WTE-W4).

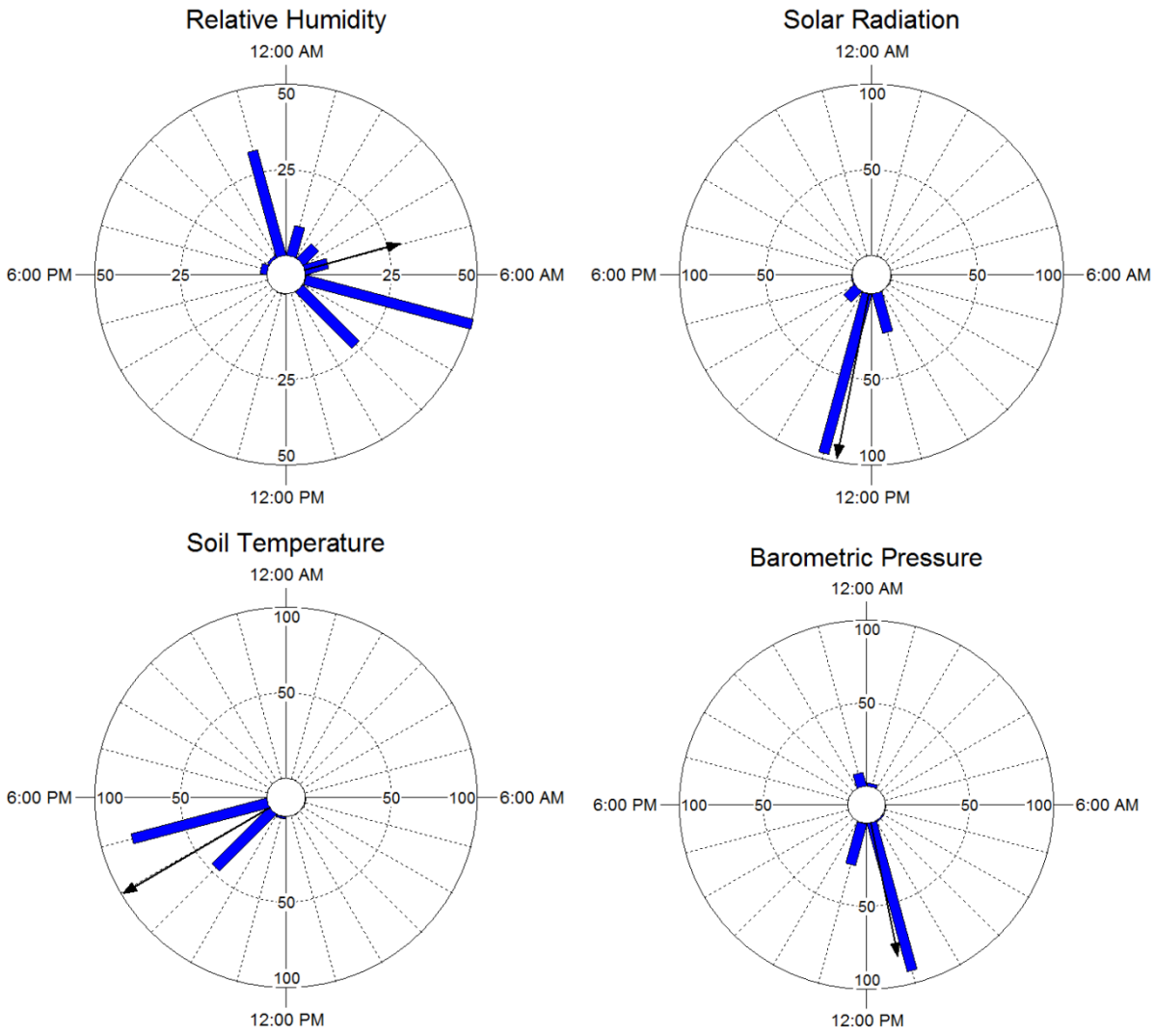

Figure 3-10. Circular histograms and mean vectors of filtered weather maximum daily values.

CHAPTER 4
MONITORING GROUNDWATER LEVELS TO PREDICT SOIL WATER CONTENT IN THE UNSATURATED ZONE OF A CALCAREOUS SOIL

Introduction

The hydrology of South Florida was significantly modified during the 1950s by a complex land drainage project to protect the agricultural and urban developing areas from flooding. This project consisted of building a drainage canal network that influenced wetlands contiguous to the Everglades National Park (ENP). An effort is currently in place through the Comprehensive Everglades Restoration Plan (CERP) to rehabilitate the natural flow and water deliveries to the ENP without affecting the developed adjacent areas. To achieve these goals, the South Florida Water Management District (SFWMD) may need to raise groundwater levels (Poole, 1996; Perry, 2004).

The Biscayne aquifer is the main source of freshwater in Southeast Florida. It is described as an unconfined aquifer consisting principally of porous limestone that increases in thickness from about 14 m in the western part of Miami-Dade County to about 30 m in the eastern part (Fish and Stewart, 1991). Typical porosity is about 0.26 and hydraulic conductivity is generally greater than 305 m/day (Chin et al., 2005). Its characteristics of unconfinement, high permeability and shallow depth result in water table fluctuations that are fairly responsive to storm events and canal system management (Pitt, 1976; Ritter and Muñoz-Carpena, 2006). According to Chin et al. (2008), the aquifer's specific yield averages 0.23 as response to direct recharge of groundwater from percolation of rainwater, and shallow saturated zone evaporation rate equals the potential evaporation rate to a depth of 1.4 m decreasing to zero at a depth of 2.5 m. The shallow nature of the Biscayne Aquifer results in the potential for it to influence soil water conditions in the unsaturated zone. Despite its high permeability, a triple porosity characteristic described by Cunningham et al. (2006) in conjunction with the local shallow

groundwater conditions suggest a capillary rise effect. The capillary rise is related to the forces in the soil that wick water upward against gravity to form a zone above the water table that remains saturated called capillary fringe. The length of the capillary fringe is defined by the pore size distribution of the soil (Todd, 1959) and its potential contribution to plant water uptake is dependent on water table depth and site elevation (Wellings and Bell, 1982).

Shallow water table contribution to plant water needs has been a subject of extensive research world-wide. A brief review of literature describing shallow groundwater contributes to crop water needs is provided in Babajimopoulos et al. (2007); shallow groundwater tables were shown to provide a portion of the crop water needs for cotton replacing 60% of the evapotranspiration (ET) (Wallender et al., 1979) and 37% of ET (Ayars and Schoneman, 1986) in San Joaquin Valley, California. A study in Pakistan suggested that irrigation could be reduced by 80% under shallow groundwater conditions (Prathapar and Qureshi, 1999). The interest in understanding this phenomenon is evident by the development of models that simulate shallow groundwater dynamics, such as Upflow (Raes and Deproost, 2003) and DRAINMOD (Skaggs, 1978a).

The relationship between soil water content and shallow groundwater level is a dynamic process of alternate cycles of wetting and drying. In a field scale situation, this relationship can be more simply evaluated by assuming hydrostatic conditions. Hydrostatic conditions refer to soil water in equilibrium (without movement). The concept of using hydrostatic conditions or "drain to equilibrium" conditions was introduced and explained in detail by Wellings and Bell (1982). If equilibrium conditions occur, water pressure potential is determined by the distance of a specific point in the soil to the water table, with positive values when the point is below the water table (saturation and hydraulic head) and negative when the point is above the water table

due to its matric potential in terms of soil water suction (Buckingham, 1907; Klute, 1986; Skaggs, 1978b) (Figure 4-1). Thus, a soil water characteristic curve in a homogenous soil profile drained to equilibrium can be obtained by collecting a series of simultaneous observations of soil water contents and groundwater levels. Soil water point of saturation would be reached when water table is zero, and its volumetric water is equal to the effective porosity (Figure 4-1) (Wellings and Bell, 1982).

Capillarity effects have been previously studied using the drained to equilibrium concept. Sumner (2007) used the idea to evaluate specific yield response to micro topography in the Everglades National Park wetlands, while Nachabe et al. (2004) tested this concept to model soil water storage capacity in Myakka fine sands of Tampa Bay, Florida. Although no studies (to the author's knowledge) have focused on capillary contribution to the soil root zone in Southeast Florida agricultural soils, previous anecdotal evidence has been reported in the region suggesting that groundwater may be contributing to plant water requirements. For example, Al-Yahyai et al. (2005) reported a lack of physiological response between irrigated and non irrigated carambola (Averrhoa carambola) and assumed this result was due to shallow groundwater capillary rise. Additional work characterizing the soil water retention in this orchard described the difficulty in obtaining suction values greater than 125 cm in the field treatments without irrigation (Al-Yahyai et al., 2006) suggesting that groundwater was contributing to soil water content. Similarly, Migliaccio et al. (2008) reported evidence of capillary influences on soil water status. They investigated soil suction in Marl soils of South Florida and identified diurnal patterns during the dry season (November to May).

The potential impact of increased soil water content by shallow groundwater is of particular concern to deep rooted crops, such as tropical fruits due to flooding tolerance and

water use efficiency (Schaffer, 1998). Understanding the hydrological interactions between groundwater level and soil water content is needed so that soil water content scenarios at given water table levels can be evaluated in terms of their benefits and challenges from water management and agronomical perspectives.

The objective of this study was to test the validity of the drain to equilibrium hydrostatic assumptions for predicting the soil water content based on shallow groundwater elevation in a typical tropical fruit grove in southeast Florida. The analysis was conducted in three steps: (i) monitoring of soil water content and groundwater level in a synchronized manner and identify when hydrostatic conditions developed; (ii) determination of soil water characteristic curves of soil profiles that were considered drained to equilibrium; and (iii) construction of simple hydrostatic models to predict soil water content based on groundwater level observations.

Materials and Methods

Experimental Site

The study was conducted in Homestead south Miami-Dade County, Florida, in a lychee (Litchi chinensis) orchard at the University of Florida (UF) Tropical Research and Education Center (TREC) (80.5^0W, 25.5^0N). The site has a mean elevation of 3.12 m National Geodetic Vertical Datum (NGVD) 1929 and a subtropical marine climate. Annual rainfall is 1,448 mm/yr (Ali and Abtew, 1999) with 80% occurring during the wet season (June to October). The dry season (November to May) is characterized by a decreasing trend in groundwater levels (Chin, 2008). The groundwater level near the site (100 m south) is monitored by USGS and depth ranges are -0.38 to 2.99 m NGVD (1929) from 1950 to 2008 (USGS, 2009).

The soils at the study site are classified as Krome calcareous very gravelly loam soils. Krome soils are loamy skeletal, carbonatic, hyperthermic Lithic Udorethents (Noble et al., 1996) made of rock plowed oolitic limestone; a technique introduced during the early 1950s to increase

the soil depth and improve agricultural production in the zone (Colburn and Goldweber, 1961). Muñoz-Carpena et al. (2002) and Al Yahyai et al. (2006) describe Krome soil's physical structure in two solid fractions, 51% coarse particles (>2 mm) and 49% loam particles. The soil is characterized by a complex bimodal water retention pattern, where the gravel fraction contributes to very rapid soil water depletion and the loamy fraction retains water. Krome soil's typical profile is constituted by a scarified layer (15 cm) of very gravelly loam texture and an underlying layer of limestone bedrock. The lychee orchard (as most tropical fruit crops in the area) is planted in rock plowed trenches 0.40 to 0.45 m wide and 0.45 to 0.60 m deep (Figure 4-2); this practice is needed to increase the soil depth for rooting growth and tree stability (Crane et al., 1994). The trenches are usually dug in parallel lines for the tree rows with another set of parallel trenches perpendicular to the first for trees spacing. Trees are planted at the intersection of the trenches (Li, 2001).

The experimental site depicted in Figure 4-2 consists of six rows: two rows with lychee trees planted in trenches (hence after referred as "lychee trench"), one row without lychee trees but with trenched soil (hence after referred as "trench"), two rows without lychee trees but with surficial roots and non trenched soil (hence after referred as "lychee no trench") and one row without lychee trees or roots and without trenches (hence after referred as "no trench"). Each lychee row consisted of 12 trees planted at a spacing of 4.6 m within rows and 7.6 m between rows; plant density was 286 trees/ha. Considering that the main purpose of the study was to explain soil water dynamics, the selection of this crop represented in general the planting and spacing of tropical fruits in Southeast Florida.

Assuming hydrostatic conditions (in equilibrium and without water movement) the soil's profile hydraulic potential (H) is equivalent to the difference between its pressure potential (h)

and gravimetric potential (z) (Figure 4-1). The pressure potential (h) at a given point is defined as the distance of the point to the water table and the gravimetric potential (z) is the distance of the given point above the reference level. If the given point is located in the unsaturated zone above the water table, its pressure potential will be negative (suction) and the hydraulic potential is expressed as the distance of the reference level to the water table (L) (Muñoz-Carpena and Ritter, 2005).

Soil Water and Groundwater Monitoring: Identifying Hydrostatic Conditions

Soil water content was measured using EnviroSCAN multi sensor capacitance probes (Sentek Ltd. Pty., Stepney, Australia). Three data loggers monitored 24 probes distributed in the six rows included in the study (Figure 4-3). Each row had four probes spaced at 13.8 m and each probe had four sensors positioned at 10, 20, 40 and 60 cm depths (Figure 4-2). The system of 96 sensors measured soil water content as a function of the apparent bulk dielectric constant of the soil described in detail by Paltineanu and Starr (1997) at a resolution of 0.1% (Buss, 1993; Fares and Alva, 2000). A sensor normalization procedure was used to determine the scaled frequency (SF):

$$SF = \frac{(F_A - F_S)}{(F_A - F_W)} \tag{4-1}$$

where F_A is the frequency reading inside the PVC probe while suspended in air, F_W is the reading inside the PVC probe in a water bath and F_S are the subsequent readings inside the PVC probe installed in the soil. Then, a regression equation for the specific soil type (i.e., Krome soil) was used to relate the scaled frequency (SF) to the volumetric water content (θ). A calibration (Equation 4-2) previously developed by Al-Yahyai et al. (2006) through the gravimetric water content method was used:

$$\theta = \left(\frac{SF - C}{A} \right)^{1/B} \quad (4\text{-}2)$$

where θ is the volumetric water content and A, B and C are coefficients fitted through nonlinear regression coefficient values are 0.011, 1 and 0.5206 for A, B and C, respectively.

Groundwater level was measured using Levelogger LT 3001 (Solinst Ltd., Ontario, Canada) pressure transducers suspended and submerged at 3.6 m depth (accuracy = 0.1%, -10^{0}C to 40^{0}C). The leveloggers were positioned in four monitoring wells located along the perimeter of the study site (Figure 4-2). Location coordinates and surveyed elevations of the monitoring well risers and their surface references are provided in Table 4-1 and Figure 4-4. Water levels were compensated using air barometric pressure measurements from a Barologger. Groundwater levels were also adjusted based on weekly manual water table depth readings.

Both soil water content and groundwater level monitoring devices were synchronized to collect readings every 15 min from 16 September 2008 to 23 March 2009. Irrigation was suspended during the study to promote drained to equilibrium conditions, although irrigation for freeze protection did occur. Daily rainfall and reference evapotranspiration (ETo) data were collected from the Florida Automated Weather Network (FAWN) station located at UF TREC, less than 100 m from the study site. Data collected when events occurred that would likely violate the drain to equilibrium assumption (e.g., storms, freeze protection events and remaining moisture greater than daily evapotranspiration) were discarded from the analysis.

Drained to Equilibrium Soil Water Characteristic Curves

The filtered groundwater level and soil water content datasets were summarized to daily means. The soil water content (after filtering) were categorized according to the installed depth and soil conditions. Thus, the soil water content dataset was subdivided into 16 different soil conditions (Table 4-2, Figure 4-2). Groundwater level data from the four piezometers were

averaged and summarized to daily means. Water table depth (WTD) values were adjusted to the distance between the soil water sensor and the water table depth (DSM). This adjustment was made to relate the pressure head or soil water content at each sensor depth to the groundwater level. Thus, the filtered soil water content data from each sensor with its correspondent DSM (pressure head) defines a field soil water relationship. This relationship was defined using the van Genuchten-Mualem model (van Genuchten, 1980). The Van Genuchten et al. (1991) RETC program was used to fit collected data by applying least squares parameter optimization and the van Genuchten (1980) equation:

$$\theta = \theta_r + \frac{(\theta_s - \theta_r)}{\left[1 + (\alpha h)^n\right]^m} \tag{4-3}$$

where θ is the volumetric water content; h is the pressure head; θ_s and θ_r represent the saturated and residual water contents, respectively; and α, n and m are empirical shape parameters. The parameters generally adopt values in the following ranges: $0 < \alpha < 1$, $n > 1$, $0 < m < 1$, $h \geq 0$.

Predicting Soil Water Based on Groundwater Observations

The fitted parameters (θ_s, θ_r, α, n and m) estimated from the soil water retention data at each sensor were used to predict soil water according to the DSM daily observations. The difference between observed values and model predictions were evaluated using the Nash and Sutcliffe (1970) coefficient of efficiency (C_{eff}) described in Equation (4-4).

$$Ceff = 1.0 - \frac{\sum_{i=1}^{n}(O_i - P_i)^2}{\sum_{i=1}^{n}(O_i - \overline{O})^2} \tag{4-4}$$

where O_i are the observed values, P_i is predicted values and $\bar{O}$ is the mean of the measured data; values for C_{eff} range between 1.0 (perfect fit) and negative infinity. C_{eff} values less than zero indicate that the mean value of the measured time series would be a better predictor of the model (Nash and Sutcliffe, 1970).

Results and Discussion

Soil Water and Groundwater Monitoring: Identifying Hydrostatic Conditions

During the study period more than 1.7 million readings of soil volumetric water content (θ) were collected from 96 capacitance sensors and about 72,500 groundwater level readings were collected from four pressure transducers. Ranges and variances found among sensors from the same soil conditions varied significantly. Thus, each sensor data set was used to develop a sensor specific soil water characteristic curve. Variability observed in the same soil conditions could be attributed to contact interference of the probe with the soil due to air gaps, instrumentation deficiencies and/or site specific conditions of soil profile.

From the soil water summary in Table 4-3 of all collected data, the greatest means of volumetric soil water content were at the shallowest depth (i.e., 10 cm) for lychee trench, lychee no trench and trench soil conditions. The standard deviations were also greater for data collected at this depth which was likely due to greater exposure of shallow soil depths to weather factors including rainfall and freeze protection irrigation. The spikes of soil water content observed in January 2009 were related to freeze protection and sensors responded differently according to their location and distance from the sprinklers.

The selected representative sensors in Figure 4-5 show the soil water dynamic response to rainfall events and mean groundwater table elevation (WTE) fluctuations. The plotted data indicates the influence of storms from the end of September 2008 to the beginning of October 2008. Data collected from the beginning of dry season (November) until March 2009 provided a period of fewer rain events. This dry period offered the conditions to collect most of the data representing a soil water state of equilibrium. This filtered data set is summarized in Table 4-3.

The groundwater level data range from field measurements was verified by comparing the range of the collected data to that of groundwater monitoring well (well 196A) maintained by the

United States Geological Survey (USGS, 2009), located less than 100 m south of the study site. Monthly groundwater records from USGS (2009) had very similar monthly means with the 4 monitoring wells (Table 4-4). The historical monthly medians (1950-2008) reported by USGS were below the monthly medians measured in the groundwater monitoring wells every month except September. All the collected values were within the USGS historical range and it could be concluded that the data collected accurately represented the groundwater level. Considering that the drained to equilibrium model's dependent variable (x-axis) is the DSM or adjusted groundwater table depth. The levels obtained during the study were higher than historical medians. However, distances from the deepest sensors (60 cm) to the groundwater level less than 120 cm were not obtained during the studied period.

Drained to Equilibrium Soil Water Characteristic Curves

Results of fitted curves and parameters are shown in Figures 4-6 to 4-8 and Tables 4-5 to 4-8. Filtering the collected dataset for points that met the drain to equilibrium assumption resulted in 75 data points (representing mean values) per sensor. Data from each sensor were used with the van Genuchten model (1980) and fitted parameters were determined (Tables 4-5 to 4-8). For each soil condition, a model was developed considering all daily mean values of the same category (e.g., one category was all data from lychee trench 10 cm depth conditions).

The fitted parameters at 10 cm in Table 4-5 indicate a greater variance in the n fitting parameter compared to the remaining soil conditions at the same depth (Table 4-6 to 4-8). Parameter n represents the slope of the curves and generally indicates the differences in rate of soil water depletion. The variability observed in the lychee trench treatment could be due to the variability in root systems and soils expected in lychee trenched conditions. Alternatively, most of the soil conditions had similar values for the saturated water content (average 0.26) and air entry ($\alpha = 0.005$). From the fitted van Genuchten equation, the inflection point derived from

Dexter and Bird (2001) for all mean soil conditions in Table 4-5 were very similar for all the sites ($\theta_{infl} = 0.14$).

Soil water results from all sensors showed certain patterns of water replenishment and depletion related to depth. Generally it is expected to find more variation in the vertical soil profile as compared to horizontal soil profile due to variability associated with structure, compaction and layering. Skaggs et al. (1978b) remarked about the vertical heterogeneity feature and explained that superficial profiles tend to have higher porosity than the deeper layers. Bruce and Luxmoore (2003) explained situations where the curves may vary more with depth than with area in response to compaction. For this study, many of the soil water characteristic curves illustrated this phenomenon (Figure 4-6, 4-7 and 4-8).

Vertical variability was observed for most sites as illustrated by the decreasing pore size distribution parameter (*n*) with increasing depth (Table 4-5). For example, *n* values calculated for all data in lychee trenched conditions were 21.123, 16.093, 10.808, and 2.115 for 10, 20, 40, and 60 cm depths, respectively. However, soil water content results also varied in small horizontal distances although it was the same soil type and soil condition. Soil horizontal variability as discussed by Becket and Webster (1971) and Warrick et al. (1977) requires interpretation according to common factors. Variation was found to be greater in sample points close to the soil surface. The horizontal variations identified in the same soil condition suggest the presence of structural heterogeneity.

The lychee trench soil water characteristic curves from probes A1 to A8 (Figures 4-6 and 4-7) generally suggest a break point of depletion at 180 cm of pressure head (DSM) not seen in the trench probes or the non trenched soil conditions. This breakpoint suggests a threshold were

bubbling pressure breaks and depletion begins. Thus, pressure head close to 180 cm could indicate the limit of capillary contribution.

Data from the lychee no trenched soil condition had similar patterns among sensor depths but different saturated water contents. In spite of the limited groundwater table range obtained during the study, the continuity found among certain curves of different depths in the same probe suggested similar soil conditions at certain depth ranges and therefore the possibility to combine datasets to increase the range of pressure head observations available to characterize the soil water content characteristic curve. Specifically, probes B1, B2, B4, B5, B6 and B7 at 40 and 60 cm depth (Figures 4-6 and 4-7) represented similar strata of the limestone and could be combined to capitalize on this benefit. These curves had a more steady depletion rate where large changes in suction responded to small changes in soil water content. In the graphs from the mentioned probes, a different curve was identified for the 10 cm depth sensor which represented the Krome scarified layer.

Water content at field capacity by definition refers to an average suction of 100 kPa (100 cm of water pressure head). If it is assumed that the saturated soil water content is close to the effective porosity and we compare the results from all the fitted curves of the study (which had a similar value, generally close to 0.26), it can be concluded that most of the curves had a very limited water holding capacity where the field capacity was very close to the saturated soil water content. These results are supported by previous in situ soil water characteristic curves by Nuñez-Elisea et al. (2001) were tensiometers at 0 suction presented the similar θs parameters found in this study at 100 cm of pressure head. This data could also help to discard the possibility of a bimodal porosity at lower suction rates. However, more information is required to determine if the soil water characteristic curves would be better described using a bimodal

porosity where more than one soil water inflection point is identified. For this condition, multimodal retention functions as described in detail by Durner (1994) could be used. If this is the case, groundwater levels at closer depths will be required to capture the gravel macro pore fraction of the soil water depletion. Finding soil water dynamics at closer DSM observations (< 0.1 m) would be required to capture this phenomenon, for the case of a dry season were drained to equilibrium conditions prevail these lengths are unusual.

Considering that fruit tree root systems that grow in trenches of calcareous soils are located in the top 30 cm of the soil profile (Zekri et al., 1999) and that most of the roots concentrate in the top 10 cm layer (Núñez-Elisea et al., 2000), it can be concluded that from all the fitted parameters in this study, lychee trenched curves at depths at 10 and 20 cm can contribute to assess irrigation practices based on capillary rise contribution.

Predicting Soil Water Based on Groundwater Level Observations

Differences among soils in terms of retention and water movement depend to a large extent on pore size and shape distributions. The interpretation of the drain to equilibrium data as a field soil water characteristic curve using van Genuchten's model (1980) adds meaning to the evaluation because the van Genuchten model is considered an analytical expression with fitted hydraulic parameters that have a physical basis. The models proposed for each sensor were determined by fitting the parameters shown in Tables 4-5, 4-6, 4-7 and 4-8 to Equation 4-3. The model's capacity to explain the relationship between groundwater level and soil volumetric water content was estimated using the C_{eff} accuracy of predictions which was in general greater than the mean value of the observed data. Time series comparisons of the 96 models (Figures 4-9, 4-10 and 4-11) indicate that groundwater level has a greater influence on the soil water content of the deepest layers of the trench (40 and 60 cm) as compared to the shallower layers of the trench (10 and 20 cm). This is evident by observing the beginning of the time series between the months

of November and December 2008. From this point, model predictions tend to underestimate soil water content compared to the predictions occurring near the end of January. During this period, soil water observations were not completely related to groundwater fluctuations as remaining moisture from precipitation and freeze protection events also influenced soil water content. This situation is more evident in the 10 and 20 cm depths where greater exposure to evapotranspiration rates occurs.

Simplifying results

The results from this study have the potential to be converted into a practical approach to assess capillary rise of a shallow groundwater table. The vertical variability in the observed soil conditions required a different prediction model for different depths. To simplify the results found in this study, a fitted parameter from all data is presented at the end of each soil condition from Table 4-5 to Table 4-8. Pair-wise multiple comparisons among means of these fitted curves was completed with Duncan test ($\alpha = 0.05$; Table 4-9). The results grouped the categories generally by depth. Similarities were found between the soil conditions of lychee trench and lychee no trench at 10 cm depth, likely due to the Krome scarified layer both categories have in common. Duncan groupings indicated that three of the four 20 cm depth conditions were not significantly different. The same result was found with the 60 cm depth. However, the 40 cm depth conditions for soil water content were shown to be significantly different. The use of Duncan means multiple comparisons suggest that different soil conditions may use a common soil water characteristic curve for only the 20 and 60 cm depth. Difference observed at 10 and 40 cm depths may be due to differences in soil structure; however, additional work is needed to verify this.

Applications of the model

The drained to equilibrium interpretation of capillary rise captured the main trends of soil water status according to water table depth. However, the model is not appropriate for estimating sub-daily soil water conditions. The methodology used in this study is applicable to different soil types, elevations and locations which makes it a practical tool. To best parameterize a model, selection of a representative site for soil water content monitoring is critical and should consider surface elevation and soil structure variations. These factors represent some of the most sensitive parameters influencing capillary contribution to plant water uptake.

Contributions from groundwater to soil water content could be assessed using the model developed in this study. This contribution could be integrated into irrigation management through the following steps:

1. Calculate soil volume according to area and depth to be irrigated.
2. Multiply the soil volume by porosity to obtain water volume to be filled.
3. Use drained to equilibrium fitted parameters in van Genuchten's equation (1980) to estimate soil water status (pick one set of "all data" parameters according to the soil conditions).
4. Estimate the field capacity of the soil with drained to equilibrium model (assuming field capacity refers to average suction of 100 cm of water pressure head).
5. Measure water table depth and use it as reference to estimate soil water status with the drained to equilibrium model.
6. Subtract the soil water status according to the water table depth from the desired field capacity.
7. Multiply the difference of soil water to be supplemented with the soil volume to be irrigated.
8. Estimate the water to be applied per hectare.

Implementing this model to assess irrigation requirements could help reduce standard irrigation. Considering that the average grower applies about 37.9 L/day, the drained to

equilibrium procedure using the lychee trench parameters at 20 cm depth could potentially reduce irrigation rates according to the water table depth (Figure 4-12). From the soil water holding capacity perspective, irrigation requirements would not be necessary if the water table is close to the root zone up to a depth of 200 cm. However, water requirements according to the phenological stage of the plant and daily ET is not considered for these purposes. If this is the case, given the low changes of soil water content in large changes of pressure, low volume high frequency irrigation is recommended if water table is between 100 and 200 cm depth were the bubbling pressure appears to break.

The importance of the drained to equilibrium conditions

In order to extend the model's capacity of prediction beyond the drained to equilibrium conditions, selected parameters from the lychee trench soil conditions were tested to predict soil water content during the entire study period. The C_{eff} results were not as satisfactory as those reported in Tables 4-5 to 4-8. The accuracy of the predictions in all the depths was reduced underestimating observations because the sensors were reporting remaining soil water from water inputs. This point highlights the importance of properly identifying drain to equilibrium for an accurate prediction.

In many circumstances, the soil water holding characteristics make it difficult to capture the drain to equilibrium condition; the effect of hysteresis is difficult to distinguish between the drying of wetting processes with field data. Nonetheless, the aquifer's high permeability and the soil's low water holding capacity are driving factors that allow the drained to equilibrium conditions to be obtained. As a result, the relationship found between soil water content and groundwater level using this simple and practical one-dimensional model is maintained when hydrostatic assumptions are valid. In this study, this corresponds to periods when water table is declining and low rainfall is reported, coinciding with the dry season in South Florida. This

season corresponds to the period when capillary rise has the potential to supply a part of the irrigation requirements, or if in excess damage the crop roots (unlikely to happen during the dry season at current levels at the study site). The simple model presented allows the determination of possible soil water content with groundwater level alteration. It is important to understand that the values of the parameters obtained from retention models are based on field observations of soil water content and pressure head. Model validity can only be assumed within the limits of the observed results (DSM range). Extrapolation of model values outside the range of input (DSM) are not reliable and should only be used as an indication of the trends. To extend the model, future research should focus on gathering field data for conditions when the groundwater level is closer to the installed sensors or to perform studies in a laboratory setting where conditions can be controlled. Finally, our results clearly indicate that groundwater level is an important factor to consider for explaining the soil water content variation in this area and that this effect needs to be considered in CERP management alternatives.

Conclusions

Soil water content is strongly related to the shallow groundwater level. Hydrostatic assumptions can be used to investigate capillary rise in shallow groundwater table conditions. This was successfully done by measuring soil water content and groundwater level and fitting data using the van Genuchten (1980) equation. Horizontal and vertical variations in the data required that each sensor be described using a different model. Field capacity was found to be very close to the saturated water content parameter confirming the low water holding capacity of the soils.

Using groundwater level as a reference to predict soil water content is possible and can be considered as a simple and useful one dimensional model technique. Accuracy of predictions had an overall $C_{eff} \approx 0.72$ and responded better at greater depths. The proposed model was able to

capture the general and most representative trends of soil water content changes in response to the shallow groundwater fluctuations. Applications of this approach to assess the soil water status using water table depth as a reference seemed to satisfy the soil water requirements when the water table depth ranges are less than 200 cm of the reference point.

Table 4-1. Monitoring well locations and elevation specifications.

Station name	ID	Latitude N (decimal degrees)	Longitude W (decimal degrees)	Well diameter (m)	Well depth to surface (m)	Riser elevation NGVD[1] 1929 (m)	Surface elevation NGVD 1929 (m)	Reference above benchmark (m)
Well 1	W1	25.5105	80.4990	0.051	8.530	3.106	3.149	0.043
Well 2	W2	25.5101	80.4990	0.051	8.530	2.941	2.954	0.013
Well 3	W3	25.5105	80.4993	0.051	8.530	3.164	3.228	0.064
Well 4	W4	25.5101	80.4993	0.051	8.530	3.057	3.057	0.000

[1] NGVD: National Geodetic Vertical Datum.

Table 4-2. Soil water sensors categorized in 16 different soil conditions.

Soil conditions	Depth (cm)	Number of sensors	Probes
Lychee Trench	10	8	A1 to A8
Lychee Trench	20	8	A1 to A8
Lychee Trench	40	8	A1 to A8
Lychee Trench	60	8	A1 to A8
Lychee No Trench	10	8	B1 to B8
Lychee No Trench	20	8	B1 to B8
Lychee No Trench	40	8	B1 to B8
Lychee No Trench	60	8	B1 to B8
Trench	10	4	A9 to A12
Trench	20	4	A9 to A12
Trench	40	4	A9 to A12
Trench	60	4	A9 to A12
No Trench	10	4	B9 to B12
No Trench	20	4	B9 to B12
No Trench	40	4	B9 to B12
No Trench	60	4	B9 to B12

Table 4-3. Summary of all and filtered volumetric soil water content daily means at each soil condition from 16 September 2008 to 23 March 2009.

Soil conditions	Depth (cm)	θ (m^3/m^3) All				θ (m^3/m^3) Filtered			
		Mean	Std Dev	Minimum	Maximum	Mean	Std Dev	Minimum	Maximum
Lychee Trench	10	0.234	0.080	0.051	0.366	0.224	0.088	0.051	0.364
Lychee Trench	20	0.204	0.045	0.069	0.278	0.200	0.046	0.079	0.276
Lychee Trench	40	0.214	0.031	0.066	0.261	0.215	0.025	0.114	0.258
Lychee Trench	60	0.219	0.015	0.196	0.260	0.217	0.014	0.196	0.257
Lychee No Trench	10	0.256	0.033	0.206	0.340	0.254	0.033	0.209	0.337
Lychee No Trench	20	0.206	0.027	0.129	0.272	0.204	0.026	0.146	0.269
Lychee No Trench	40	0.212	0.019	0.167	0.262	0.211	0.019	0.167	0.255
Lychee No Trench	60	0.218	0.030	0.144	0.266	0.218	0.029	0.144	0.260
Trench	10	0.240	0.032	0.131	0.295	0.238	0.030	0.166	0.290
Trench	20	0.236	0.021	0.182	0.280	0.235	0.020	0.198	0.278
Trench	40	0.240	0.021	0.195	0.283	0.241	0.020	0.203	0.281
Trench	60	0.230	0.014	0.198	0.264	0.230	0.013	0.201	0.259
No Trench	10	0.197	0.044	0.021	0.309	0.189	0.039	0.022	0.300
No Trench	20	0.172	0.039	0.009	0.248	0.165	0.031	0.032	0.242
No Trench	40	0.189	0.038	0.108	0.264	0.185	0.038	0.133	0.245
No Trench	60	0.227	0.020	0.195	0.274	0.225	0.021	0.195	0.261

Table 4-4. Summary of entire dataset of groundwater daily means and comparison with USGS well 196A historical database.

Month	Year	Well ID	Surface Elevation NGVD 1929 (m)	Water Table Elevation NGVD 1929 (m)				
				Mean	Std Dev	Minimum	Maximum	Median
September	2008	W1	3.15	1.14	0.06	1.01	1.39	1.12
September	2008	W2	2.95	1.14	0.06	1.02	1.38	1.13
September	2008	W3	3.23	1.20	0.06	1.08	1.43	1.18
September	2008	W4	3.06	.	.	.	.	.
September	2008	USGS 196A	3.15	1.14		1.06	1.36	
September	1950-2008	USGS 196A	3.15			0.72	2.15	1.28
October	2008	W1	3.15	1.31	0.09	1.16	1.57	1.29
October	2008	W2	2.95	1.30	0.09	1.15	1.61	1.29
October	2008	W3	3.23	1.37	0.09	1.23	1.64	1.36
October	2008	W4	3.06	1.32	0.08	1.21	1.60	1.31
October	2008	USGS 196A	3.15	1.33		1.22	1.60	
October	1950-2008	USGS 196A	3.15			0.88	1.83	1.24
November	2008	W1	3.15	1.15	0.03	1.06	1.21	1.15
November	2008	W2	2.95	1.09	0.05	0.91	1.21	1.09
November	2008	W3	3.23	1.19	0.03	1.13	1.25	1.19
November	2008	W4	3.06	1.14	0.06	0.96	1.29	1.14
November	2008	USGS 196A	3.15	1.15		1.08	1.21	
November	1950-2008	USGS 196A	3.15			0.70	1.89	1.05
December	2008	W1	3.15	1.07	0.02	1.02	1.15	1.06
December	2008	W2	2.95	1.04	0.03	0.95	1.12	1.04
December	2008	W3	3.23	1.13	0.02	1.08	1.18	1.12
December	2008	W4	3.06	1.08	0.03	0.99	1.16	1.09
December	2008	USGS 196A	3.15	1.06		1.04	1.09	
December	1950-2008	USGS 196A	3.15			0.43	1.32	0.96
January	2009	W1	3.15	1.02	0.03	0.91	1.06	1.03
January	2009	W2	2.95	0.96	0.04	0.85	1.04	0.96
January	2009	W3	3.23	1.08	0.03	1.00	1.12	1.09
January	2009	W4	3.06	1.02	0.04	0.88	1.12	1.02
January	2008	USGS 196A	3.15	1.01		0.94	1.05	
January	1950-2008	USGS 196A	3.15			0.30	1.39	0.89
February	2009	W1	3.15	0.87	0.02	0.81	0.94	0.87
February	2009	W2	2.95	0.83	0.06	0.72	0.97	0.80
February	2009	W3	3.23	0.95	0.04	0.85	1.04	0.94
February	2009	W4	3.06	0.86	0.07	0.73	1.06	0.84
February	2009	USGS 196A	3.15	0.87		0.83	0.93	
February	1950-2008	USGS 196A	3.15			0.23	1.19	0.83
March	2009	W1	3.15	0.84	0.08	0.74	1.05	0.81
March	2009	W2	2.95	0.80	0.08	0.69	1.02	0.76
March	2009	W3	3.23	0.89	0.08	0.79	1.11	0.85
March	2009	W4	3.06	0.83	0.09	0.70	1.07	0.80
March	2009	USGS 196A	3.15	0.87		0.74	1.02	
March	1950-2008	USGS 196A	3.15			0.07	1.15	0.82

Table 4-5. Drained to equilibrium fitted parameters of van Genuchten's model (1980) used to describe field soil water characteristic curves at 10 cm depth of Krome soil in a lychee orchard at four different soil conditions.

Soil conditions	Probe ID	θ_s [a]	θ_r [b]	α [c]	n [d]	m [e]	r^2 [f]	C_{eff} [g]
Lychee Trench	A1-10	0.257	0.000	0.005	14.987	0.933	0.786	0.781
Lychee Trench	A2-10	0.229	0.000	0.004	5.950	0.832	0.834	0.834
Lychee Trench	A3-10	0.405	0.000	0.004	3.570	0.720	0.645	0.646
Lychee Trench	A4-10	0.285	0.000	0.005	14.973	0.933	0.819	0.819
Lychee Trench	A5-10	0.266	0.000	0.005	43.027	0.977	0.887	0.887
Lychee Trench	A6-10	0.274	0.000	0.005	29.074	0.966	0.734	0.734
Lychee Trench	A7-10	0.373	0.000	0.004	9.791	0.898	0.546	0.546
Lychee Trench	A8-10	0.251	0.000	0.005	56.777	0.982	0.733	0.733
Lychee Trench	All data*	0.286	0.000	0.005	21.122	0.953	0.811	0.809
Trench	A9-10	0.235	0.000	0.005	16.767	0.940	0.823	0.823
Trench	A10-10	0.299	0.000	0.004	9.620	0.896	0.759	0.759
Trench	A11-10	0.351	0.000	0.004	2.320	0.569	0.759	0.753
Trench	A12-10	0.260	0.000	0.005	15.511	0.936	0.780	0.779
Trench	All data*	0.270	0.000	0.005	12.582	0.921	0.797	0.497
Lychee No Trench	B1-10	0.261	0.000	0.005	11.926	0.916	0.677	0.677
Lychee No Trench	B2-10	0.272	0.000	0.004	5.761	0.826	0.637	0.638
Lychee No Trench	B3-10	0.269	0.000	0.005	13.090	0.924	0.795	0.794
Lychee No Trench	B4-10	0.293	0.000	0.004	10.455	0.904	0.799	0.793
Lychee No Trench	B5-10	0.406	0.000	0.006	2.012	0.503	0.690	0.689
Lychee No Trench	B6-10	0.393	0.039	0.009	1.251	0.201	0.168	0.169
Lychee No Trench	B7-10	0.298	0.000	0.004	4.469	0.776	0.743	0.744
Lychee No Trench	B8-10	0.271	0.000	0.004	7.501	0.867	0.704	0.704
Lychee No Trench	All data*	0.359	0.000	0.005	2.457	0.593	0.631	0.631
No Trench	B9-10	0.304	0.000	0.005	4.582	0.782	0.891	0.891
No Trench	B10-10	0.383	0.000	0.005	1.831	0.454	0.650	0.649
No Trench	B11-10	0.233	0.000	0.005	7.251	0.862	0.710	0.710
No Trench	B12-10	2.537	0.000	0.115	1.804	0.446	0.788	0.788
No Trench	All data*	0.352	0.000	0.006	4.521	0.779	0.848	0.848

[a] Saturated water content (θ_s).
[b] Residual water content (θ_r).
[c] Inverse of the air entry value (α).
[d] Dimensionless measure of pore size distribution (slope) (n).
[e] Curve shape parameter ($m=1-1/n$) (m).
[f] Coefficient of determination of observed values and fitted curve (r^2).
[g] Nash-Sutcliffe (1970) coefficient of efficiency of observed and predicted values (C_{eff}).
[*] Fitted parameters considering all daily mean values of the soil condition.

Table 4-6. Drained to equilibrium fitted parameters of van Genuchten's model (1980) used to describe field soil water characteristic curves at 20 cm depth of Krome soil in a lychee orchard at four different soil conditions.

Soil conditions	Probe ID	θ_s [a]	θ_r [b]	α [c]	n [d]	m [e]	r^2 [f]	C_{eff} [g]
Lychee Trench	A1-20	0.267	0.000	0.005	10.077	0.901	0.796	0.796
Lychee Trench	A2-20	0.227	0.000	0.005	7.087	0.859	0.844	0.844
Lychee Trench	A3-20	0.281	0.000	0.005	11.013	0.909	0.854	0.854
Lychee Trench	A4-20	0.260	0.000	0.005	12.604	0.921	0.836	0.836
Lychee Trench	A5-20	0.278	0.000	0.005	31.136	0.968	0.864	0.863
Lychee Trench	A6-20	0.253	0.000	0.006	25.541	0.961	0.806	0.806
Lychee Trench	A7-20	0.256	0.000	0.005	18.278	0.945	0.837	0.838
Lychee Trench	A8-20	0.234	0.000	0.005	19.841	0.950	0.607	0.607
Lychee Trench	All data*	0.256	0.000	0.005	16.093	0.938	0.836	0.836
Trench	A9-20	0.256	0.000	0.005	12.603	0.921	0.852	0.852
Trench	A10-20	0.261	0.000	0.005	7.950	0.874	0.901	0.901
Trench	A11-20	0.341	0.000	0.005	2.021	0.505	0.856	0.857
Trench	A12-20	0.625	0.000	0.017	1.750	0.429	0.697	0.697
Trench	All data*	0.266	0.000	0.005	10.339	0.903	0.872	0.872
Lychee No Trench	B1-20	0.219	0.000	0.005	12.133	0.918	0.747	0.746
Lychee No Trench	B2-20	0.220	0.000	0.005	7.582	0.868	0.775	0.775
Lychee No Trench	B3-20	0.256	0.000	0.005	7.928	0.874	0.762	0.762
Lychee No Trench	B4-20	0.276	0.000	0.005	9.195	0.891	0.836	0.835
Lychee No Trench	B5-20	0.260	0.000	0.005	8.006	0.875	0.763	0.762
Lychee No Trench	B6-20	0.258	0.000	0.005	6.272	0.841	0.741	0.741
Lychee No Trench	B7-20	0.247	0.000	0.004	7.254	0.862	0.763	0.763
Lychee No Trench	B8-20	0.250	0.000	0.005	6.651	0.850	0.772	0.771
Lychee No Trench	All data*	0.254	0.000	0.005	6.281	0.841	0.741	0.740
No Trench	B9-20	0.301	0.000	0.006	4.971	0.799	0.899	0.898
No Trench	B10-20	0.328	0.000	0.007	1.900	0.474	0.524	0.522
No Trench	B11-20	0.313	0.000	0.006	3.428	0.708	0.825	0.825
No Trench	B12-20	0.401	0.000	0.009	2.536	0.606	0.832	0.832
No Trench	All data*	0.290	0.000	0.006	4.883	0.795	0.828	0.825

[a] Saturated water content (θ_s).
[b] Residual water content (θ_r).
[c] Inverse of the air entry value (α).
[d] Dimensionless measure of pore size distribution (slope) (n).
[e] Curve shape parameter ($m=1-1/n$) (m).
[f] Coefficient of determination of observed values and fitted curve (r^2).
[g] Nash-Sutcliffe (1970) coefficient of efficiency of observed and predicted values (C_{eff}).
* Fitted parameters considering all daily mean values of the soil condition.

Table 4-7. Drained to equilibrium fitted parameters of van Genuchten's model (1980) used to describe field soil water characteristic curves at 40 cm depth of Krome soil in a lychee orchard at four different soil conditions.

Soil conditions	Probe ID	θ_s [a]	θ_r [b]	α [c]	n [d]	m [e]	r^2 [f]	C_{eff} [g]
Lychee Trench	A1-40	0.268	0.000	0.006	10.078	0.901	0.775	0.775
Lychee Trench	A2-40	0.270	0.000	0.005	4.587	0.782	0.822	0.822
Lychee Trench	A3-40	0.260	0.000	0.005	11.043	0.909	0.866	0.866
Lychee Trench	A4-40	0.335	0.000	0.006	2.185	0.542	0.798	0.799
Lychee Trench	A5-40	0.253	0.000	0.005	10.057	0.901	0.825	0.825
Lychee Trench	A6-40	0.238	0.000	0.006	25.638	0.961	0.872	0.872
Lychee Trench	A7-40	0.244	0.000	0.005	10.726	0.907	0.879	0.879
Lychee Trench	A8-40	0.314	0.000	0.005	2.567	0.610	0.877	0.877
Lychee Trench	All data*	0.256	0.000	0.005	10.808	0.907	0.869	0.869
Trench	A9-40	0.245	0.000	0.005	15.336	0.935	0.820	0.819
Trench	A10-40	0.246	0.000	0.005	10.617	0.906	0.908	0.907
Trench	A11-40	0.342	0.000	0.006	1.584	0.369	0.880	0.881
Trench	A12-40	0.261	0.000	0.005	14.539	0.931	0.872	0.874
Trench	All data*	0.272	0.000	0.005	5.365	0.814	0.843	0.843
Lychee No Trench	B1-40	0.280	0.000	0.007	1.679	0.404	0.798	0.799
Lychee No Trench	B2-40	0.253	0.000	0.005	5.863	0.829	0.890	0.890
Lychee No Trench	B3-40	0.242	0.000	0.005	6.062	0.835	0.880	0.880
Lychee No Trench	B4-40	0.331	0.000	0.006	2.040	0.510	0.881	0.880
Lychee No Trench	B5-40	0.307	0.000	0.006	2.207	0.547	0.835	0.835
Lychee No Trench	B6-40	0.307	0.000	0.007	2.224	0.550	0.869	0.869
Lychee No Trench	B7-40	0.324	0.000	0.007	1.755	0.430	0.871	0.871
Lychee No Trench	B8-40	0.218	0.166	0.008	8.318	0.880	0.658	0.657
Lychee No Trench	All data*	0.306	0.000	0.007	2.045	0.511	0.862	0.862
No Trench	B9-40	0.207	0.000	0.006	2.827	0.646	0.728	0.728
No Trench	B10-40	0.287	0.000	0.009	1.539	0.350	0.553	0.553
No Trench	B11-40	0.465	0.000	0.387	1.169	0.144	0.169	0.436
No Trench	B12-40	0.275	0.160	0.011	3.907	0.744	0.786	0.882
No Trench	All data*	0.375	0.163	0.027	2.048	0.512	0.798	0.796

[a] Saturated water content (θ_s).
[b] Residual water content (θ_r).
[c] Inverse of the air entry value (α).
[d] Dimensionless measure of pore size distribution (slope) (n).
[e] Curve shape parameter ($m=1-1/n$) (m).
[f] Coefficient of determination of observed values and fitted curve (r^2).
[g] Nash-Sutcliffe (1970) coefficient of efficiency of observed and predicted values (C_{eff}).
[*] Fitted parameters considering all daily mean values of the soil condition.

Table 4-8. Drained to equilibrium fitted parameters of van Genuchten's model (1980) used to describe field soil water characteristic curves at 60 cm depth of Krome soil in a lychee orchard at four different soil conditions.

Soils conditions	Probe ID	θ_s [a]	θ_r [b]	α [c]	n [d]	m [e]	r^2 [f]	C_{eff} [g]
Lychee Trench	A1-60	0.263	0.000	0.006	5.845	0.829	0.830	0.830
Lychee Trench	A2-60	0.228	0.209	0.008	41.366	0.976	0.753	0.754
Lychee Trench	A3-60	0.331	0.000	0.008	1.735	0.424	0.753	0.754
Lychee Trench	A4-60	0.318	0.000	0.007	2.009	0.502	0.839	0.839
Lychee Trench	A5-60	0.301	0.000	0.007	2.390	0.582	0.832	0.832
Lychee Trench	A6-60	0.466	0.099	0.020	2.198	0.545	0.895	0.895
Lychee Trench	A7-60	0.249	0.000	0.006	5.856	0.829	0.903	0.903
Lychee Trench	A8-60	0.326	0.000	0.008	1.879	0.468	0.847	0.848
Lychee Trench	All data*	0.313	0.000	0.007	2.115	0.527	0.870	0.870
Trench	A9-60	0.295	0.000	0.007	2.236	0.553	0.807	0.807
Trench	A10-60	0.280	0.000	0.005	1.776	0.437	0.471	0.777
Trench	A11-60	0.318	0.000	0.009	1.551	0.355	0.918	0.918
Trench	A12-60	0.337	0.000	0.008	1.679	0.404	0.842	0.842
Trench	All data*	0.325	0.000	0.009	1.630	0.386	0.856	0.856
Lychee No Trench	B1-60	0.513	0.216	0.024	5.889	0.830	0.024	-2.391
Lychee No Trench	B2-60	0.285	0.000	0.008	1.709	0.415	0.936	0.936
Lychee No Trench	B3-60	0.252	0.000	0.012	1.708	0.415	0.812	0.812
Lychee No Trench	B4-60	0.308	0.000	0.007	1.534	0.348	0.948	0.949
Lychee No Trench	B5-60	0.349	0.024	0.037	1.266	0.210	0.923	0.922
Lychee No Trench	B6-60	0.288	0.108	0.109	1.173	0.147	0.147	0.397
Lychee No Trench	B7-60	0.271	0.000	0.007	1.336	0.252	0.560	0.766
Lychee No Trench	B8-60	0.428	0.218	0.026	2.523	0.604	0.417	0.416
Lychee No Trench	All data*	0.268	0.000	0.006	1.514	0.339	0.757	0.757
No Trench	B9-60	0.288	0.000	0.012	1.350	0.259	0.529	0.528
No Trench	B10-60	0.239	0.080	0.073	1.092	0.084	0.052	0.052
No Trench	B11-60	0.237	0.361	0.004	1.971	0.493	0.049	0.049
No Trench	B12-60	0.193	0.226	1.244	1.122	0.109	0.001	-0.028
No Trench	All data*	0.270	0.086	0.027	1.130	0.115	0.281	0.281

[a] Saturated water content (θ_s).
[b] Residual water content (θ_r).
[c] Inverse of the air entry value (α).
[d] Dimensionless measure of pore size distribution (slope) (n).
[e] Curve shape parameter ($m=1-1/n$) (m).
[f] Coefficient of determination of observed values and fitted curve (r^2).
[g] Nash-Sutcliffe (1970) coefficient of efficiency of observed and predicted values (C_{eff}).
[*] Fitted parameters considering all daily mean values of the soil condition.

Table 4-9. Duncan mean multiple comparison of soil water characteristic curves at each soil condition.

Duncan Grouping		θ_{mean} (m^3/m^3)	Soil condition	Depth (cm)
A		0.276	Lychee No Trench	10
B	A	0.269	Lychee Trench	10
B	C	0.262	Trench	10
B	C	0.257	Trench	20
C		0.253	No Trench	10
D		0.229	Trench	40
D		0.225	Lychee Trench	20
E	D	0.223	Trench	60
E	D	0.222	Lychee No Trench	20
E	D	0.222	No Trench	60
E	D	0.217	No Trench	20
E	D	0.215	Lychee No Trench	40
E	D	0.215	Lychee No Trench	60
E		0.210	Lychee Trench	40
	F	0.194	No Trench	40
	F	0.189	Lychee Trench	60

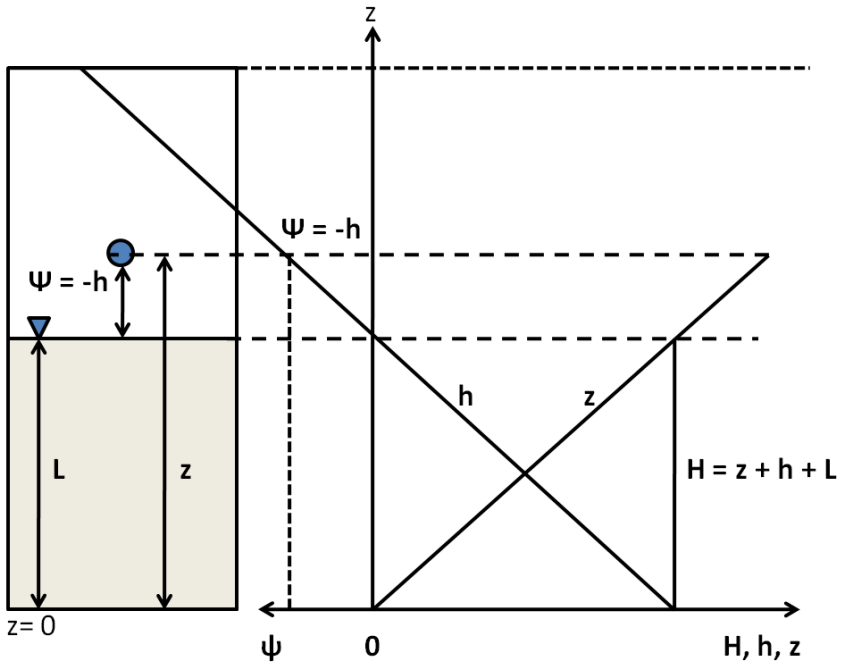

Figure 4-1. Soil water potential in an unsaturated soil column at drained to equilibrium conditions. H=hydraulic potential, h=pressure potential, z=gravimetric potential, L=water table elevation

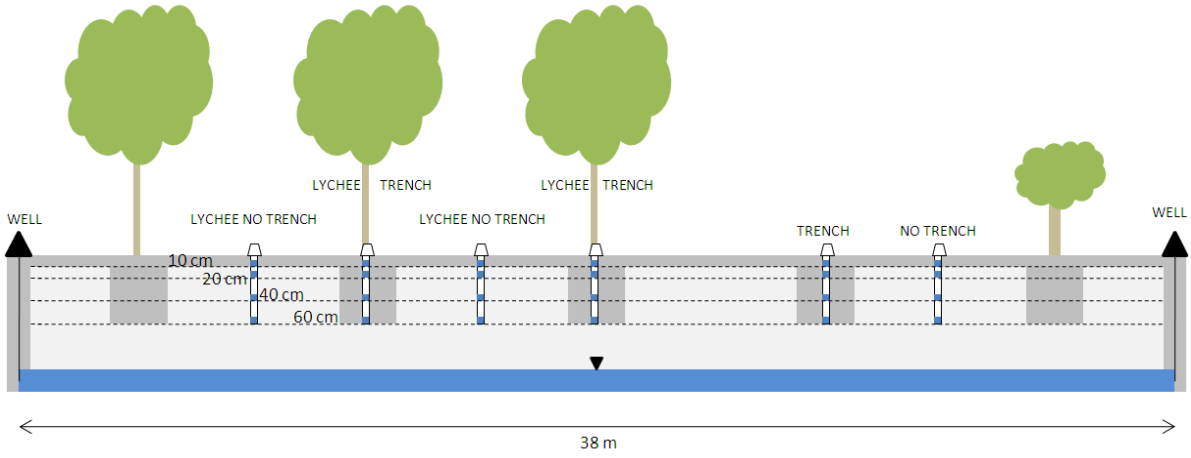

Figure 4-2. Side view schematic of soil conditions studied using monitoring wells and multisensor capacitance probes in the Krome scarified (gray) and limestone bedrock (light) soil profile.

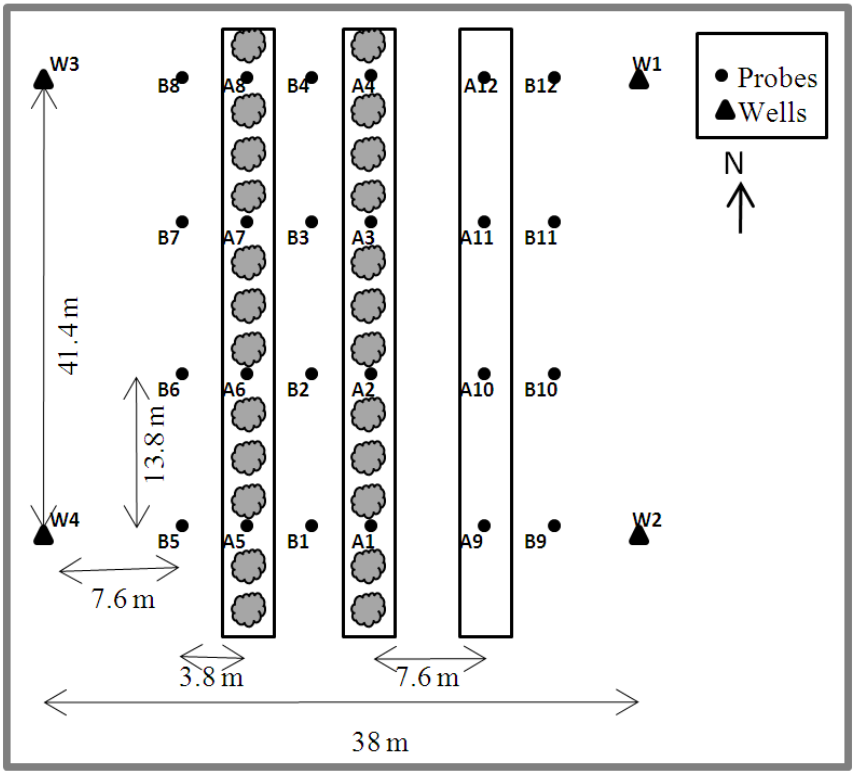

Figure 4-3. Schematic of experimental site at University of Florida Tropical Research and Education Center (TREC), Homestead, FL. “A” symbolized probes located in a trench Krome soil condition and “B” symbolizes probes located in a non trenched limestone soil condition.

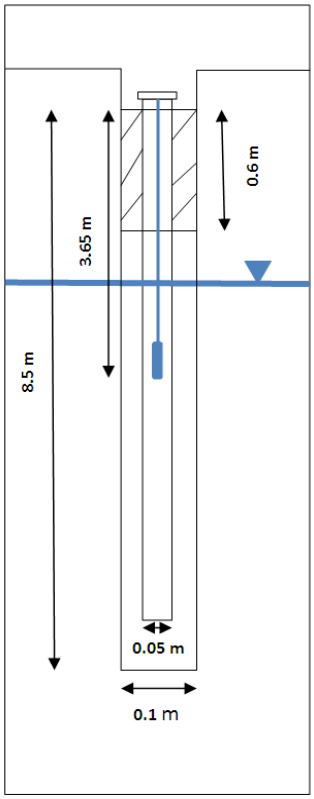

Figure 4-4. Schematic of monitoring well geometry and Levelogger location for monitoring groundwater levels.

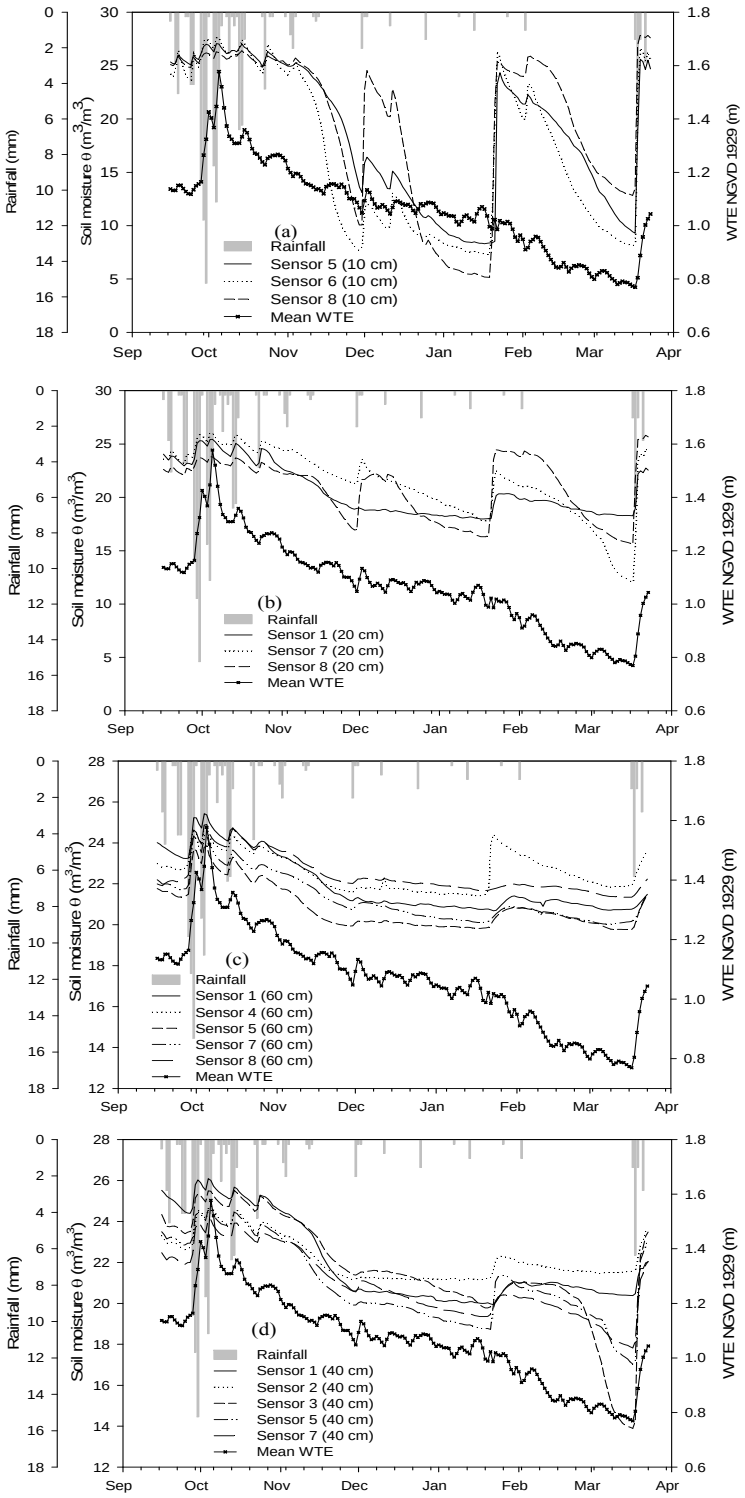

Figure 4-5. Soil water response to groundwater fluctuations from September 2008 to March 2009 in Lychee trench selected sensors at (a) 10 cm, (b) 20 cm, (c) 40 cm and (d) 60 cm depths.

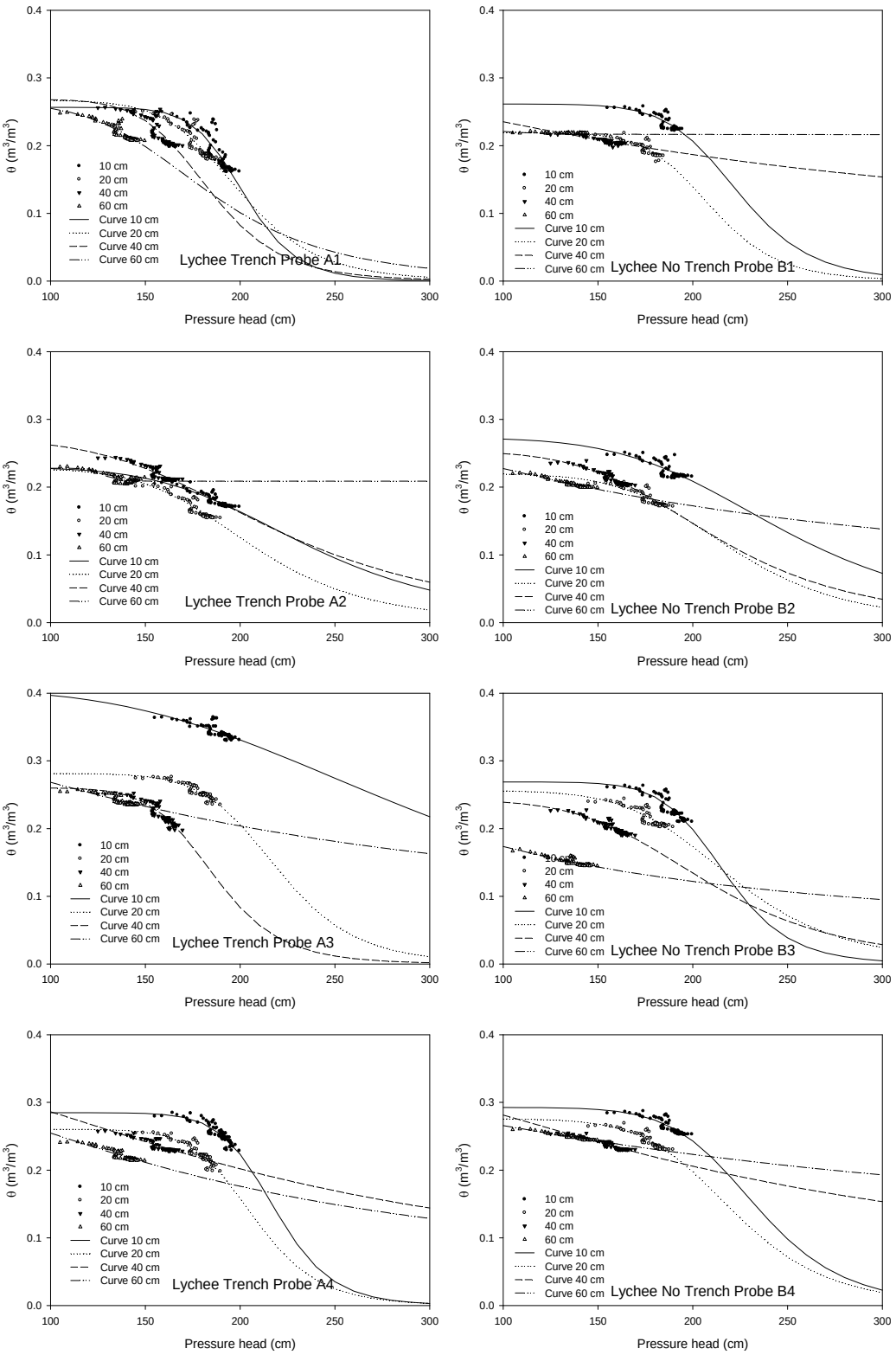

Figure 4-6. Soil water characteristic curves for probes A1 to A4 and B1 to B4 at 10, 20, 40 and 60 cm depths.

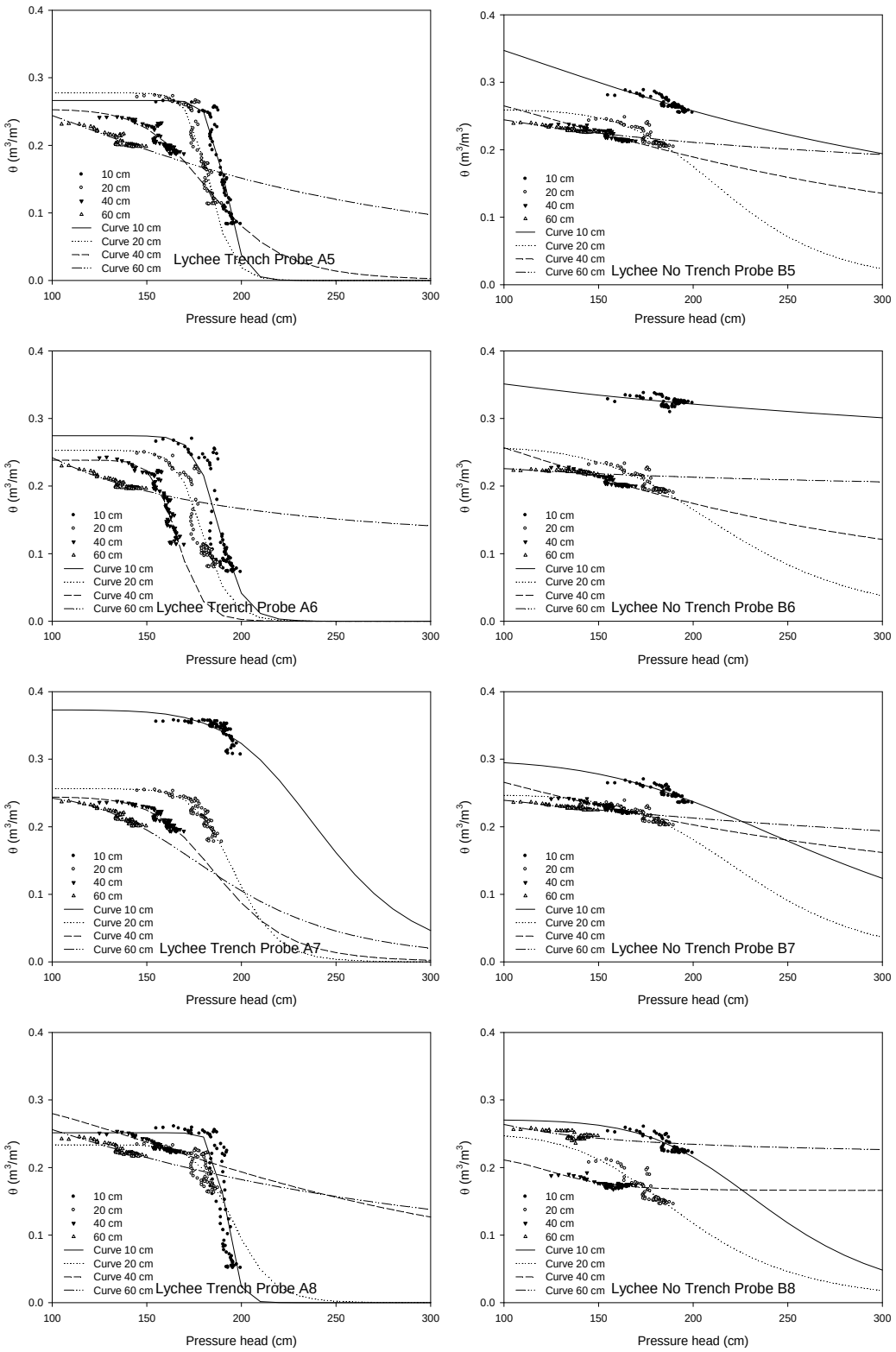

Figure 4-7. Soil water characteristic curves for probes A5 to A8 and B5 to B8 at 10, 20, 40 and 60 cm depths.

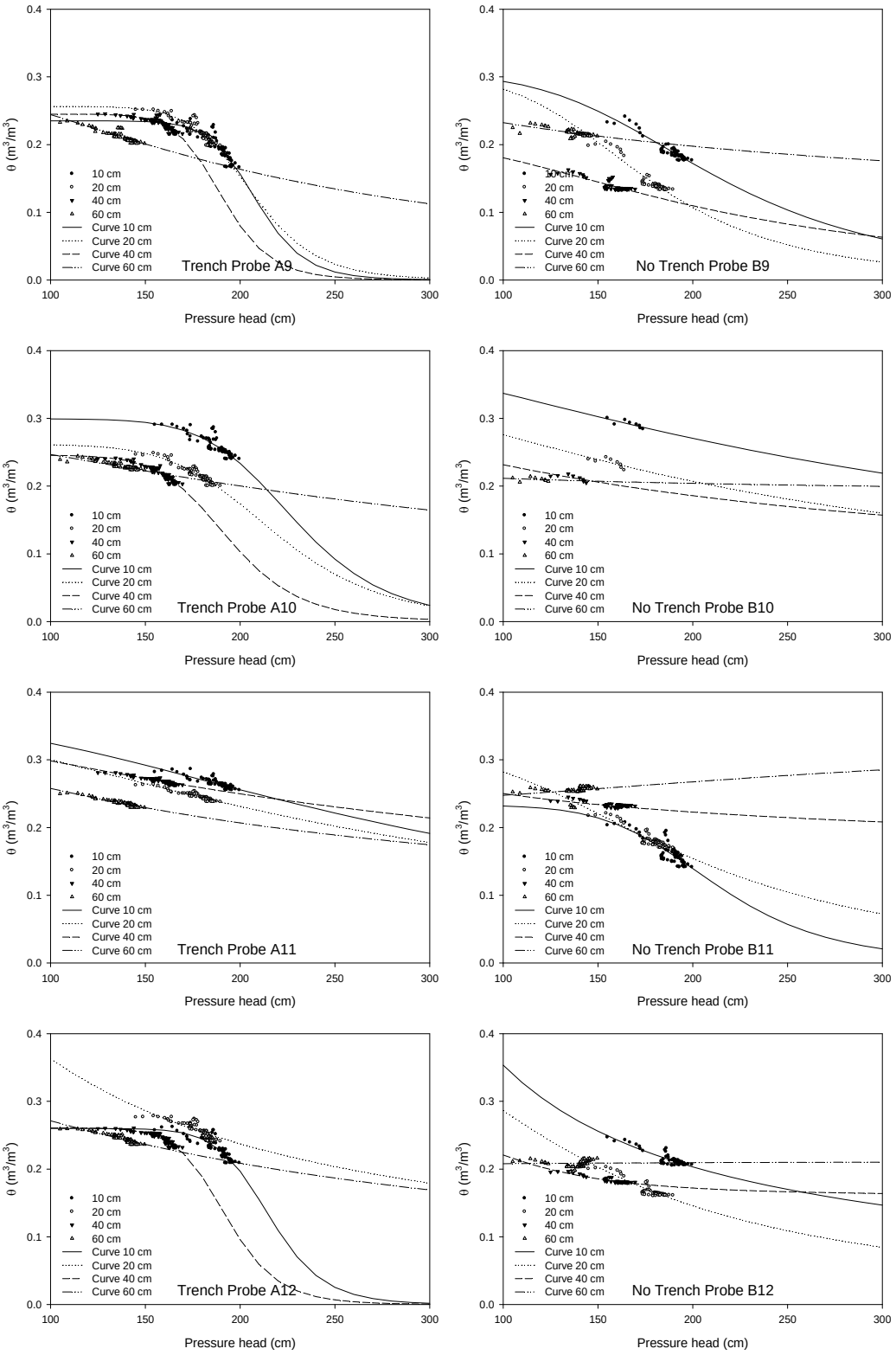

Figure 4-8. Soil water characteristic curves for probes A9 to A12 and B9 to B12 at 10, 20, 40 and 60 cm depths.

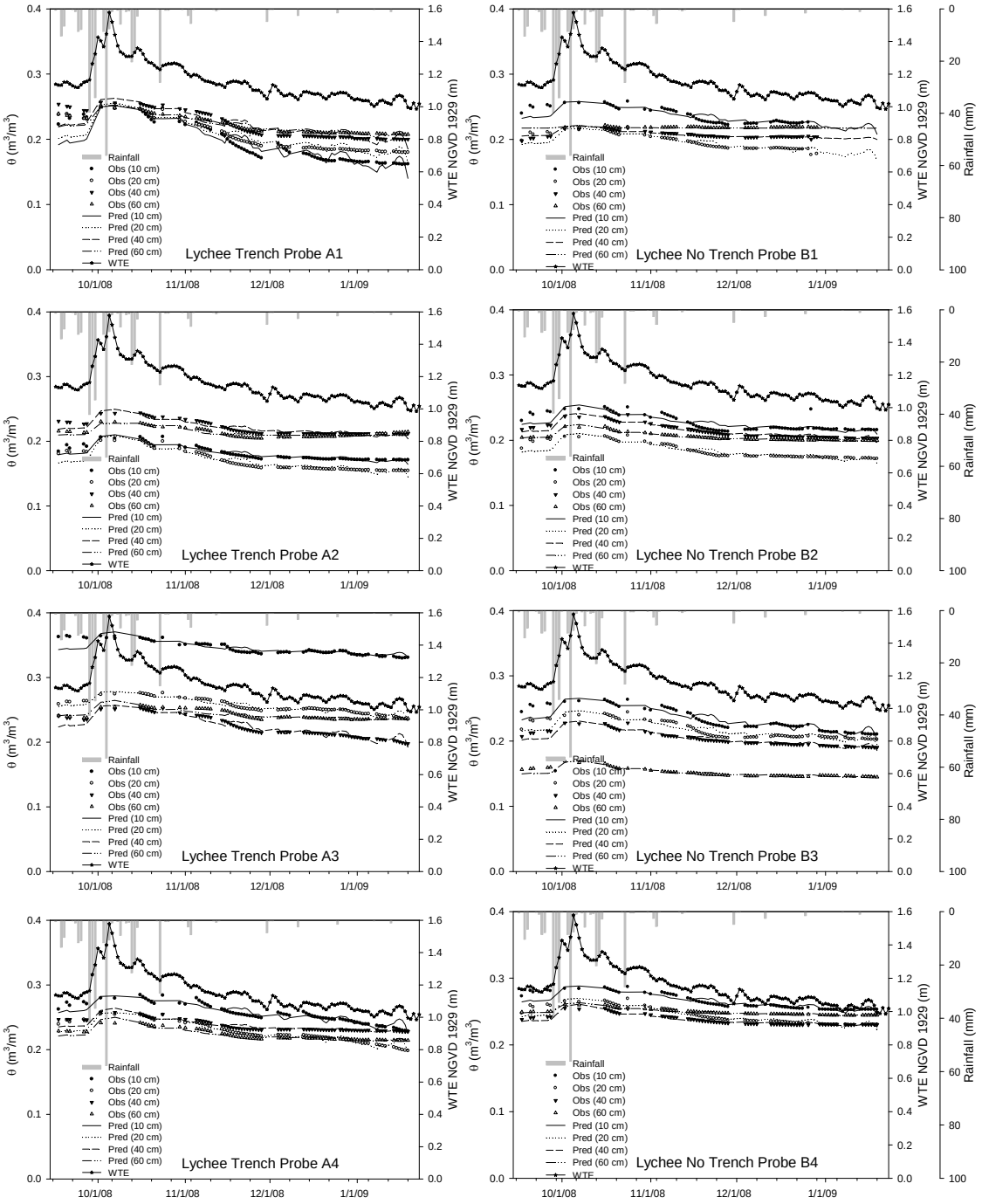

Figure 4-9. Soil water prediction using groundwater level as reference with the fitted parameters of van Genuchten model (1980) for probes A1 to A4 and B1 to B4 at 10, 20, 40 and 60 cm depths.

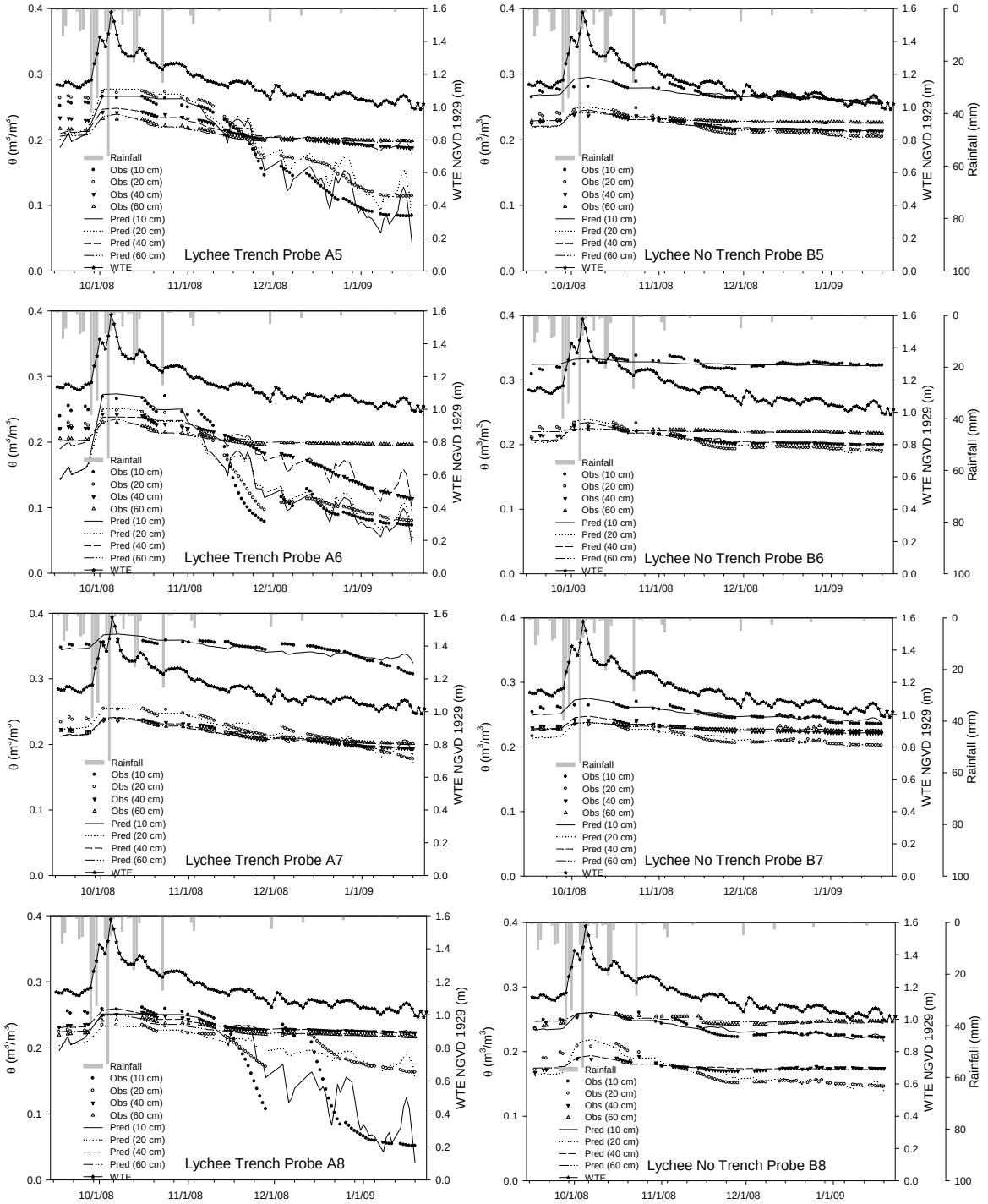

Figure 4-10. Soil water prediction using groundwater level as reference with the fitted parameters of van Genuchten model (1980) for probes A5 to A8 and B5 to B8 at 10, 20, 40 and 60 cm depths.

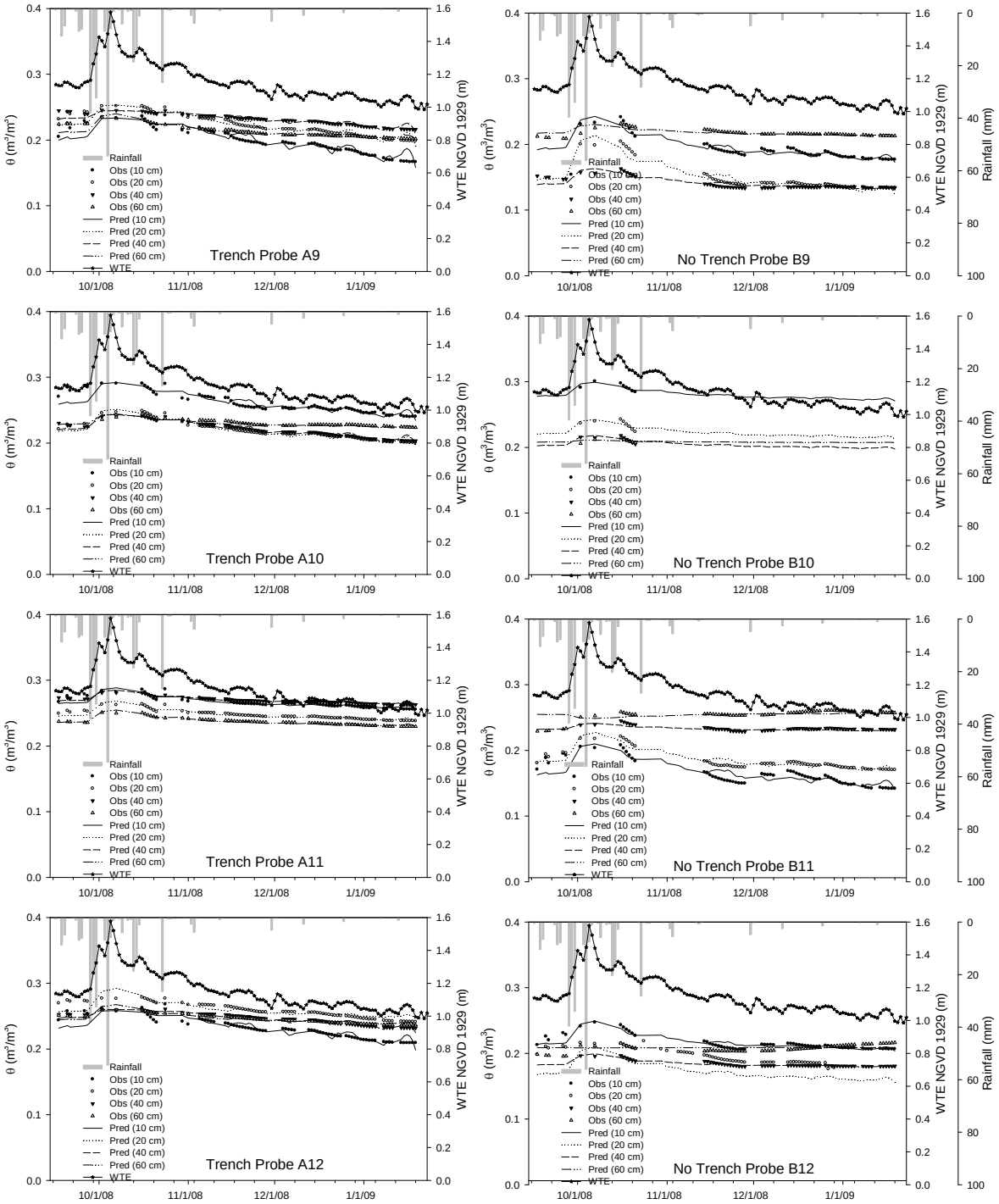

Figure 4-11. Soil water prediction using groundwater level as reference with the fitted parameters of van Genuchten model (1980) for probes A9 to A12 and B9 to B12 at 10, 20, 40 and 60 cm depths.

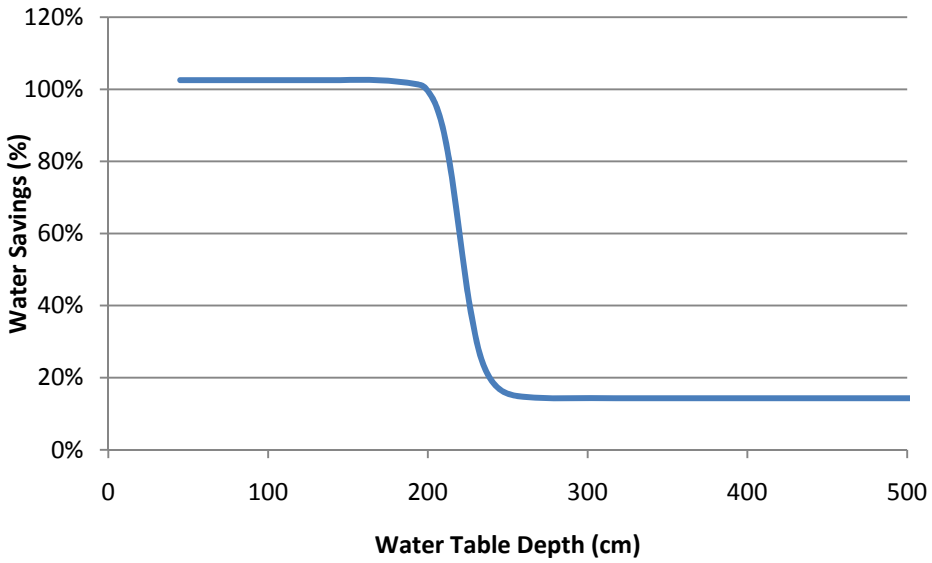

Figure 4-12. Estimation of water savings based on drained to equilibrium assessment of irrigation requirements. Drained to equilibrium model assumes field capacity at 100 H2O cm of suction and compares supplemented irrigation with average grower (10.8 m3/ha).

CHAPTER 5
EXECUTIVE SUMMARY

Quantifying the relationship between groundwater table level and root zone soil water content in shallow groundwater conditions is important in South Florida due to the potential changes in groundwater level related to the Comprehensive Everglades Restoration Plan (CERP) and the resulting impacts these changes may have on deep rooted agriculture. The topic requires long and comprehensive research in multiple disciplines. This study represents a small contribution through three different objectives: soil water instrument calibration, methods of capillary rise interpretation and modeling the unsaturated zone of the soil profile. Results are intended to provide growers with science-based information on the benefits and challenges of the shallow groundwater table in this area.

Objective 1

Laboratory soil water characteristic curves helped to identify similarities in soil water retention patterns and low water holding capacity properties of gravel and limestone bedrock, attributing Krome soils water holding capacity to the loam fraction of the soil. Although gravel and limestone retention patterns were low, the soil water depletion was characterized to have very low volumetric water content changes in large increments of suction.

Onsite calibration of multi sensor capacitance probes using synchronized suction values from tensiometers as a reference to determine volumetric water content is a promising technique for conditions were standard calibration procedures are not possible. However limestone heterogeneity limited the results to an unpractical site specific calibration. Regression equations for instrument calibration in limestone bedrock conditions were characterized by their spatial and depth variability. As a result four regression models were proposed for calibration purposes. Relationships between Al-Yahyai et al. (2006) calibration regression model of Krome soils and

the proposed models were similar at equilibrium conditions, confirming the possibility to use a single calibration equation in Krome scarified and limestone bedrock.

Objective 2

Circular statistics represent a practical approach to interpret diurnal fluctuations of soil water content and groundwater level. Locations of statistically significant mean vectors were confirmed in all instruments and variables with Rayleigh test although many of the vectors were influenced by multimodal distributions attributed to multivariate effects. Mean vectors of soil water content at deeper depths were more related to mean vectors of groundwater; mean vectors of soil water content at shallower depths were more related to solar radiation and soil temperature. Circular-circular correlation analysis confirm in general a weak relationship between diurnal peaks of soil water content and the peaks found in groundwater and weather variables.

Objective 3

A hydrostatic model based on the drained to equilibrium principle was proposed to use groundwater level as a reference to predict soil water content. Predictions indicated this approach can be considered as a simple and useful reference of one-dimensional model technique. The proposed model was able to capture the general and most representative trends of soil water content changes in response to the shallow groundwater fluctuations although accuracy of predictions responded better at greater depths. Results have the potential to improve irrigation practices by considering groundwater contribution to the soil water status in the unsaturated zone.

LIST OF REFERENCES

Abtew, W. 1996. Evapotranspiration measurements and modeling for three wetland systems in South Florida. *Water resources bulletin* 32: 465.

Ali, A., and Abtew. W. 1999. Regional rainfall frequency analysis for central and South Florida. hydrologic reporting unit, South Florida, West Palm Beach, FL.: Water management district water resources evaluation.

Al-Yahyai, R., B. Schaffer, F.S. Davies, and J.H. Crane. 2005. Four levels of soil water depletion minimally affect carambola phenological cycles. *Horttechnology* 15: 623-630.

Al-Yahyai, R., B. Schaffer, F.S. Davies, and R. Munoz-Carpena. 2006. Characterization of soil-water retention of a very gravelly loam soil varied with determination method. *Soil Science* 171: 85-93.

Ayars, J.E., and R.A. Schoneman. 1986. *Use* of saline water from a shallow water table by cotton. *Transactions of the ASAE* 29: 1674-1678.

Babajimopoulos, C., A. Panoras, H. Georgoussis, G. Arampatzis, E. Hatzigiannakis, and D. Papamichail. 2007. Contribution to irrigation from shallow water table under field conditions. *Agricultural Water Management* 92: 205-210.

Batschelet, E. 1981. *Circular Statistics in Biology*. New York: Academic Press.

Bauer, P., G. Thabeng, F. Stauffer, and W. Kinzelbach. 2004. Estimation of the evapotranspiration rate from diurnal groundwater level fluctuations in the Okavango Delta, Botswana. *Journal of Hydrology* 288: 344–355.

Beckett and Webster. 1971. Soil variability: a review. *Soils and Fertilizers.* 34: 1–15.

Beran, R.J. 1969. Asymptotic theory of a class of tests for uniformity of a circular distribution. *Annals of Mathematical Statistics* 40: 1196-1206.

Berger, E. 1976. Partitioning the parameters of stony soils, important in moisture determinations into their constituents. *Plant and Soil* 44: 201-207.

Black, A. and A. Werritty. 1997. Seasonality of flooding: a case study in North Britain. *Journal of Hydrology*, 195: 1-25.

Bouyoucos, G. T. 1915. Effect of temperature on the movement of water vapor and capillary moisture in soil. *Journal of Agricultural Research* 5: 141-172.

Bruce, R.R., and R.J. Luxmoore. 2003. Water Retention: Field Methods. In *Methods of Soil Analysis, Soil Science Society of America Book Series* 5: 663-686.

Buckingham, E. 1907. *Studies on the movement of soil moisture*. Govt. print. off., Washington.

Buss, P. 1993. The use of capacitance based measurements of real time soil water profile dynamics for irrigation scheduling. In National Conference of the Irrigation, Australia and the National Committee on Irrigation and Drainage, Launceston, Tasmania.

Chin, D.A., and R.D. Patterson. 2005. Quantification of hydrologic processes and assessment of rainfall-runoff models in Miami-Dade County, Florida. Information Services, Reston, VA, Denver, CO.: U.S. Geological Survey.

Chin, D.A. 2008. Phenomenological models of hydrologic processes in South Florida. *Journal of Hydrology* 349: 230-243.

Coile, T.S. 1953. Moisture Content of Small Stone in Soil. *Soil Science* 75(3):203-208.

Colburn, B., and S. Goldweber. 1961. Preparation of oolitic limestone soil for agricultural. *Proceedings of the Florida State Horticultural Society* 74: 343-345.

Crane, J. 2008. *Tropical fruit crop production and research; HOS 5555* course notes, pp. 267. University of Florida.

Crane, J. H., and B. Schaffer. 2004. Increased exposure to cool ambient temperatures increased yield of 'Mauritius' lychee (Litchi chinensis) in Homestead Florida. In *Proceedings of the Florida State Horticultural Society* 117: 206-208.

Crane, J., C. Balerdi, R. Campbell, C. Campbell, and S. Goldweber. 1994. Managing Fruit Orchards to Minimize Hurricane Damage. *HortTechnology* 4: 21-27.

Cunningham, K. J., R. A. Renken, M. A. Wacker, M. R. Zygnerski, E. Robinson, A. M. Shapiro, and G. L. Wingard. 2006. Application of carbonate cyclostratigraphy and borehole geophysics to delineate porosity and preferential flow in the karst limestone of the Biscayne aquifer, South Florida. *Geological Society of America* 404: *191-208.*

Cunningham, K.J., J.I. Carlson, and N.F. Hurley. 2004. New method for quantification of vuggy porosity from digital optical borehole images as applied to the karstic Pleistocene limestone of the Biscayne aquifer, southeastern Florida. *Journal of Applied Geophysics* 55: 77-90.

Delin, G.N., R.W. Healy, M.K. Landon, and J.K. Bohlke. 2000. Effects of topography and soil properties on recharge at two sites in an agricultural field. *American Water Resources Association* 36: 1401-1416.

Dexter, A.R., and N.R.A. Bird. 2001. Methods for predicting the optimum and the range of soil water contents for tillage based on the water retention curve. *Soil and Tillage Research* 57: 203-212.

Durner, W. 1994. Hydraulic conductivity estimation for soils with heterogeneous pore structure. *Water Resources Research* 30: 211-223.

Fares, A., and A.K. Alva. 2000. Soil water components based on capacitance probes in a sandy soil. *Soil Science Society of America Journal* 64: 311-318.

Fernald, E.A., and E.D. Purdum. 1998. Water Resources Atlas of Florida. Tallahassee, Florida State University, Institute of Science and Public Affairs. Available at: www.evergladesvillage.net/atlas_of_fla/atlas.html. Accessed 19 February 2009.

Fish, J. E., and M. Stewart. 1991. Hydrogeology of the surficial aquifer system, Dade County, Florida. Report 90-4108, 50 p.: U. S. Geological Survey Water Resources Investigations.

Fisher, N.I., and A.J. Lee. 1983. A correlation coefficient for circular data. *Biometrika* 70: 327-332.

Gardner, C.M.K., T.J. Dean, and J.D. Cooper. 1998. Soil water content measurement with a high-frequency capacitance sensor. *Journal of Agricultural Engineering Research* 71: 395-403.

Greenwood, J. A., and D. Durand. 1955. The distribution of length and components of the sum of n random unit vectors. *Annals of Mathematical Statistics* 26: 233-246.

Hanson, C.T., and R.L. Blevins. 1979. Soil water in coarse fragments. *Soil Science Society of America Journal* 43: 819-820.

Hassan, SF, Hussin, AG, Zubairi, YZ, 2009. Analysis of Malaysian wind direction data using ORIANA. *Modern Applied Science* 3(3):115-119.

Jabro, J.D., Lieb, B.G., and Jabro, A.D. 2005. Estimating soil water content using site-specific calibration of capacitance measurements from sentek enviroscan systems. *Applied Engineering in Agriculture* 21(3): 393-399.

Klein, H., and J.E. Hull. 1978. Biscayne aquifer, southeast Florida. Tallahassee, Florida.: U.S. Geological Survey, Water Resources Division.

Klute, A. 1986. Water Retention: Laboratory Methods. In *Methods of Soil Analysis, Soil Science Society of America Book Series* 1: 635-662.

Kovach, W. L. 2009. *Oriana for Windows, version 3.01*. Pentraeth, Wales, UK.: Kovach Computing Services.

Li, Y. 2001. Calcareous soils in Miami-Dade County. University of Florida. Cooperative extension service, Institute of Food and Agriculture Sciences, EDIS SL183, Gainesville, Fla.

Magilligan, F. and B. Graber. 1996. Hydroclimatological and geomorphic controls on the timing and spatial variability of floods in New England, USA. *Journal of Hydrology*, 178: 159-180.

Mead, R. M., J. E. Ayars, and J. Liu. 1995. Evaluating the influenceog soil texture, bulk density and soil water salinity on a capacitance probe calibration. ASAE Pap. 95-3264, St. Joseph, MI.: ASAE.

Mennill, D. J. and Ratcliffe, L. M. 2004. Nest cavity orientation in black-capped chickadees Poecile atricapillus: do the acoustic properties of cavities influence sound reception in the nest and extra-pair matings? *Journal of Avian Biology* 35: 477-482.

Merritt, M.L. 1996. Simulation of the water-table altitude in the Biscayne aquifer, southern Dade County, Florida, water years 1945-89.: U.S. Geological Survey Water-Supply Paper 2458.

Meyer, A. F. 1960. Effect of temperature on groundwater levels. *Journal of Geophysical Research* 65 (6): 1747-1752.

Migliaccio, K., B. Schaffer, J. Crane, Y. Li, and R. Muñoz-Carpena. 2008a. Assessing capillary rise in a field nursery considering irrigation management. In *Proceedings of ASABE. ASABE Annual International Meeting,* June 29 – July 2, 2008, Providence, Rhode Island.

Migliaccio, K.W., B. Schaffer, Y.C. Li, E. Evans, J.H. Crane, and R. Munoz-Carpena. 2008b. Assessing benefits of irrigation and nutrient management practices on a Southeast Florida royal palm (Roystonea elata) field nursery. *Irrigation Science* 27: 57-66.

Minkowski, K., and B. Bruce Schaffer. 2001. Section 1: A geographic information system for Miami – Dade County agriculture. In *Miami-Dade County agricultural land retention study, Vol. 2*. Florida agricultural market research center, Gainesville, FL. p. 110: Institute of Food and Agricultural Sciences, University of Florida.

Morgan, K. T., L. R. Parsons, T. A. Wheatson, D. J. Pitts, and T. A. Obreza. 1999.Field calibration of a capacitance water content probe in fine sand soils. *Soil Science Society of America Journal* 63 (4): 987-989.

Muñoz-Carpena, R., and A. Ritter. 2005. *Hidrología Agroforestal*. Canarias, Spain: MundiPrensa.

Muñoz-Carpena, R., Y. Li, and T. Olczyk. 2002. Alternatives of low cost soil moisture monitoring devices for vegetable production in South Miami-Dade County. University of Florida Cooperative Extension Service, Institute of Food and Agriculture Sciences, EDIS ABE333, Gainesville, FL.

Nash, J.E., and J.V. Sutcliffe. 1970. River flow forecasting through conceptual models part I A discussion of principles. *Journal of Hydrology 10*: 282-290.

Nielsen, D. 2006. *Environmental site characterization and ground-water monitoring*, 208-244. 2nd editon. Boca Raton, FL.: Taylor & Francis.

Noble, C.V., R.W. Drew, and J.D. Slabaugh. 1996. Soil survey of Dade County area, Florida. In: IFAS USDA/NRCS in cooperation with the University of Florida, Agricultural Experiment Stations, Soil and Water Science Department, t.F.D.o.A.a.C. Services, t.S.D.S.a.W.C. District and a.t.F.D.o. Transportation (Eds).

Nuñez-Elisea, R., B. Schaffer, M. Zekri, S.K. O Hair, and J.H. Crane. 2001. In situ soil-water characteristic curves for tropical fruit orchards in trenched calcareous soil. *Horttechnology* 11: 65-68.

Núñez-Elisea, R., B. Schaffer, M. Zekri, S.K. O'Hair, and J.H. Crane. 2000. Monitoring soil water content in tropical fruit orchards in South Florida with multisensor capacitance probes and tensiometers. *Hort-Science* 35: 487.

Oliveira, E.G., Srygley, R.B. and R. Dudley. 1998. Do neotropical migrant butterflies navigate using a solar compass? *Journal of Experimental Biology*, 201: 3317-3331.

Paltineanu, I.C., and J.L. Starr. 1997. *Real*-time Soil water dynamics using multisensor capacitance probes: laboratory calibration. *Soil Science Society of America Journal* 61: 1576.

Paton, Peter W. C., Timm, Brad and Tupper, Todd, 2003. Monitoring pond breeding amphibians. Report from the *USGS Patuxent Wildlife Research Center*, Wellfleet, MA.

Peach, M. B., 2003. Rheotaxis by epaulette sharks, Hemiscyllium ocellatum (Chondrichthyes hemiscylliidae), on a coral reef flat. *Australian Journal of Zoology* 50(4) 407-414.

Peck, A.J. 1960. The water table as affected by atmospheric pressure. *Journal of Geophysical Research* 65: 2383.

Perry, W. 2004. Elements of South Florida's Comprehensive Everglades Restoration Plan. *Ecotoxicology* 13: 185-193.

Pitt, W.. 1976. Response of ground-water levels to flood control operations in three basins, Southeastern Florida, Geological Survey, Tallahassee: U.S. Dept. of the Interior.

Polyakov, V., A. Fares, and M. Ryder. 2005. Calibration of a capacitance system for measuring water content of tropical soil. *Vadose Zone Journal* 4: 1004-1010.

Poole, CE. 1996. *Environmental resources for South Florida ecosystem restoration*. State University System of Florida Monographic holdings.

Prathapar ,and Qureshi. 1999. Modelling the effects of deficit irrigation on soil salinity, depth to water table and transpiration in semi-arid zones with monsoonal rains. *International Journal of Water Resources Development* 15: 141-159.

Raes, D., and P. Deproost. 2003. Model to assess water movement from a shallow water table to the root zone. *Agricultural Water Management* 62: 79-91.

Rasmussen, T.C., and L.A. Crawford. 1997. Identifying and removing barometric pressure effects in confined and unconfined aquifers. *Ground Water* 35: 502-511.

Ritter, A., and R. Muñoz-Carpena. 2006. Dynamic factor modeling of ground and surface water levels in an agricultural area adjacent to Everglades National Park. *Journal of Hydrology* 317: 340-354.

Saxena, S.K. 1982. Geotechnical properties of calcareous rocks in Southern Florida. In *Geotechnical properties, behavior, and performance of calcareous soils*, *ASTM STP 777*, 340-358. American Society for Testing and Materials.

Schaffer, B. 2008. *Ecophysiology of subtropical and tropical fruit crops; HOS 5555* course notes. University of Florida.

Schaffer, B. 1998. Flooding responses and water-use efficiency of subtropical and tropical fruit trees in an environmentally-sensitive wetland. *Annals of Botany* 81: 475-481.

Skaggs, R.W. 1978a. A water management model for shallow water table soils. *Water Resources Research Institute of the University of North Carolina, Raleigh.*

Skaggs, R.W., L.G. Wells, and S.R. Ghate. 1978b. Predicted and measured drainable porosities for field soils. *Transactions of the ASAE* 21: 522-528.

Smith, W. O. 1939. Thermal transfer of moisture in soils. *Transactions American Geophysical Union* 24(2): 511-524.

Sumner, D.M. 2007. Effects of capillarity and microtopography on wetland specified yield. *Wetlands* 27: 693-701.

Taylor, S. A. 1962. Influence of temperature upon the transfer of water in soil systems. *Mededelingers, Landbouwhogeschool, Gent. Belgium.* 27: 535-551.

Todd, D.K. 1959. *Groundwater hydrology*. New York: Wiley.

Towner, G. 1980. Theory of time response of tensiometers. *European Journal of Soil Science* 31(4): 607 – 621.

Tromble, J.M. 1977. Water requirements for mesquite (Prosopis juliflora). *Journal of Hydrology* 34: 171–179.

Turk, L. J. 1975. Diurnal fluctuations of water tables induced by atmospheric pressure changes. *Journal of Hydrology* 26: 1-16.

USGS. 2009. Ground-water watch:site number:253029080295601-S-196A. US Geological Survey Ground-Water Watch. Available at: http://groundwaterwatch.usgs.gov. Accessed 28 March 2009.

Van Genuchten, M.T. 1980. A closed-form equation for predicting the hydraulic conductivity of unsaturated soils. *Soil Science Society of America Journal* 44: 892-898.

Van Genuchten, M.T., F.J. Leij, S.R. Yates, and S.K.E.R.L. Robert. 1991. The RETC code for quantifying the hydraulic functions of unsaturated soils. Robert S. Kerr Environmental Research Laboratory, Office of Research and Development, U.S. E.P.A., Ada, Okla.

Wallender, W.W., D.W. Grimes, D.W. Henderson, and L.K. Stromberg. 1979. Estimating the Contribution of a perched water table to the seasonal evapotranspiration of cotton. *Agronomy Journal* 71: 1056-1060.

Warrick, A. W., G. J. Mullen, and D. R. Nielsen. 1977. Scaling field-measured soil hydraulic properties using a similar media concept. *Water Resources Research* 13(2): 355–362.

Weeks, E.P. 1979. Barometric fluctuations in wells tapping deep unconfined aquifers. *Water Resources Research* 15(5): 1167–1176.

Wellings, S. R., and J. P. Bell. 1982. Physical controls of water movement in the unsaturated zone. *Quarterly Journal of Engineering Geology* 15: 235 – 241.

White, W.N.1932. A method of estimating groundwater supplies based on discharge by plants and evaporation from soil. Utah.U.S. Geological Survey Water-Supply Paper. Results of Investigations in Escalante Valley, *659-A*, 165 p.

Zekri, M., R. Núñez-Elisea, B. Schaffer, S.K. O'Hair, and J.H. Crane. 1999. Multi-sensor capacitance probes for monitoring soil water dynamics in the oolitic limestone soil of South Florida. In *Proceeding of the Florida State Horticultural Society* 112: 178–181.

BIOGRAPHICAL SKETCH

Luis Pablo Barquin Valle was born in Guatemala de la Asuncion, Guatemala. Luis went to EARTH University in Costa Rica for his undergraduate education in Agronomy and Natural Resources in 2001. During his undergraduate internship in 2003, Luis worked for Dr Rafael Muñoz Carpena and Dr Bruce Schaffer with the hydrology and environmental physiology laboratories. This experience helped him to define his interests for water resources engineering which motivated him to do his agronomy degree thesis related to the response of banana production with improved drainage conditions. After graduating from EARTH University in December 2004, Luis worked as a farm supervisor for two years with AV- CMI Group, the biggest poultry corporation in Central America. In 2007, Luis came to the U.S. and worked as a research assistant for Dr Yuncong Li with UF-TREC Soil and Water Science Laboratory. In August 2007, Luis was accepted to the University of Florida graduate school at the Agricultural and Biological Engineering Department, joining Dr. Kati Migliaccio's research team to work on his Master of Science thesis focused on modeling capillary rise of groundwater in South Florida calcareous soils.